5-2015

Targeted Inhibition Of Pi3K, Mtor, And Igf1R For The Treatment Of Undifferentiated Pleomorphic Sarcoma

Caitlin Denise May

TARGETED INHIBITION OF PI3K, MTOR, AND IGF1R FOR THE TREATMENT OF UNDIFFERENTIATED PLEOMORPHIC SARCOMA

by

Caitlin Denise May, BS

APPROVED:

_____

Keila E. Torres, MD, PhD
Chair, Supervisory Committee

_____

Menashe Bar-Eli, PhD

_____

Dennis P. M. Hughes, MD, PhD

_____

Alexander J. Lazar, MD, PhD

_____

Li Ma, PhD

APPROVED:

_____

Dean, Graduate School of Biomedical Sciences
The University of Texas Health Science Center at Houston

TARGETED INHIBITION OF PI3K, MTOR, AND IGF1R FOR THE TREATMENT OF UNDIFFERENTIATED PLEOMORPHIC SARCOMA

A

DISSERTATION

Presented to the Faculty of

The University of Texas

Health Science Center at Houston

Graduate School of Biomedical Sciences

and

The University of Texas

M. D. Anderson Cancer Center

Graduate School of Biomedical Sciences

In Partial Fulfillment

Of the Requirements

For the Degree of

DOCTOR OF PHILOSOPHY

by

Caitlin Denise May, BS

May, 2015

Dedication

To my parents, Paul and Catherine May – for your encouragement during the hard times, your joy during the best times, and, above all else, your unfaltering and unconditional love.

And to my grandparents – Claude and Catherine Allen and Merle and Noreen May – for all of your love and prayers throughout your lives and mine. You are truly missed.

Acknowledgements

I would like to thank Dr. Keila E. Torres for her support and guidance during my graduate career. Thank you for allowing me to take control of my dissertation project and really letting me make it my own. Working in your lab has allowed me grow, improve, and mature, both personally and professionally, and for that I am very appreciative. To the members of the sarcoma research lab, both past and present, thank you for all of your help and encouragement, day in and day out. In particular, I would like to thank Svetlana Bolshakov for her tough love and to Dr. Jeannine Garnett for helpful discussions regarding my project. Also, many thanks to Kelsey Watson-Schertz for all of her help with the clinical databases and her statistical support and also for helping me put things into perspective.

To Dr. Ghadah al-Sannaa, thank you for scoring all of the immunohistochemical stains and for your constant uplifting positivity and kind words.

To my advisory committee members, Dr. Menashe Bar-Eli, Dr. Dennis Hughes, Dr. Alexander Lazar, and Dr. Li Ma, thank you for your helpful discussions concerning my dissertation project and for your interest in my career development as a young scientist. Your questions and suggestions have improved my critical thinking, scientific writing, and oral presentation skills. The advice you have given has been invaluable and I am very grateful for it.

To my supervisory and exam committee members, Dr. Dina Lev, Dr. Elsa Flores, Dr. Randy Johnson, Dr. Johnathan Kurie, Dr. Min-Gyu Lee, and Dr. Michael Galko, thank you for your guidance during the beginning of my graduate career.

To Dr. Lisa Chen and Brian Menegaz, thank you for troubleshooting experiments with me and being great sources of encouragement.

I would like to acknowledge the Amschwand Sarcoma Cancer Foundation and the Andrew Sowell-Wade Huggins Endowed Scholarship Fund, for their financial support during my graduate training.

To my Mom and Dad. You were my first teachers who fostered a love and a thirst for knowledge. You have not only shown me how to be a great parent, but to be a great spouse, a great friend, and a great scientist. Thank you for showing me what truly matters in life and for believing in me all the way.

To my sisters, Molly, Erin, and Shannon, thank you for all of your support and encouragement when I was down, for the reality checks when I needed them, and for being so understanding when I missed important events because of the distance. It hasn't been easy, living so far away, but it has made me truly treasure the time we spend together as a family. You three are extraordinarily smart, funny, and compassionate women and it is a tremendous privilege to be your sister.

To my other sisters Mallory and Ashley. Even though we have spent the better part of the last 16 years separated by distance (and sometimes even an ocean or two!), we are as close as ever. Thank you for the laughs, for somehow always knowing when I needed a card in the mail or a phone call to brighten my day, and for being my family.

To my Houston friends – thank you for making the transition from Michigan to Texas an easier one. A special thanks to Christine M. Kivlin, BS Biology, for sharing an office with me for two years, all day, every day, troubleshooting and wordsmithing, and for still

being willing to hang out afterwards. Solidarity, sister! Thank you to Davis Ingram for challenging me to expand my mind and to learn more about the world around me.

And to Frank J. Lowery III – my partner in crime and in life. Thank you for sharing in the laughter and the tears and for pushing me forward when I didn't think I could. I am constantly inspired by your strength, your (seemingly endless) patience, and your ability to calmly handle anything that comes your way. You are the absolute best and I am so excited to see what the future has in store for us.

Abstract

Targeted inhibition of PI3K, mTOR, and IGF1R for the treatment of undifferentiated pleomorphic sarcoma

Caitlin Denise May, BS

Supervisory Professor: Keila E. Torres, MD, PhD

Undifferentiated pleomorphic sarcoma (UPS) is an aggressive mesenchymal malignancy largely devoid of indicators for its originating tissue. Surgery remains the standard of care, as radiation therapy and systemic chemotherapy have limited efficacy in UPS patients with localized and metastatic disease, respectively. Therefore, it is imperative to identify and evaluate novel therapeutic targets in UPS in order to provide more efficacious treatment options for patients. Previous studies have revealed that members of the phosphatidylinositol-3-kinase/mammalian target of rapamycin (PI3K/mTOR) signaling pathway can be used to predict patient outcome in cohorts containing patients with various subtypes of soft tissue sarcoma. Furthermore, we have previously shown that high levels of phosphorylated AKT correlate to poorer disease-specific survival in UPS patients, indicating that PI3K/mTOR activity may contribute to the aggressiveness of disease. In this dissertation, we demonstrate that the PI3K/mTOR pathway is active in UPS patient-derived tumor samples and cell strains/lines. Pharmacologic blockade of this pathway using second-generation dual PI3K/mTOR small molecule inhibitors as single agents attenuates UPS cell proliferation, migration, and invasion *in vitro*. In addition, daily or twice daily drug administration reduces tumor volume and weight in a mouse model harboring a UPS tumor implant. However, single agent therapy was insufficient to eliminate tumor growth, and immunohistochemical analysis revealed that PI3K/mTOR inhibition activates insulin-like

growth factor 1 receptor (IGF1R), potentially as a mechanism of adaptive resistance. Combined inhibition of PI3K, mTOR, and IGF1R via small molecule inhibitors resulted in a drastically reduced tumor volume *in vivo*, despite the lack of substantial antiproliferative effects *in vitro*. Furthermore, the drug combination significantly decreased UPS cell migration and invasion, due in part to the re-localization of the cyclin-dependent kinase inhibitor $p27^{KIP1}$ to the nucleus. Taken together, our data indicate that targeted inhibition of key nodes in the PI3K/mTOR pathway in combination with IGF1R reduces UPS tumorigenicity and should be further explored as a novel therapeutic avenue for UPS patients.

Table of Contents

List of Illustrations

List of Tables

Abbreviations

4EBP1: eukaryotic translation-initiation factor 4E (eIF4E)-binding protein 1

CC3: cleaved caspase 3

CDKi: cyclin-dependent kinase inhibitor

DSS: disease-specific survival

EGFR: epidermal growth factor receptor

eIF4E: eukaryotic translation-initiation factor 4E

ERK: extracellular signal-related kinase

FOXO: forkhead box O

GAP: GTPase-activating protein

GEF: guanine exchange factor

H&E: hematoxylin and eosin

(h)MSC: (human) mesenchymal stem cell

HR: hazard ratio

IGF1/IGF2: insulin-like growth factor 1/insulin-like growth factor 2

IGF1R: insulin-like growth factor 1 receptor

IHC: immunohistochemistry

IR: insulin receptor

IRS1-4: insulin receptor substrate 1-4

LIMK: LIM kinase

LMS: leiomyosarcoma

mAb: monoclonal antibody

MAPK: mitogen-activated protein kinase

MEK: mitogen-activated protein kinase kinase (MAPKK)

MFH: malignant fibrous histiocytoma

MPNST: malignant peripheral nerve sheath tumor

mTORC1/2: mammalian target of rapamycin complex 1/2

mTOR: mammalian target of rapamycin

OS: overall survival

p27: $p27^{KIP1}$

PDK1: phosphoinositide-dependent kinase 1

PI3K: phosphatidylinositol-3-kinase

PIP_2: phosphatidylinositol-4,5-bisphosphate

PIP_3: phosphatidylinositol-3,4,5-bisphosphate

PKB: protein kinase B, also called AKT

PDGFRA/B: platelet-derived growth factor receptor A/B

P-REX1: PIP_3-dependent Rac1 exchanger 1

PTEN: phosphatase and tensin homologue

RA-STS: radiation-associated soft tissue sarcoma

RA-UPS: radiation-associated undifferentiated pleomorphic sarcoma

RHEB: RAS homologue enriched in brain

ROCK: Rho-associated kinase

RTK: receptor tyrosine kinase

S6K: p70 ribosomal protein S6 kinase

S6RP: S6 ribosomal protein

SCF^{SKP2}: S-phase kinase associated protein 1 [SKP1]/Cullin/F-box protein: SK2 complex, E3 ubiquitin ligase

SKP2: S phase kinase-associated protein 2

STS: soft tissue sarcoma

TSC1/2: tuberous sclerosis protein 1/2

UPS: undifferentiated pleomorphic sarcoma

WHO: World Health Organization

Chapter 1

Introduction

1.1 Soft tissue sarcoma

Soft tissue sarcoma (STS) accounts for approximately 1% of adult and 7-15% of pediatric cancers, with more than 12,000 new diagnoses and 5,000 deaths related to STS in the United States annually (1-3). The term STS does not refer to a single entity; rather, it encompasses more than 80 histologically distinct subtypes of rare mesenchymal malignancies, classified and named according to their putative or known originating tissue (4, 5). As these tumors are putatively derived from connective tissues or more primitive precursor cells, including fat, nerve, and muscle, STS can develop in all regions of the body, most commonly in the extremities (5, 6). The standard of care is surgical resection, as many STS patients have limited response to conventional chemotherapies (4, 5). Currently, the five-year overall survival rate for all STS patients with localized disease is approximately 82%; for patients with metastatic disease, survival drops dramatically to 18% (7, 8).

STS can be further characterized into two categories based on genomic criteria (9-13). The first includes those associated with specific recurring genetic alterations and relatively simple karyotypes. The second is comprised of complex and unbalanced karyotypes and inherent high levels of genomic instability and include tumors that are generally more pleomorphic. Undifferentiated pleomorphic sarcoma, previously termed malignant fibrous histiocytoma, is one such karyotypically complex STS subtype (13-15).

1.2 Undifferentiated pleomorphic sarcoma

Reclassification of malignant fibrous histiocytoma

Malignant fibrous histiocytomas (MFHs) were once the most commonly diagnosed STS in adults, accounting for nearly 40% of cases in the 1970s-1990s (16). First described in the early 1960s, this STS subtype was thought to be derived from histiocytes (local tissue macrophages) which could assume fibroblastic characteristics (17, 18). MFHs display a wide range of morphological patterns that include storiform (cartwheel-like)-pleomorphic, myxoid, giant cell, and inflammatory growth patterns (19, 20). The inclusive nature caused concern in some pathologists that MFH was being over-diagnosed (20-22). Moreover, it was proposed that the pleomorphic growth pattern observed in MFH represented a specific morphology, rather than an STS subtype (23, 24).

During the 1990s and early 2000s, the majority of MFH cases were reclassified as specific STS subtypes or other non-mesenchymal neoplastic entities, such as melanoma or poorly differentiated carcinoma, as a result of improved diagnostic techniques (25-28). Furthermore, identification of cell type-specific markers detectable by immunohistochemistry revealed that many MFH cases more closely resembled stromal spindle cells such as fibroblasts or myofibroblasts, rather than histiocytes (29). In 2002, the World Health Organization (WHO) designated the myxoid and angiomatoid subtypes of MFH as distinct diagnostic entities; moreover, the remaining tumors previously called MFHs were reclassified as undifferentiated pleomorphic sarcomas

(UPSs) (22, 30). In 2013, the UPS concept was further refined to account for non-pleomorphic histologies (31).

Incidence and clinical features

UPS accounts for approximately 5-15% of STS cases and is the most commonly diagnosed STS subtype in patients over 40 years of age, with a slight predominance towards males (1.2 to 1) (4, 13, 21, 22). These tumors are generally higher grade, deep-seated masses most often located in the lower extremity and, to a lesser extent, the upper extremity and retroperitoneum (4, 5, 13, 30). UPSs are often asymptomatic, with only extremely fast growing tumors tending to cause discomfort and approximately 5% of patients have evidence of metastatic disease at time of initial diagnosis (30).

Molecular characteristics

The key defining characteristic of UPS is the lack of a distinct discernible line of differentiation able to be identified by electron microscopy, immunohistochemistry, or other methodologies (32). Therefore, UPS is considered a diagnosis of exclusion, reserved for any STS with a pleomorphic or spindle cell histology and an absence of specific diagnostic markers that cannot be placed in another diagnostic category. However, recent reports have suggested that UPS may arise from mesenchymal stem cells (MSCs) which are malignantly transformed through the inactivation of the Wnt pathway and/or the activation of known oncogenes (33-36). The broader application of these findings to the broad class of UPS is not known.

In contrast to STS subtypes characterized by chromosomal translocations or gene amplifications or mutations, UPSs are karyotypically complex malignancies with non-recurrent chromosomal gains and losses. Reports of specific recurring aberrations

unique to UPS are rare. However, several studies have reported similar chromosomal rearrangements in UPS and leiomyosarcoma (LMS), a STS subtype showing smooth muscle differentiation (37-39). Additionally, transcriptome analyses could not distinguish UPS from other pleomorphic STS subtypes, further confounding differential diagnoses (40-43).

Available treatment options

As with most STS, surgical resection is the standard-of-care for patients with localized tumors (11, 44, 45). Chemotherapy and/or radiation therapy has been used in conjunction with surgery for patients with large (>5 cm in diameter) and/or aggressive disease. For patients with metastatic or unresectable disease, chemo- and/or radiotherapy are the only available therapeutic options (45). However, like other subtypes of STS, UPS is generally chemoresistant to most available systemic therapies (46). In addition, clinical trials evaluating imatinib, sunitinib, or other targeted therapies against receptor tyrosine kinases (RTKs) which have proved effective in other STS subtypes have reported poor response rates in UPS patients (47-50).

Patient outcome

The local recurrence rate for patients with sporadic UPS is approximately 19-31% (51-54). More than one-third of UPS patients will experience metastatic disease, most often to the lung (80%), bone (8%), or liver (1%) (5, 51-54). The five-year survival rate for patients with sporadic UPS is only 65-70% (51-54).

Radiation-associated UPS

Neoadjuvant or adjuvant radiation therapy is often a part of a multidisciplinary treatment regimen for cancer patients. A rare consequence of radiation therapy is the development of a second malignancy. STS is one of the most common types of post-radiation tumors, with an incidence rate from 0.03% - 0.80% (5, 55). In order for a tumor to be classified as a radiation-associated STS (RA-STS), it must develop in an area of the body which was exposed to radiation, such as a treatment modality for an unrelated disease. The median latency between initial radiation exposure and STS development has been reported to be approximately 8-10 years, although the mandatory latency period for diagnosis has not yet been explicitly defined (56-58). Approximately 25-36% of RA-STS are classified as radiation-associated UPS (RA-UPS), which in turn account for 3% of all UPS cases (30, 31, 58, 59). Patients with RA-UPS generally have a poorer prognosis than those with sporadic UPS, with a 5-year disease-specific survival rate of 36-52% and a recurrence rate of 55% (56-58, 60).

1.3 The PI3K/mTOR signaling cascade

The phosphatidylinositol-3-kinase/mammalian target of rapamycin (PI3K/mTOR) signaling axis is summarized in Figure 1. Briefly, PI3K is composed of two subunits: the p110α catalytic subunit and the p85 regulatory subunit. Activation of PI3K can be initiated when a ligand binds to a RTK, resulting in phosphorylation of tyrosine residues located on the intracellular portion of the RTK (61, 62). These phosphotyrosines recruit PI3K to the cell membrane by providing docking sites for the p85 subunit of PI3K, causing a conformational change in the p85 subunit which allows for p110α catalytic activity (63, 64). Activated PI3K then generates the second messenger phosphatidylinositol-3,4,5-triphosphate (PIP_3) through phosphorylation of phosphatidylinositol-4,5-bisphosphate (PIP_2) (65). PIP_3 is able to recruit the

serine/threonine kinase AKT (also called protein kinase B; PKB) and 3-phosphoinositide-dependent kinase 1 (PDK1) to the plasma membrane by providing docking sites for the proteins' pleckstrin homology domains. PDK1 phosphorylates AKT at T308 in the activation loop; an additional phosphorylation on S473 by the mammalian target of rapamycin complex 2 (mTORC2) is essential for the full activation of the protein (65, 66). Activated AKT promotes cellular processes like proliferation, survival, and motility through the phosphorylation of downstream effector molecules (67-69).

The serine/threonine kinase mTOR is a member of the PI3K-related kinase family due to the strong homology between their catalytic domains (70). mTOR is essential for the integration of extracellular and intracellular stimuli to coordinate the activation of metabolic processes which support cell growth, proliferation, and survival; furthermore, there is evidence that mTOR can regulate cell motility (70-72). Mammalian target of rapamycin complex 1 (mTORC1) and mTORC2 are two large multiprotein complexes which contain mTOR and are linked to PI3K signaling, but vary in both protein composition and function (73-75). In addition, mTORC1 is sensitive to the macrolide rapamycin, while mTORC2 is not directly inhibited by the compound; however, sustained rapamycin treatment can block mTORC2 function (75-77).

The regulation and function of mTORC1 has been extensively characterized. mTORC1 can be activated in response to several stimuli, including nutrient levels, cell energy status, and growth factors (70). Stimulation of upstream RTKs by growth factors results in PI3K activity and AKT phosphorylation. AKT indirectly activates mTORC1 through the inhibitory phosphorylation of tuberous sclerosis 2 (TSC2) (78-80). The TSC1/2 heterodimer acts as a GTPase activating protein (GAP) and promotes the

GDP-bound (inactive) state of RAS homologue enriched in brain (RHEB), a small G protein essential for mTORC1 activation (81, 82). Inhibition of the TSC1/2 complex allows GTP-bound (active) RHEB to bind and activate mTORC1 (83).

Figure 1. The PTEN–PI3K–AKT–mTOR pathway.

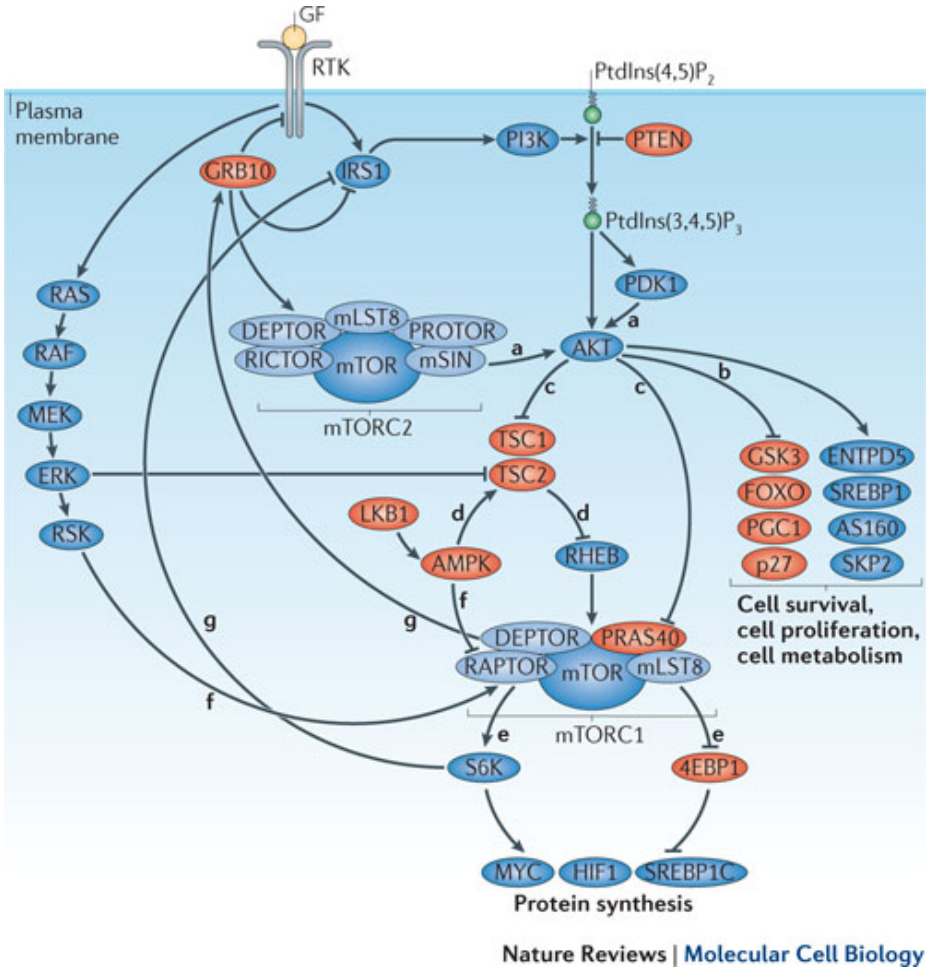

Phosphatase and tensin homologue (PTEN) opposes phosphoinositide 3-kinase (PI3K) function, leading to inactivation of AKT and mammalian target of rapamycin (mTOR) signalling. Following PTEN loss, phosphatidylinositol-3,4,5-trisphosphate (PtdIns(3,4,5)P3) accumulation recruits the pleckstrin homology (PH) domain-containing proteins AKT and 3-phosphoinositide-dependent kinase 1 (PDK1). Once positioned at the membrane, AKT is activated by PDK1-mediated phosphorylation at Thr308 and phosphorylation at Ser473 by mTOR complex 2 (mTORC2; composed of mTOR, DEP domain-containing mTOR-interacting protein (DEPTOR), mammalian lethal with SEC13 protein 8 (mLST8), stress-activated MAP kinase-interacting protein 1 (mSIN1), Pro-rich protein 5 (PRR5; also known as PROTOR) and rapamycin insensitive companion of mTOR (RICTOR)) (a). Active AKT drives cell survival, proliferation and cellular metabolism through inhibitory phosphorylation of downstream proteins, including glycogen synthase kinase 3 (GSK3), forkhead box O (FOXO), peroxisome proliferator-activated

receptor-γ (PPARγ) co-activator 1α (PGC1) and p27, and through activatory phosphorylation of ectonucleoside triphosphate diphosphohydrolase 5 (ENTPD5), sterol-responsive element-binding protein 1C (SREBP1C), AS160 and S phase kinase-associated protein 2 (SKP2) (b). AKT can also activate mTORC1 (composed of mTOR, DEPTOR, mLST8, 40 kDa Pro-rich AKT1 substrate 1 (PRAS40) and regulatory associated protein of mTOR (RAPTOR)) by mediating the inhibitory phosphorylation of its negative regulators tuberous sclerosis protein 2 (TSC2) and PRAS40 (c). TSC2 is also phosphorylated by extracellular signal-regulated kinase (ERK), which inhibits the ability of TSC2 to function as a GTPase-activating protein (GAP) towards RAS homologue enriched in brain (RHEB), whereas AMP-activated protein kinase (AMPK)-mediated phosphorylation positively regulates the GAP activity of TSC2 (d). mTORC1 phosphorylates p70 ribosomal protein S6 kinase (S6K) and eukaryotic translation-initiation factor 4E (eIF4E)-binding protein 1 (4EBP1) to activate protein translation and cell survival (e). p90 ribosomal protein S6K (RSK)-mediated phosphorylation of RAPTOR contributes the activation of mTORC1 signalling, whereas AMPK-mediated phosphorylation of RAPTOR results in the inhibition of mTORC1 signalling (f). Genetic inactivation or pharmacological inhibition of mTORC1 can activate AKT by preventing a negative feedback loop mediated by the mTORC1–S6K-induced phosphorylation of insulin receptor substrate 1 (IRS1) and growth factor receptor-bound protein 10 (GRB10) (g). Blue- and red-coloured molecules represent activators and repressors of the signalling pathway, respectively. GF, growth factor; HIF1, hypoxia-inducible factor 1; LKB1, liver kinase B1; MEK, mitogen-activated protein kinase kinase; RTK, receptor Tyr kinase.

Once activated, mTORC1 is able to positively regulate cell metabolism and biosynthesis through the promotion of anabolic processes, which it achieves by phosphorylating several downstream proteins. In particular, activated mTORC1 increases protein synthesis by phosphorylating the eukaryotic initiation factor 4E (eIF4E)-binding protein 1 (4EBP1) and the p70 ribosomal S6 kinase (S6K) (73, 74, 85, 86). Phosphorylation of the translational repressor 4EBP1 blocks its binding to eIF4E and thus facilitates the initiation of cap-dependent translation (87, 88). Similarly, S6K activation also promotes cap-dependent translation and elongation; furthermore, S6K promotes ribosome biogenesis via phosphorylation of S6 ribosomal protein (S6RP) (89, 90).

Compared to mTORC1, not much is currently known about mTORC2 regulation and function. Like mTORC1, mTORC2 is a regulator of cell metabolism, despite not showing any sensitivity towards cellular nutrient levels. Rather, activation of mTORC2 is dependent on growth factor-mediated PI3K activation and the subsequent generation of PIP_3, although the details of mTORC2 activation are poorly understood (91). In addition, mTORC2-mediated phosphorylation of AKT results in maximal activation of the kinase and regulates cancer cell migration and invasion, further linking mTORC2 to PI3K signaling (66, 92).

Implication of the PI3K/mTOR signaling pathway in tumorigenesis

The PI3K/mTOR pathway is one of the most commonly activated pathways in cancer (61, 93-95). The tumorigenic potential of the PI3K/mTOR pathway lies within its regulation of cellular processes such as cell growth, proliferation, migration, and angiogenesis; furthermore, constitutive activation of this pathway has been linked to

resistance to systemic chemotherapies and inhibition of specific molecule targets (62, 69, 95-97). Aberrant or constitutive activation can be achieved in cancer cells through upregulation of receptor tyrosine kinase signaling, activating mutations in molecular pathway components (such as *PIK3CA*), and/or loss of tumor suppressors like the phosphatase and tensin homologue (PTEN) (61, 94, 95).

Oncogenic PI3K/mTOR signaling contributes to cancer cell proliferation, migration, and invasion in part through its regulation of the cyclin-dependent kinase inhibitor (CDKi) $p27^{Kip1}$ (hereafter called p27) (72, 98-100) (Figure 1, 2). In normal cells, p27 functions as a master regulator of cell proliferation through its direct interactions with cyclin-CDK complexes. In G_0 and early G_1, nuclear p27 blocks the G_1-S transition by binding to and inhibiting cyclin E-CDK2; in late G_1, cytoplasmic p27 promotes G_1 progression by facilitating the assembly and import of cyclin D-CDK4/6 complexes (100-102). Furthermore, the contribution of p27 activity in cell motility has been observed independently of its CDK-regulatory functions (98, 99, 103).

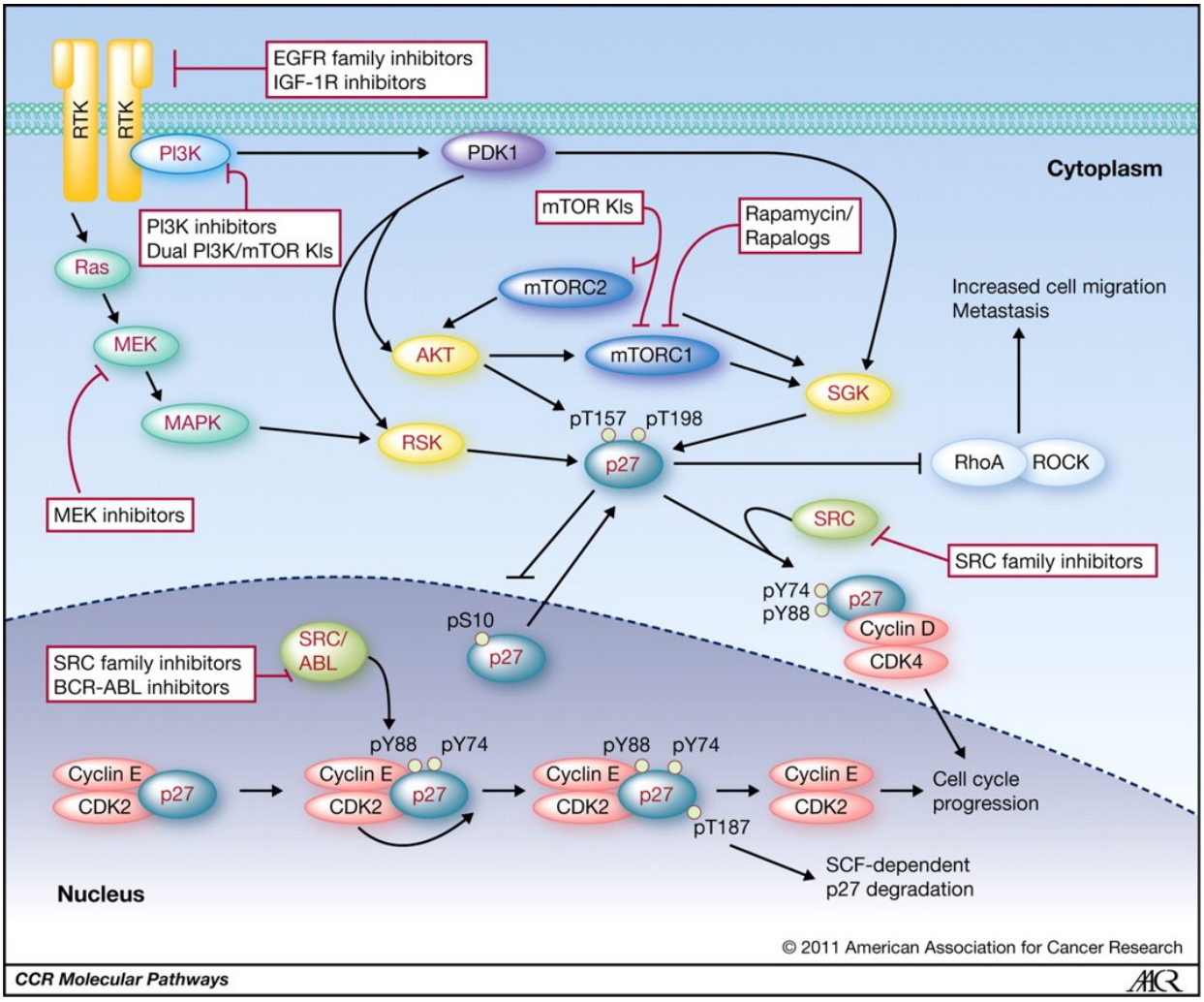

Figure 2. p27 plays multifaceted roles in the regulation of cell proliferation and cell migration. This schematic depicts p27 regulation and function as it relates to the protein's subcellular localization. While in the nucleus, p27 binds to and inhibits cyclin E-CDK2, preventing G1-S transit. Following SRC/ABL-mediated tyrosine phosphorylation and cyclin E-CDK2–mediated T187 phosphorylation, nuclear p27 is targeted for SCF^{SKP2}-dependent degradation, allowing cell cycle progression. S10 phosphorylation promotes nuclear export; whereas in the cytoplasm, p27 may play several roles. Oncogenic signal transduction via PI3K/PDK1 or Ras/MAPK results in the hyperactivation of several AGC family kinases (including AKT, SGK, and RSK), which all mediate C-terminal phosphorylation of p27 at T157 and T198. These phosphorylation events cooperate to sequester and stabilize p27 within the

cytoplasm, where it promotes cell proliferation (via cyclin D-CDK4 assembly) and cell motility (via inhibition of RhoA/ROCK signaling). Potential sites of targeted therapeutic intervention are highlighted in the figure.

Reprinted from Clinical Cancer Research, 2011, 17 (1), 12-18, SA Wander, D Zhao and JM Slingerland, p27: A Barometer of Signaling Deregulation and Potential Predictor of Response to Targeted Therapies, with permission from AACR (102).

Changes in p27 levels during the cell cycle are generally post-translationally regulated. p27 translation and stability are maximal during G_0 and early G_1, where it binds cyclin E-CDK2 and inhibits the G_1-S transition (104-107). These levels begin to fall during G_1 progression due to a series of phosphorylation events which target p27 for nuclear export and/or proteolysis. In early G_1, members of the ABL and SRC kinase family phosphorylate p27 on several tyrosine residues (Y74, Y88, and Y89) on the CDK-inhibitory domain (108, 109). This allows p27-bound cyclin E-CDK2 to further phosphorylate p27 on T187, which targets p27 for proteolysis by SCF^{SKP2} (S-phase kinase associated protein 1 [SKP1]/Cullin/F-box protein: SKP2 complex, E3 ubiquitin ligase) (99, 108, 109). Interestingly, a recent study reported that mTORC2 reduced nuclear p27 levels through the upregulation of the SKP2 ubiquitin ligase complex independently of phosphorylation of T187, demonstrating that PI3K/mTOR signaling can directly regulate nuclear p27 protein levels (110).

Subcellular localization can also regulate p27 function (Figure 2). Phosphorylation of p27 on S10 by kinase-interacting stathmin (KIS) or minibrain-related kinase (MIRK) during early G_1 promotes nuclear export of p27 by exportin 1, preventing p27-mediated cyclin E-CDK2 inhibition and targeting p27 for proteolysis by a SCF-independent mechanism (111-115). Cytoplasmic p27 is further phosphorylated by AKT at T157 and T198, effectively blocking its nuclear import while increasing its cytoplasmic stability; furthermore, these modifications promote the assembly of cyclin D-CDK4/6-p27 complexes (116-120). Further phosphorylation of these complexes enables their nuclear import and promotes subsequent cell cycle progression (99).

Cytoplasmic sequestration of p27 as a result of constitutive PI3K/mTOR signaling can facilitate increased cancer cell migration and invasion through the inhibition of the

RhoA/ROCK pathway (98, 100, 121). This pathway mediates the reorganization of the actin cytoskeleton and therefore regulates cell morphology, adhesion, and migration. The small GTPase RhoA activates Rho-associated kinase (ROCK), which in turn activates LIM kinase (LIMK) (103, 122, 123). LIMK negatively regulates cofilin, a member of the actin-depolymerizing protein (ADP) family which dissembles actin filaments. As a result, there is an increase in the formation and stability of actin stress fibers and focal adhesions, which promotes cell adhesion. Cytoplasmic p27 directly binds and inhibits RhoA by preventing RhoA from binding its upstream activators, Rho-guanine exchange factors (Rho-GEFs) (124). The resulting actin cytoskeleton instability and loss of stress fibers and focal adhesions following RhoA pathway inhibition facilitates cell migration.

Prognostic potential of PI3K/mTOR pathway members

The PI3K/mTOR pathway has been reported as a driver of tumorigenesis in numerous STS subtypes (125-129). In addition, markers of pathway activation have been investigated as molecular prognosticators for disease progression and outcome for STS patients. Constitutive activation of the pathway, as measured by the expression of activated (phosphorylated) pathway components AKT, mTOR, S6K, and 4EBP1, correlated with poor prognosis for STS patients (130-133). Furthermore, two studies identified phosphorylated AKT as an independent negative prognosticator for overall survival (OS) and disease-specific survival (DSS), while a third found that high levels of activated AKT correlated to a higher probability of metastatic disease (130, 132, 134). Similarly, previous work from our lab focusing on UPS patients determined that the high level of phosphorylated AKT expressed by a subset of tumors (approximately 20% of the cohort) significantly correlated to shorter DSS (135).

Targeted therapy against PI3K/mTOR signaling and the potential for resistance

As constitutive PI3K/mTOR signaling is frequently observed in cancer and contributes to tumorigenesis, disease progression, and resistance to systemic and targeted therapies, recent drug development efforts have focused on specific small molecule inhibitors against the PI3K/mTOR pathway (62, 85, 93, 136-139). However, many studies have reported limited efficacy and/or resistance to these targeted agents, often resulting in activation of compensatory signaling pathways, suggesting that combination therapy involving PI3K/mTOR pathway inhibition may have superior anti-tumor results (61, 95, 140-145).

The PI3K/mTOR pathway is regulated by several negative feedback loops which are disrupted upon targeted inhibition of the pathway members (70, 95). Both mTORC1 and its downstream kinase S6K negatively regulate growth factor signaling by phosphorylating the adaptor protein insulin receptor substrate 1 (IRS1) and reducing its stability (74, 146, 147). Inhibition of aberrant mTORC1 activity by treatment with rapamycin or its derivatives (called rapalogues) relieves the negative regulation of IRS1 by S6K and mTORC1 and activates the PI3K-AKT axis via RTK signaling, resulting in increased levels of phosphorylated AKT (140, 148, 149). In order to overcome the compensatory increase in PI3K signaling, treatment strategies expanded to include targeted therapy of both mTORC1 and mTORC2 (95). In addition, some second generation mTOR inhibitors also block PI3K catalytic activity as a result of the high structural homology and sequence identity in their ATP binding domains (93, 150).

Dual PI3K/mTOR inhibitors efficiently blocked AKT activation and reduced cancer cell proliferation, generally through a G_1 cell cycle arrest, although an increase in

apoptosis has been reported; in addition, treatment with dual inhibitors attenuated xenograft growth *in vivo* (151-160). Blockade of the PI3K/mTOR pathway via the use of dual inhibitors enhanced or restored sensitivity to chemotherapy, radiation therapy, or other targeted therapies (161-173). These preclinical data and safety profiles have promoted the evaluation of several dual PI3K/mTOR inhibitors in early stage clinical trials both alone and in combination with chemotherapy or other targeted agents (174-180).

Although dual PI3K/mTOR inhibitors display strong anti-cancer effects in preclinical and clinical settings, adaptive resistance through alternative pathway activation and upregulation of RTK activity has been reported following treatment (61, 71, 144, 148, 181, 182). One potential resistance mechanism involves insulin-like growth factor 1 receptor (IGF1R). Increased expression and activation of IGF1R was noted in matrix-attached ovarian cancer cells treated with the dual PI3K/mTOR inhibitor BEZ235; shRNA-mediated knockdown of IGF1R restored sensitivity to PI3K/mTOR inhibition (145). In addition, targeted AKT inhibition induced IGF1R expression and activation through the activation of the FOXO transcription factor family and the suppression of S6K activity (142). Furthermore, synergistic proapoptotic and anti-tumorigenic effects were observed in models of hepatocellular carcinoma treated with the combination of PI3K/mTOR pathway inhibitors RAD001 (against mTOR), MK2206 (against AKT), and BEZ235 (against PI3K and mTOR) with the IGF1R-targeting agent AEW541 (167). Taken together, these data indicate that a vertical blockade combining pharmacologic blockade of PI3K/mTOR pathway with targeted IGF1R inhibition would prevent resistance to single agent therapy and yield a superior therapeutic benefit.

1.4 Insulin-like growth factor 1 receptor (IGF1R) signaling

IGF1R is a tetrameric receptor tyrosine kinase composed of two half-receptors, each containing an extracellular ligand-binding α-subunit and an intracellular β-subunit, which is further divided into the transmembrane and catalytic domains (Figure 3). The insulin receptor (IR) is similarly composed and highly homologous to IGF1R, with 84% sequence identity in the kinase domain and 95% sequence identity in the ATP-binding domain (183, 184). Furthermore, hybrid receptors consisting of one IGF1R half-receptor and one IR half-receptor have been reported in cells that express both receptors (185, 186). The extracellular domains of IGF1R can bind one of three ligands: insulin-like growth factor 1 (IGF1), IGF2, or insulin. The sequence homology between IGF1 and IGF2 is 62%, while the homology between the IGFs and insulin in 42% (187).

IGF1R preferentially binds IGF1 and binds IGF2 and insulin with a 5-10 and 100 fold lower affinities, respectively (188). Ligand binding to the extracellular domains of IGF1R results in a conformational change and subsequent autophosphorylation of tyrosine residues 1131, 1135, and 1136 in the intracellular catalytic domain. These events promote the phosphorylation of juxtamembrane tyrosines and C-terminus serines, resulting in docking sites which recruit adaptor proteins to the receptor (189-191). These proteins, such as IRS1-4 (IR substrate 1-4) or SHC (Src homology/collagen domain protein), activate signaling through the PI3K/mTOR or mitogen-activated protein kinase (MAPK) pathways. Signaling transduction through IGF1R and its downstream pathways results in cell growth, proliferation, metabolism, and survival; furthermore, IGF1R regulates migration, invasion, adhesion, and angiogenesis (191, 192).

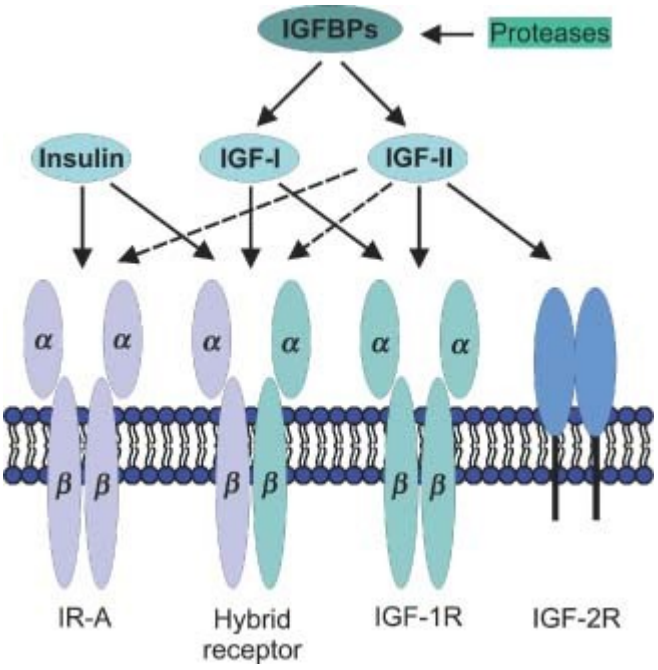

Figure 3. The components of the IGF system. IGF-I, IGF-II and insulin interact with their cognate receptors as indicated. IGF-II has a high affinity for the insulin receptor isoform A (IR-A) but not for IR-B. IGF-1R and insulin receptor isoforms can form heterodimers, called hybrid receptors. The function of IGF-I and IGF-II is modulated by IGF binding proteins (IGFBP-1–6), which in their turn are subjected to cleavage by proteases.

Reprinted with permission from [The insulin-like growth factor system and sarcomas/ B Rikhof, S de Jong, AJH Suurmeijer, C Meijer and WTA van der Graaf/The Journal of Pathology, Volume 217, Issue 4. Copyright (c) [2008] [Pathological Society of Great Britain and Ireland] (190).

Tumorigenic role of IGF1R

IGF1R is critical for malignant transformation by several oncogenes; furthermore, IGF1R signaling facilitates cancer cell proliferation and survival, angiogenesis, and metastasis through the activation of PI3K/mTOR and other downstream pathways (188, 191, 193-196). Cancer-specific amplifications of or mutations in IGF1R are rare; rather, the main route of IGF1R dysregulation in tumorigenesis is aberrant activation due to increased expression and/or the development of autocrine or paracrine signaling loops (191, 196). Moreover, overexpression and/or activation of IGF1R have been reported in cancer cells previously treated with inhibitors of the PI3K/mTOR pathway, indicating that receptor activity can also circumvent targeted therapy (142, 145, 197).

In addition, IGF1R has been identified as a molecular prognosticator in numerous cancers, including STS. High IGF1R expression is linked to tumor aggressiveness and poor metastasis-free survival in myxoid liposarcoma and synovial sarcoma (198, 199). Similarly, IGF1R expression inversely correlated with overall survival in MPNST and rhabdomyosarcoma (133, 200, 201). In addition, IGF1R expression could distinguish between low, intermediate, and high grade disease in multiple STS subtypes, including UPS, with increasing levels of IGF1R corresponding to higher grade lesions (202).

Targeted therapy against IGF1R

In addition to identifying IGF1R as an important regulator of several tumorigenic processes, preclinical studies also linked IGF1R activity with resistance to therapy

(189, 196, 203-207). Therefore several anti-IGF1R monoclonal antibodies (mAbs) and small molecule inhibitors were developed (192, 208). mAbs against IGF1R or its ligands function to prevent growth factor binding and subsequent signal transmission to downstream pathways (mainly PI3K/mTOR) as well as to increase the rate of receptor internalization, reducing the number of receptors on the cell surface, while small molecule inhibitors block the ATP binding site of the receptor's tyrosine kinase domain (209). Small molecule inhibitors are generally less specific than mAbs, due to the high homology between IGF1R and IR; however, some small molecule inhibitors show selectivity towards IGF1R (209-212).

Several clinical trials evaluating IGF1R mAbs as single agent or in combination with cisplatin or targeted chemotherapies were discontinued due to lack of efficacy, with one Phase II trial reporting poorer overall patient survival in the treatment arm (213-215). The failure of these trials to result in any anti-tumor effects could be attributed to increased IR signaling. While targeting of IGF1R reduces the number of IGF1R homodimers and hybrid IGF1R:IR heterodimers through receptor internalization, IR homodimers are unaffected and expression has been reported to increase in response to therapy, which would attenuate the response to mAb-mediated IGF1R inhibition (213). In addition, the use of IGF1R mAbs has been linked to dysregulated endocrine signaling through increased growth hormone levels which promotes IR activation through increased IGF1 and insulin production (191, 208).

The disappointing results of initial clinical trials have highlighted the need to identify predictive biomarkers to discern patient populations that could benefit from this type of therapy (208, 214, 216). Furthermore, IGF1R-targeted therapy development has begun to exploit the role of IGF1R as a mediator of chemoresistance. Several preclinical

studies and clinical trials have evaluated combination therapy with an IGF1R inhibitor and cytotoxic chemotherapy or other targeted agent (167, 217-222). Furthermore, the identification of potential resistance mechanisms to IGF1R-targeted therapy is prompting the evaluation of novel combinations for their anti-tumor efficacy. The combination of anti-IGF1R mAbs with rapalogues has been investigated in Phase I clinical trials in patients with advanced solid tumors, with some antitumor responses reported (216, 223-225); however, additional clinical studies of the anticancer efficacy of combined inhibition of IGF1R and other components of the PI3K/mTOR pathway have yet to be conducted.

1.5 Hypothesis and specific aims

In summary, UPS is a karyotypically complex STS subtype with no discernible line of differentiation, nor any specific recurring genetic aberrations (31). The absence of consistent genomic abnormalities in UPS has hindered the identification and evaluation of potential therapeutic targets. Furthermore, the moderate response of UPS patients to available therapeutic options is reflected in the current five-year overall survival rate of only 65-70%, highlighting the crucial need to identify and evaluate targeted therapies for their efficacy (4, 5). Previous studies have revealed that active PI3K/mTOR signaling denotes a worse prognosis for STS patients (131). Our lab has further shown that 20% evaluated UPS patient samples expressed high levels of phosphorylated AKT, which correlated to a poorer patient outcome (135). These findings indicate that the PI3K/mTOR pathway may be a driver of UPS tumorigenesis and thus represents a potential therapeutic target. However, IGF1R activation has been reported in response to PI3K/mTOR inhibition, suggesting a potential mechanism of adaptive resistance (142, 145).

Therefore, I hypothesize that dysregulation of the PI3K/mTOR signaling axis contributes to the aggressive nature of UPS and targeting specific components of this pathway will have anti-tumorigenic effects; furthermore, combining targeted therapy against PI3K/mTOR and IGF1R will yield a greater therapeutic benefit.

To pursue this hypothesis, I developed the following specific aims:

- **Specific Aim 1:** Determine the activation status of the PI3K/mTOR signaling cascade in UPS tumors and cell lines and investigate prognostic significance.
- **Specific Aim 2:** Examine the consequences of therapeutic blockade of PI3K/mTOR pathway components on the tumorigenic characteristics of UPS cells.
- **Specific Aim 3:** Evaluate the efficacy of PI3K/mTOR inhibition in combination with targeted therapy against IGF1R to yield synergistic anti-tumorigenic effects.

Chapter 2

Materials and Methods

Immunohistochemical and statistical analysis of UPS tissue microarrays (TMAs)

A previously constructed TMA comprised of sporadic-UPS tissue samples was utilized for immunohistochemical analysis (n = 173); an additional TMA of RA-UPS samples (n = 35) was developed as previously described and was included for analysis (135). All samples evaluated were derived from primary tumors. Immunohistochemistry for pAKT, AKT, pS6RP, S6RP, and p4EBP1 was performed by the histology core facility at The Virginia Harris Cockrell Cancer Research Center at Science Park histology core (Smithville, TX, USA). Immunohistochemistry for MET, cyclin D1, pEGFR, IGF1R, c-KIT, PDGFRα, and PDGFRβ was performed by the MD Anderson Cancer Center Clinical and Research Core facilities. Immunostaining for pIGF1R, pMEK, MEK, pMET, and AXL was conducted in our laboratory as follows. Formalin-fixed, paraffin-embedded tumor specimens were cut into 4µm sections, which were deparaffinized in xylene and rehydrated using a graded ethanol series. Sections were subjected to antigen retrieval at 100℃ for 45 minutes in Tris-EDTA, pH 8 and endogenous peroxidase blocking in 3% H2O2 in PBS for 12 minutes. Primary antibody incubation took place at 4℃ overnight using pIGF1R rabbit monoclonal antibody #3024 diluted 1:25, pMEK rabbit monoclonal antibody #2338 diluted 1:50, MEK rabbit

polyclonal primary antibody #9122 diluted 1:50, pMET rabbit monoclonal antibody #3077 diluted 1:100, or AXL rabbit monoclonal antibody #4566 diluted 1:100 (Cell Signaling Technology). Primary antibody was visualized using the 4plus two-step HRP detection system (Biocare Medical) and diaminobenzidine. Sections were counterstained with hematoxylin and mounted with Permount (Fisher).

The percentage of tumor cells expressing the marker was recorded. Cyclin D1 revealed a nuclear localization while pAKT, AKT, p4EBP1, and 4EBP1 showed both cytoplasmic and nuclear staining. All other markers exhibited cytoplasmic localization. For cyclin D1, AXL, c-KIT, pEGFR, IGF1R, PTEN, pS6RP, and p4EBP1, samples were considered positive if ≥ 10% of cells were stained. For pMET, pIGF1R, pAKT, AKT, and S6RP, samples were analyzed as 2 groups: negative/low (≤60% of cells positive for stain) and high (>60% of cells positive). A regularly updated prospective database was available for retrieval of clinicopathologic variables (age, sex, disease setting, and tumor size [diameter in cm]) pertaining to UPS patient samples.

Mann-Whitney and Fisher's exact tests were utilized to evaluate protein expression differences between sporadic UPS and RA-UPS. Correlations between protein markers were determined by Spearman's rank correlation coefficient. Survival times were estimated by Kaplan-Meier curves. Multivariate Cox regression models were constructed to assess associations between protein expression and survival outcome adjusting for clinical covariates. To construct the most parsimonious models, variables in univariate analysis at $p < 0.10$ were fitted in multivariate models. Overall survival (OS) time was measured from date of diagnosis by pathological confirmation to date of death of any cause or last day of follow-up and disease-specific survival (DSS) was measured to date of sarcoma-related death or last day of follow-up. p values <0.05

were considered statistically significant unless otherwise indicated. All analyses were performed using SPSS version 21. Kaplan-Meier curves were constructed using GraphPad Prism, version 6.05.

UPS cell isolation and tissue cultures

The isolation of UPS cells from patient tumor samples was conducted by our laboratory with the approval of the Institutional Review Board at The University of Texas MD Anderson Cancer Center (UTMDACC) and patients' written informed consent. Surgical specimens were obtained from 5 patients who presented at UTMDACC from July 2010 to November 2011. RIS-DL-620, UPS-186, and UPS-DL-511 were isolated as previously described (226), while RIS-819.1 and UPS-DL-271.1 were isolated from patient surgical specimens serially passaged in hairless severe combined immunodeficient (SCID) mice. The clinical characteristics of these bioresources are detailed in Table 1. In brief, fresh sterile samples from surgically resected tumors were minced in 1x PBS and then digested via incubation with collagenase type I (3%), DNase I (0.02%), and hyaluronidase (1.5 mg/ml) at 37 °C for 2–4 h. The sample was strained through a wire mesh screen, and undigested tissue was discarded. After centrifugation, washes, and resuspension in PBS, the sample was gently transferred to Histopaque tubes containing 10 ml Histopaque (100%; Sigma) overlayed with 15 ml of Histopaque (75%). The tubes were then centrifuged at 40 °C for 30 min at 1200 *g*. After centrifugation, tumor cells located in the top interface (over 75% Histopaque) were collected and plated. Cells were cultured and passaged in DMEM supplemented with 10% FBS and 1% penicillin/streptomycin. UPS-186 and RIS-819.1 were passaged more than 40 times and considered cell lines. UPS cell strains and cell lines were validated by STR DNA fingerprinting using the Promega 16 High Sensitivity

STR Kit (Catalog # DC2100). The STR profiles were compared to online search databases (DSMZ/ATCC/JCRB/RIKEN) of 2455 known profiles; along with the MD Anderson Characterized Cell Line Core (CCLC) database of 2556 know profiles. The STR profiles of cell strains and cell lines matched originating tumor DNA fingerprints. STR-confirmed cell strains and cell lines were deposited in an in-house cell bank and were pulled every 9-12 months for experimental use to ensure low passage numbers and no cross-contamination. The results of STR fingerprinting are presented in Table 2.

Bone-derived human mesenchymal stem cells were purchased from PromoCell (cat# C-12974) and maintained in Mesenchymal Stem Cell Growth Medium (PromoCell, cat# C-28010).

Drugs and vehicles

XL765 was provided by Sanofi-Aventis as part of a collaboration. BGT226 (NVP-BGT226, cat# S2749) and AEW541 (NVP-AEW541, cat# S1034) were purchased from Selleck Chemicals. All drugs were resuspended as stock concentrations in DMSO for *in vitro* applications. For *in vivo* administration, XL765 was resuspended in water and 10 mM HCl. BGT226 was resuspended in N-Methyl-2-pyrrolidone (NMP) and this stock solution was stable at 4℃ for 1 week. Immediately prior to administration, the NMP/BGT226 stock solution was diluted in PEG300 (10% NMP/BGT226 plus 90% PEG300). AEW541 was solubilized in 25 mM L(+)-tartaric acid for use in mice.

Cell proliferation assay

Cell proliferation was evaluated using CellTiter 96 AQueous One Solution Cell Proliferation Assay (3-(4,5-dimethylthiazol-2-yl)-5-(3-carboxymethoxyphenyl)-2-(4-sulfophenyl)-2H-tetrazolium, inner salt; MTS) (Promega, cat# G3580) according to the

manufacturer's instructions. For MTS experiments requiring stimulation with recombinant IGF1 (R&D Systems, cat# 291-G1-200), cells were incubated with half the total volume of DMEM-10% FBS with or without 2x concentrated dose(s) of drug(s) 24 hours after seeding. After 2 hours, the remaining media containing 40 ng/mL recombinant IGF1 was added to the wells (final concentration: 20 ng/mL IGF1, 1x concentrated drug).

Evaluation of drug synergism

The potential synergistic drug interactions between BGT226 and AEW541 were analyzed by the Chou-Talalay method for drug combination (227). MTS assays were used to quantify cell viability after 96 hours of treatment and cell proliferation relative to the DMSO + recombinant IGF1 control was calculated. Drug concentrations along with the corresponding drug effects (drug effect = 1 – relative cell proliferation) were entered into the CompuSyn software (Version 1.0) and combination index (CI) values were obtained. A CI value <1 indicates drug synergy; values near 1 designates additivity and those >1 are indicative of antagonism. Heat maps displaying CI values and %drug effects obtained from each combination were generated using Microsoft Excel (Microsoft, Redmond, WA).

Preparation of whole cell lysates and immunoblotting

UPS cell lysates were made by scraping cells in whole cell lysis buffer (10% glycerol, 1% NP-40, 50 mM TrisCl, 150 nM NaCl, 50 mM NaF, 1mM EDTA, 2mM PMSF, 1 mM Na3VO4, plus protease inhibitor [Roche cat# 11 697 498 001] and phosphastase inhibitor cocktails #2 and #3 [Sigma cat# P5726 and P0044]). For assessment of drug treatment on protein expression, cells were incubated with drug for the indicated time

point and immediately harvested. For AEW541 and combination treatments, cells were incubated with or without drug for 2 hours, stimulated with 20 ng/mL recombinant IGF1 for 15 minutes, and harvested in whole cell lysis buffer.

Standard protocols for western blot analysis were followed. Commercially available antibodies were used for detection of PI3K/mTOR and MAPK pathway components: AKT (cat# 9272), pAKT S473 (#9271), S6K (#9202), pS6K T389 (#9206), 4EBP1 (#9452), p4EBP1 T37/46 (#2855), ERK (#9102), pERK T202/T204 (#9106), pMEK1/2 S221 (#2338), IGF1R (#3018), and pIGF1Rβ Y1135/1136/insulin receptor β Y1150/1151 (#3024) (Cell Signaling Technology). Antibodies against p-p27 T157 (cat# AF1555) and p-p27 T198 (cat# AF3994) were obtained from R&D Systems and anti-p27 (cat# sc-1641) and anti-β-actin-HRP (cat# sc-47778) were purchased from Santa Cruz Biotechnology.

Reverse phase protein array (RPPA)

One sporadic UPS cell line and one RA-UPS cell line were exposed to 5 μM XL765 for 48 hours prior to harvest. RPPA protein expression profiles were generated by the RPPA Core Facility at UTMDACC using standard procedures (228). Protein dilution curves were fitted with the Supercurve fitting logistical model and RPPA data were normalized to loading controls. Normalized data were transformed by $\log_2$ and used for further analyses. Heat maps displaying the linear ratio of the protein expression of XL765-treated cells by that of untreated control cells were created in Microsoft Excel.

Cell cycle and apoptosis assays

Cell cycle distribution was determined by propidium iodine-fluorescence associated cell sorting (PI-FACS) analysis. Cells were treated with the indicated inhibitor for 48

hours, then fixed in 70% ethanol. Fixed cells were resuspended in a PI staining solution containing 75 µg/mL PI and 10 µg/mL RNase A. Apoptosis was measured in UPS cells after 96 hours of treatment using the Apoptosis Detection Kit I (BD Biosciences cat# 556547) according to the manufacturer's instructions. Cells in both early and late stages of apoptosis were reported as total apoptosis. Cell cycle and apoptosis were analyzed in a Gallios Flow Cytometer (Beckman Coulter) located in the Flow Cytometry and Cellular Imaging Core at MDACC. Data from these experiments were analyzed using the Multicycle Program in FCS Express (De Novo Software).

Assessment of in vitro *migration and invasion*

In vitro cell migration and invasion was assessed via modified Boyden chamber assays. For migration analysis, 2.5 x 104 cells were resuspended in low-serum (1% FBS) DMEM/F12 and seeded into the upper compartment of each BD BioCoat Control Insert (cat# 354578). For invasion assays, cell number was increased to 5.0 x 104 and cells were seeded in BD BioCoat Matrigel Invasion Chambers (cat# 354480). DMEM/F12 supplemented with 5% FBS served as the chemoattractant in the lower compartment. In assays interrogating the effects of PI3K/mTOR or IGF1R inhibition, drug(s) were added to both the upper and lower compartment of the chamber at the indicated concentrations. For experiments with AEW541 or combination treatment, the lower chamber included 100 ng/mL recombinant IGF1 as an additional chemoattractant. After a 16 hour incubation at 37℃, cells were fixed with 10% glutaraldehyde and stained with 0.2% crystal violet in 20% methanol. Chambers were photographed at 20x magnification, with 5 images showing different fields of view taken for each chamber. Migratory cells were quantified using ImageJ 1.47V software

(http://rsbweb.nih.gov/ij/index.html) and invasive cells were counted manually (84, 229, 230).

In vivo *tumor studies*

All animal procedures were approved by the Institutional Animal Care and Usage Committee (IACUC) at UTMDACC. Six-week old female hairless SCID mice (Charles River Laboratory, Strain Code 488) were implanted in the flank with 2-3 mm pieces of RIS-819.1 tumor. Therapeutic interventions began when tumors reached an average volume of 100 mm^3 in each group. BGT226 and AEW541 were administered daily (5 days/week unless otherwise indicated) via oral gavage. When tumors in the vehicle arm reached a maximum volume of 1500 mm^3, all animals were euthanized.

Immunohistochemical analysis of xenografts

Xenograft-derived specimens were analyzed for PI3K/mTOR signaling activity through IHC for pAKT, pS6RP, and p4EBP1 by the histology core facility at the MD Anderson Cancer Center at Science Park. These tissues were further interrogated by immunostaining for Ki67 (cell proliferation marker) and cleaved caspase 3 (CC3; apoptosis marker), which was performed by the MD Anderson Cancer Center Clinical and Research Core facilities. IHC for pIGF1R was conducted in our laboratory as described above.

Nuclear and cytoplasmic fractionation

RIS-819.1 cells were treated with 1 μM AEW541, 25 nM BGT226, or a combination of the two drugs in low serum (1% FBS) DMEM/F12 for 16 hours. Following treatment, nuclear and cytoplasmic fractions were isolated using the NE-PER Cytoplasmic and Nuclear Extraction Reagents (Pierce, cat#7833) per the manufacturer's instructions. Lamin A/C (Santa Cruz, cat# sc-6215) and α-tubulin (Santa Cruz, cat# sc-5286) were used as nuclear and cytoplasmic purity controls, respectively. Densitometric quantification of protein expression was performed with ImageJ 1.47V software (http://rsbweb.nih.gov/ij/index.html).

Assessment of RhoA activity

UPS cells were grown to 70-80% confluency and serum starved (1% FBS in DMEM/F12) for 16 hours. After stimulation with 5% FBS and 100 ng/mL IGF1 for 60 seconds, cells were immediately lysed. RhoA activity was detected using the G-LISA RhoA Activation Assay (Cytoskeleton, Inc., cat# BK124) per the manufacturers' instructions.

Statistical analysis of in vitro *and* in vivo *experiments*

Data are presented as the mean +/- the standard error of the mean (SEM). Each experiment was repeated in triplicate unless otherwise indicated in the figure legend. The Student's t-test was used to evaluate statistically significant differences between experiment groups. p values were considered statistically significant when $p < 0.05$.

Table 1. Clinical characteristics of cell strains and cell lines generated from UPS patient tumors

Designation	Patient age	Patient sex	Tumor type	Site	Disease setting
RIS-620	50	F	Recurrent	Chest	Radiation-associated
RIS-819.1	46	F	Primary	Chest	Radiation-associated
UPS-186	46	F	Metastasis	Buttock	Sporadic
UPS-271.1	60	M	Recurrent	Thigh	Sporadic
UPS-511	73	M	Recurrent	Chest	Sporadic

Table 2. UPS cell strain and cell line DNA fingerprinting results*

Tumor and cell strain/line	AMEL	CSF1PO	D13S317	D16S539	D5S818	D7S820	TH01	TPOX	vWA
RIS-620 tumor	X	12	11,12	9,11	9,10	8	7,9	8,11	17,18
RIS-620 cell strain	X	12	11,12	9,11	9,10	8	7,9	8,11	17,18
RIS-819 tumor	X	11,12	10,14	11,13	11,13	10,12	7,9	10,11	17
RIS-819.1 cell line	X	11,12	14	11	11,13	10,12	7,9	10,11	17
UPS-186 tumor	X	10	11,12	11	11,12	10,11	6,7	8,10	17,18
UPS-186 cell line	X	10	11	11	12	10,11	7	10	18
UPS-271 tumor	X,Y	10,11	8,13	13	10,11	10,11	6,7,9.3	8,11	18,19
UPS-271.1 cell strain	X,Y	10,11	8,13	13	10,11	10,11	6,7,9.3	8,11	18,19
UPS-511 tumor	X,Y	12	8,13	11,12	10,11	8,12,13	6,9.3	8,10	15,17
UPS-511 cell strain	X	12	8	11	10,11	8,13	6	8,10	17

*As per HIPPA regulations and Institutional policy not all markers are provided. Marker selection followed ATCC database reporting.

Chapter 3

PI3K/mTOR signaling is active in UPS patient samples.

A previous study by our research group revealed that 20% of sporadic UPS patient samples examined harbored high levels of phosphorylated AKT (pAKT) and that increased expression significantly correlated with disease-specific survival (DSS) in a multivariate model. In our study, we utilized two UPS TMAs comprising 173 sporadic and 35 RA-UPS samples to interrogate PI3K/mTOR pathway activity through the expression of downstream effectors S6 ribosomal protein (S6RP; a surrogate for S6K activity) and 4EBP1; a downstream transcriptional target, cyclin D1; and the tumor suppressor PTEN, a negative regulator of PI3K activity. AKT expression was again evaluated in these TMAs to maintain consistency with the inclusion of the newly constructed TMA as well as to accommodate the longer follow-up period in the previously utilized microarray. We also determined the expression level of AXL and c-KIT as well as the levels of total and phosphorylated EGFR (epidermal growth factor receptor), IGF1R, MET, and platelet-derived growth factor receptors A and B (PDGFRA/B), as these upstream RTKs can stimulate PI3K/mTOR signaling. Finally, we determined total and active MEK (mitogen-activated protein kinase kinase) expression

to indicate activation of the MAPK (mitogen-activated protein kinase) pathway, which is dysregulated in numerous cancer types and also can be activated in response to PI3K/mTOR inhibition (231).

Tumor and patient characteristics are summarized in Table 3. The total cohort consisted of 208 patients with a median age of 64 years old. All 208 samples were obtained from primary/index tumors. The majority of tumors were high grade (76%), located in the extremity (73%), and superficial (87%). Nearly one-third (31%) of patients received chemotherapy, while 57% of patients were treated with radiation. The majority of resection margins (70%) were negative.

Protein marker expression can vary based on disease setting

The majority of the biomarkers of interest (16/21, 76%) were able to be evaluated in survival analysis. Homogenous expression of MET, PDGFRA, PDGFRB, and total and phosphorylated MEK, was detected at high levels (>80% of cells strongly positive) in all samples; therefore, these stains could not be stratified in univariate or multivariate analysis (data not shown). The expression of evaluable protein markers for the entire cohort, both combined and divided into disease settings (sporadic UPS and RA-UPS), is summarized in Table 4. Positive expression (≥10% of cells positive for marker presence) of AXL, pEGFR, and nuclear p4EBP1 was detected in the majority of samples (52%, 74%, and 80% of samples, respectively). In addition, high expression (>60% of cells positive) of nuclear pAKT and total S6RP was noted in 53% and 76% of tumors, respectively. PTEN was expressed in most samples (96.0%), with only 10 samples exhibiting a loss. Interestingly, we noted that the expression of some markers varied significantly depending on disease setting (sporadic versus radiation-associated

UPS). A higher percentage of sporadic UPS samples were positive for pEGFR than RA-UPS (81% versus 45%, $p < 0.001$). Excitingly, more RA-UPS samples were positive for IGF1R (53% versus 25% of sporadic samples, $p = 0.003$); furthermore, 80% of RA-UPS samples exhibit high pIGF1R staining compared with only 29% of sporadic UPS samples ($p < 0.001$).

Table 3. Tumor and patient characteristics

Variable	Sporadic	Radiation-Associated	Entire Cohort
n	173 (83.2%)	35 (16.8%)	208 (100.0%)
Age			
Median (range)	65.0 (22-87)	62.0 (17-87)	64.0 (17-87)
Tumor size, cm			
Median (range)	8.0 (1.0-35.0)	6.0 (0.9-30.0)	7.5 (0.9-35.0)
Grade			
Low	4 (2.3%)	2 (5.7%)	6 (2.8%)
Intermediate	38 (21.9%)	0 (0.0%)	38 (18.2%)
High	130 (75.1%)	27 (77.1%)	157 (75.5%)
Unknown	1 (0.6%)	6 (17.1%)	7 (3.4%)
Location			
Head & neck	0 (0.0%)	6 (17.1%)	6 (2.9%)
Trunk	12 (6.9%)	13 (37.1%)	25 (12.0%)
Extremity	143 (82.7%)	9 (25.7%)	152 (73.1%)
Retroperitoneum	18 (10.4%)	7 (20.0%)	25 (12.0%)
Depth			
Deep to investing fascia	25 (14.5%)	3 (8.6%)	28 (13.5%)
Superficial	148 (85.5%)	32 (91.4%)	180 (86.5%)
Therapy received			
Chemotherapy	57 (32.9%)	8 (22.9%)	65 (31.2%)
Radiation	99 (57.2%)	19 (54.3%)	118 (56.7%)
Resection Margins			
R0	119 (68.8%)	26 (74.3%)	145 (69.7%)
R1	51 (29.5%)	6 (17.1%)	57 (27.4%)
R2	1 (0.6%)	2 (5.7%)	3 (1.4%)
Unknown	2 (1.2%)	1 (2.9%)	3 (1.4%)

Table 4. Protein expression by disease setting

	Total			Sporadic			Radiation-Associate	
	n	**Negative**	**Positive**	***n***	**Negative**	**Positive**[◊]	***n***	**Negative**
Cyclin D1	167	56.8%	43.1%	137	58.4%	41.6%	30	50.0%
AXL	136	47.8%	52.2%	114	50.0%	50.0%	22	36.4%
c-KIT	172	88.4%	11.6%	141	87.2%	12.8%	31	93.5%
pEGFR	162	25.9%	74.1%	131	19.1%	80.9%	31	54.8%
IGF1R	150	69.3%	30.7%	120	75.0%	25.0%	30	46.7%
PTEN	175	4.0%	96.0%	144	3.5%	96.5%	31	6.5%
pS6RP	173	63.0%	37.0%	142	63.4%	36.6%	31	61.3%
p4EBP1 *(Cytoplasmic)*	169	55.6%	44.4%	140	57.1%	42.9%	29	48.3%
p4EBP1 *(Nuclear)*	49	20.4%	79.6%	48	20.8%	79.2%	1	0.0%
	N	**Negative-low**	**High**	**N**	**Negative-low**	**High**[**]	**N**	**Negative-low**
pIGF1R	116	57.8%	42.2%	86	70.9%	29.1%	30	20.0%
pMET	64	85.9%	14.1%	35	91.4%	8.6%	29	79.3%
pAKT *(Cytoplasmic)*	163	63.8%	36.2%	134	66.4%	33.6%	29	51.7%
pAKT *(Nuclear)*	163	46.6%	53.4%	134	46.3%	53.7%	29	48.3%
AKT *(Cytoplasmic)*	157	62.4%	37.6%	127	63.8%	36.2%	30	56.7%
AKT *(Nuclear)*	157	64.3%	35.7%	127	67.7%	32.3%	30	50.0%
S6RP	170	24.1%	75.9%	139	25.9%	74.1%	31	16.1%

*Significant at level of $p < 0.05$

[◊]Samples were considered positive if there was labeling present in ≥ 10% of cells.

[**]Samples were considered to have high expression if there was labeling in >60% of cells.

The PI3K/mTOR pathway is active in a subset of UPS patient samples

In order to determine whether the PI3K/mTOR signaling cascade is activated, we correlated the expression of active pathway components using a Spearman's correlation. Positive correlation coefficients obtained when pAKT, pS6RP, and p4EBP1 staining patterns (both cytoplasmic and nuclear) were examined indicated that the PI3K/mTOR signaling cascade is active in UPS samples regardless of disease setting; in addition, these correlations were strongly significant (Figure 4). As expected, PTEN expression negatively correlated with all downstream effectors examined. Expression of pIGF1R and pMET positively correlated with one another, while both negatively

correlated with pEGFR. Active IGF1R expression weakly correlated with cytoplasmic pAKT and pS6RP, while pEGFR significantly correlated with pS6RP and cytoplasmic p4EBP1.

Several protein markers can predict OS and DSS for UPS patients

The follow-up period for patients ranged from 0.8 to 20.75 years. The median overall survival (OS) was 8.5 years, with a 5-year survival estimate of 55% (Figure 5A). The 5-year DSS was 63% (Figure 5B). A univariate Cox proportional hazard ratio model determined that age (<61 years old), disease setting (sporadic), tumor size (<10 cm in diameter), and margins (negative) were significant prognosticators of both OS and DSS (OS: hazard ratio [HR] 0.36, 0.44, 0.51, and 0.61, $p < 0.001$, <0.001, 0.001, and 0.016; DSS: HR 0.41, 0.37, 0.48, and 0.62, $p = 0.001$, <0.001, 0.002, and 0.051, respectively) (Table 5).

Figure 4. Correlation of the expression of PI3K/mTOR pathway components and upstream RTKs from TMA samples. A heat map was generated using Spearman's correlation coefficients obtained from the correlation between the expression of PI3K/mTOR signaling components and/or upstream RTKs. C = cytoplasmic stain, N = nuclear stain. Gold indicates a positive correlation, while blue indicates a negative correlation. Bold values = $p < 0.05$; bold and italicized values = $p < 0.01$; bold and italicized values surrounded by a bold box = $p < 0.001$.

	pEGFR	pIGF1R	pMET	PTEN	pAKT C	pAKT N	pS6RP	p4EBP1 C	p4EBP1 N
pEGFR									
pIGF1R	***-0.341***								
pMET	-0.096	***0.44***							
PTEN	-0.029	0.086	0.23						
pAKT C	-0.023	0.165	-0.052	**-0.178**					
pAKT N	0.043	-0.071	-0.186	-0.139	***0.341***				
pS6RP	***0.301***	0.029	0.057	-0.081	**0.18**	***0.231***			
p4EBP1 C	***0.309***	-0.076	-0.063	-0.143	**0.189**	***0.303***	***0.584***		
p4EBP1 N	0.219	0.107	0.396	-0.163	***0.426***	**0.332**	**0.301**	***0.756***	
pMEK	-0.05	0.001	0.171	-0.115	0.097	0.097	-0.161	0.015	0.265

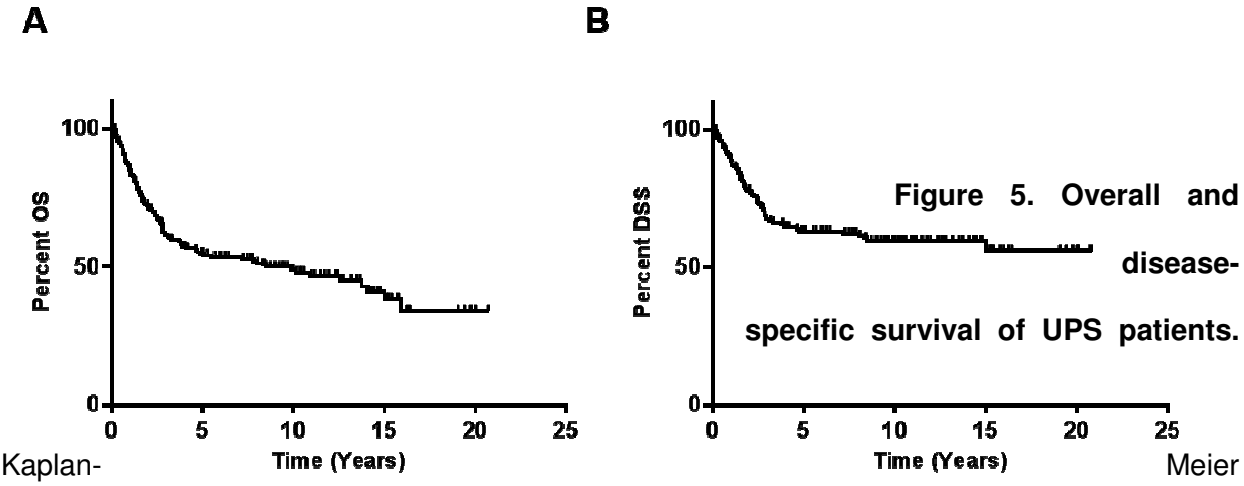

Figure 5. Overall and disease-specific survival of UPS patients. Kaplan-Meier curves depicting (A) OS and (B) DSS of the UPS patient cohort included in TMA analysis.

Table 5. Overall and disease-specific survival analysis including clinical variables

	Overall Survival				Disease-specific Survival			
	Univariable		Multivariable		Univariable		Multivariable	
Covariate, (indicator)	**HR (95% CI)**	***p* value**	**HR (95% CI)**	***p* value**	**HR (95% CI)**	***p* value**	**HR (95% CI)**	***p* value**
Age, (<61) v. ≥ 61	0.36 (0.23-0.57)	<0.001*	0.17 (0.08-0.38)	<0.001*	0.41 (0.24-0.67)	0.001*	0.22 (0.08-0.55)	0.001*
Sex, male v. female	1.13 (0.74-1.69)	0.555			1.21 (0.75-1.98)	0.430		
Setting, sporadic v. RAS	0.44 (0.28-0.69)	<0.001*	0.36 (0.16-0.79)	0.011*	0.37 (0.22-0.63)	<0.001*	0.19 (0.08-0.46)	<0.001*
Size, <10 cm v. ≥ 10 cm	0.51 (0.34-0.76)	0.001*	0.45 (0.24-0.84)	0.012*	0.48 (0.30-0.77)	0.002*	0.33 (0.16-0.71)	0.004*
Depth, superficial v. deep	0.78 (0.43-1.42)	0.415			0.63 (0.29-1.84)	0.253		
Grade, low-intermediate v. high	0.22 (0.31-1.58)	0.132			0.29 (0.04-2.06)	0.285		
Chemotherapy, yes v. no	0.92 (0.59-1.45)	0.732			0.93 (0.55-1.54)	0.763		
Radiation, yes v. no	1.04 (0.70-1.54)	0.830			1.04 (1.18-1.69)	0.851		
Margins, negative v. positive	0.61 (0.40-0.91)	0.016*	0.24 (0.24-0.84)	<0.001*	0.62 (0.38-1.00)	0.051*	0.26 (0.11-0.62)	0.002*
Ki67, negative v. positive	0.75 (0.48-1.19)	0.228			0.90 (0.52-1.56)	0.904		
Cyclin D1, negative v. positive	1.40 (0.89-2.21)	0.145			1.73 (0.98-3.05)	0.060**	1.36 (0.59-3.12)	0.475
CD31, negative-low v. high	1.26 (0.51-3.14)	0.617			1.10 (0.39-3.07)	0.850		
p53, negative v. positive	0.81 (0.52-1.26)	0.350			0.86 (0.51-1.45)	0.562		
AXL *(Cytoplasmic),* negative v. positive	0.66 (0.40-1.06)	0.085**	0.91 (0.46-1.83)	0.797	0.46 (0.25-0.86)	0.015*	0.50 (0.21-1.19)	0.119
AXL *(Nuclear),* negative v. positive	1.36 (0.76-2.41)	0.298			1.50 (0.76-2.96)	0.239		
c-kit, negative v. positive	1.38 (0.66-2.87)	0.391			1.43 (0.57-3.58)	0.447		
pEGFR, negative v. positive	1.81 (1.12-2.91)	0.015*	0.69 (0.35-1.35)	0.278	1.94 (1.09-3.43)	0.023*	0.58 (0.26-1.30)	0.186
pIGF1R, negative-low v. high	0.58 (0.35-0.97)	0.036*	0.92 (0.47-1.76)	0.804	0.49 (0.27-0.90)	0.022*	0.59 (0.27-1.33)	0.208
IGF1R, negative v. positive	0.67 (0.41-1.07)	0.091*	0.87 (0.42-1.79)	0.706	0.65 (0.37-1.13)	0.130		
pMET, negative-low v. high	0.97 (0.38-2.51)	0.955			0.88 (0.30-2.55)	0.814		
PTEN, negative v. positive	7.70 (3.47-17.1)	<0.001*	6.73 (2.48-18.3)	<0.001*	10.3 (4.55-23.4)	<0.001*	20.8 (6.34-68.2)	<0.001*
pAKT *(Cytoplasmic),* negative-low v. high	0.83 (0.53-1.32)	0.434			0.74 (0.43-1.26)	0.261		
pAKT *(Nuclear),* negative-low v. high	0.86 (0.55-1.35)	0.520			1.05 (0.62-1.78)	0.854		
AKT *(Cytoplasmic),* negative-low v. high	1.04 (0.65-1.67)	0.861			1.15 (0.64-2.05)	0.629		
AKT *(Nuclear),* negative-low v. high	0.61 (0.39-0.96)	0.034*	0.78 (0.39-1.54)	0.468	0.83 (0.47-1.45)	0.827		
pS6RP, negative v. positive	1.23 (0.77-1.96)	0.380			1.58 (0.88-2.86)	0.128		
S6RP, negative-low v. high	0.78 (0.46-1.35)	0.379			0.67 (0.35-1.31)	0.241		
p4EBP1 *(Cytoplasmic),* negative v. positive	0.97 (0.62-1.50)	0.879			1.04 (0.61-1.76)	0.890		

*Significant at level of $p < 0.05$
**Significant at level of $p < 0.10$

Furthermore, univariate analysis revealed that better OS and DSS was predicted by negative-low expression of pIGF1R (OS: HR 0.58, $p = 0.036$; DSS: HR 0.49, $p = 0.022$ DSS) and the presence of PTEN (OS: HR 7.70; DSS: HR 10.3, both: $p < 0.001$), while worse survival outcomes were associated with negative pEGFR expression (OS: HR 1.81, $p = 0.015$, DSS: HR 1.94, $p = 0.023$; Figures 6 and 7). Negative-low staining for nuclear AKT was significantly associated with improved OS (HR 0.61, $p = 0.034$). Although not reaching statistical significance at $p < 0.05$, a strong trend revealed that negative-low AXL and IGF1R expression was indicative of better OS (HR 0.66 and 0.67, $p = 0.085$ and 0.091, respectively) and negative expression of cyclin D1, a downstream transcriptional target of the PI3K/mTOR pathway and a key regulator of cell cycle progression through the G_1/S checkpoint, correlated with a less favorable DSS (HR 0.46, $p = 0.060$; Figure 8).

Clinical factors and PTEN loss retain prognostic value in multivariate analysis

Only those markers or clinicopathologic features that were found significant at $p < 0.10$ in univariate analysis were included in multivariate analysis. Age (<61 years old), disease setting (sporadic), tumor size (<10 cm in diameter), margins (negative) and PTEN expression maintained their prognostic value in the multivariate model for both OS and DSS (Table 5). The prognostic value of AXL, cyclin D1, pEGFR, pIGF1R, IGF1R, and nuclear AKT expression was lost in multivariate analysis. Exclusion of clinical variables did not strongly alter these results; all protein markers except PTEN lost their prognostic value in a multivariate model (Table 6). In addition, patients with

high pIGF1R expression had significantly poorer DSS outcomes when *p* was set at 0.1 (HR 0.58, *p* = 0.092).

Table 6. Overall and disease-specific survival analysis excluding clinical variables

	Overall Survival				Disease-specific Survival			
	Univariable		Multivariable		Univariable		Multivariable	
Covariate, (indicator)	**HR (95% CI)**	***p* value**	**HR (95% CI)**	***p* value**	**HR (95% CI)**	***p* value**	**HR (95% CI)**	***p* value**
Ki67, negative v. positive	0.75 (0.48-1.19)	0.228			0.90 (0.52-1.56)	0.904		
Cyclin D1, negative v. positive	1.40 (0.89-2.21)	0.145			1.73 (0.98-3.05)	0.060**	1.04 (0.58-1.87)	0.892
CD31, negative-low v. high	1.26 (0.51-3.14)	0.617			1.10 (0.39-3.07)	0.850		
p53, negative v. positive	0.81 (0.52-1.26)	0.350			0.86 (0.51-1.45)	0.562		
AXL *(Cytoplasmic)*, negative v. positive	0.66 (0.40-1.06)	0.085**	0.77 (0.42-1.43)	0.409	0.46 (0.25-0.86)	0.015*	0.79 (0.43-1.39)	0.395
AXL *(Nuclear)*, negative v. positive	1.36 (0.76-2.41)	0.298			1.50 (0.76-2.96)	0.239		
c-kit, negative v. positive	1.38 (0.66-2.87)	0.391			1.43 (0.57-3.58)	0.447		
pEGFR, negative v. positive	1.81 (1.12-2.91)	0.015*	1.09 (0.57-2.09)	0.800	1.94 (1.09-3.43)	0.023*	1.07 (0.57-2.04)	0.841
pIGF1R, negative-low v. high	0.58 (0.35-0.97)	0.036*	0.72 (0.38-1.35)	0.309	0.49 (0.27-0.90)	0.022*	0.58 (0.31-1.09)	0.092
IGF1R, negative v. positive	0.67 (0.41-1.07)	0.091*	0.91 (0.49-1.71)	0.775	0.65 (0.37-1.13)	0.130		
pMET, negative-low v. high	0.97 (0.38-2.51)	0.955			0.88 (0.30-2.55)	0.814		
PTEN, negative v. positive	7.70 (3.47-17.1)	<0.001*	8.42 (3.15-22.5)	<0.001	10.3 (4.55-23.4)	<0.001*	10.6 (4.05-27.6)	<0.001
pAKT *(Cytoplasmic)*, negative-low v. high	0.83 (0.53-1.32)	0.434			0.74 (0.43-1.26)	0.261		
pAKT *(Nuclear)*, negative-low v. high	0.86 (0.55-1.35)	0.520			1.05 (0.62-1.78)	0.854		
AKT *(Cytoplasmic)*, negative-low v. high	1.04 (0.65-1.67)	0.861			1.15 (0.64-2.05)	0.629		
AKT *(Nuclear)*, negative-low v. high	0.61 (0.39-0.96)	0.034*	0.79 (0.42-1.47)	0.448	0.83 (0.47-1.45)	0.827		
pS6RP, negative v. positive	1.23 (0.77-1.96)	0.380			1.58 (0.88-2.86)	0.128		
S6RP, negative-low v. high	0.78 (0.46-1.35)	0.379			0.67 (0.35-1.31)	0.241		
p4EBP1 *(Cytoplasmic)*, negative v. positive	0.97 (0.62-1.50)	0.879			1.04 (0.61-1.76)	0.890		
p4EBP1 *(Nuclear)*, negative v. positive	0.47 (0.11-2.04)	0.314			0.34 (0.04-2.63)	0.300		

*Significant at level of $p < 0.05$
**Significant at level of $p < 0.10$

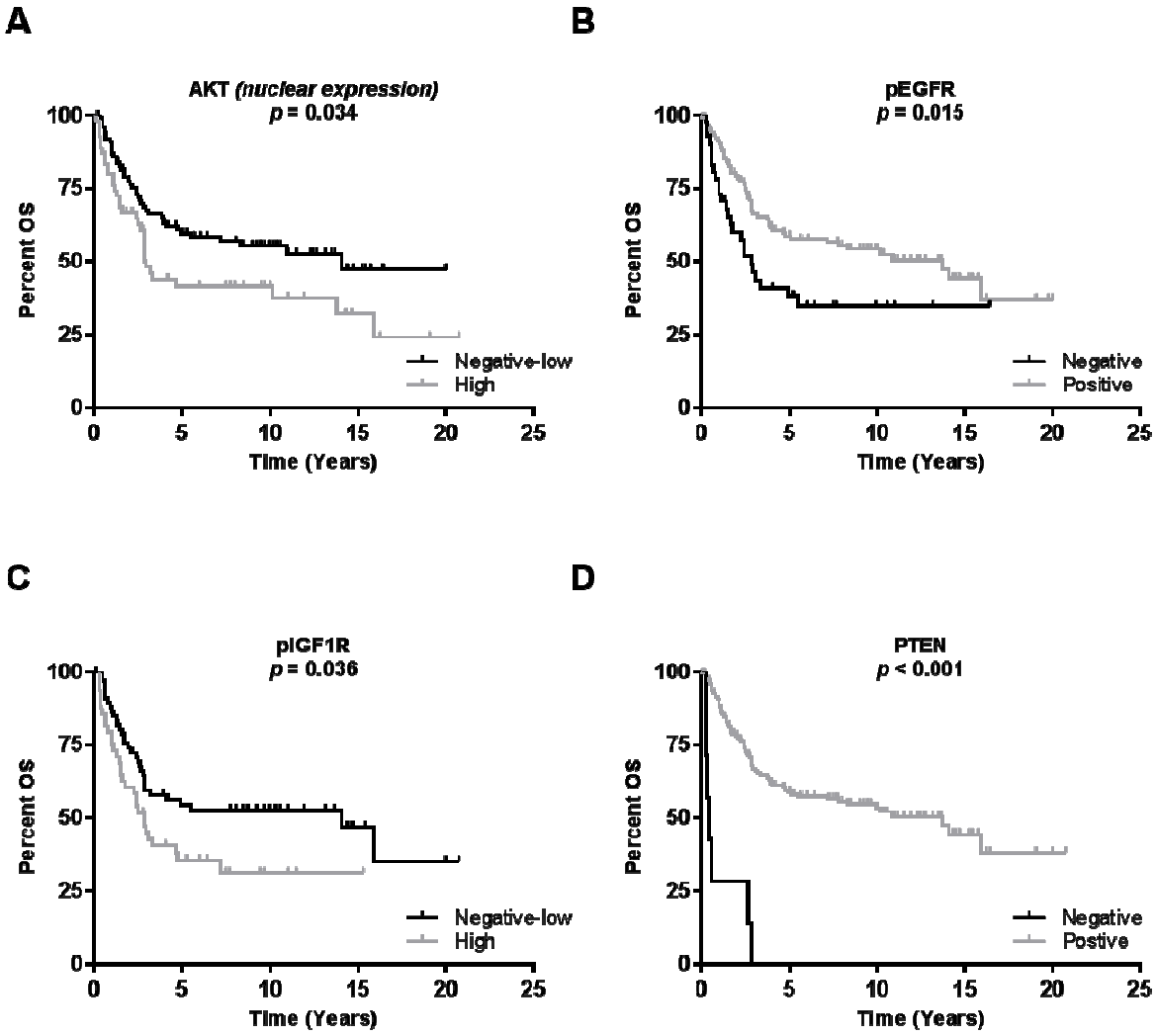

Figure 6. Kaplan-Meier OS curves based on protein marker expression ($p < 0.05$). Primary UPS tumor samples (n = 208) were assessed for (A) nuclear AKT, (B) pEGFR, (C) pIGF1R, and (D) PTEN immunostaining and Kaplan-Meier curves for OS were constructed.

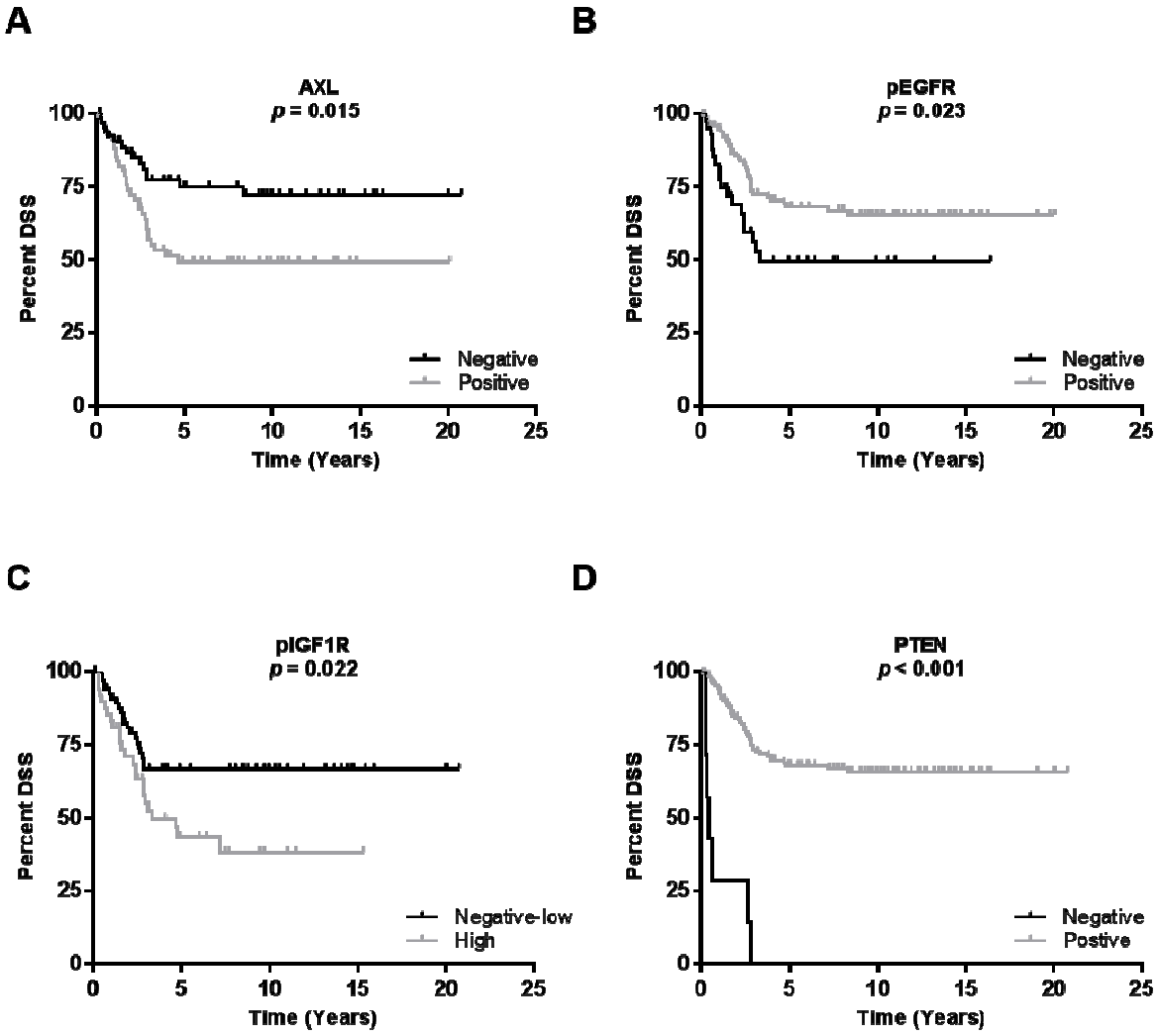

Figure 7. Kaplan-Meier DSS curves based on protein marker expression ($p < 0.05$). Primary UPS tumor samples (n = 208) were assessed for (A) AXL, (B) pEGFR, (C) pIGF1R, and (D) PTEN expression and Kaplan-Meier DSS curves were constructed.

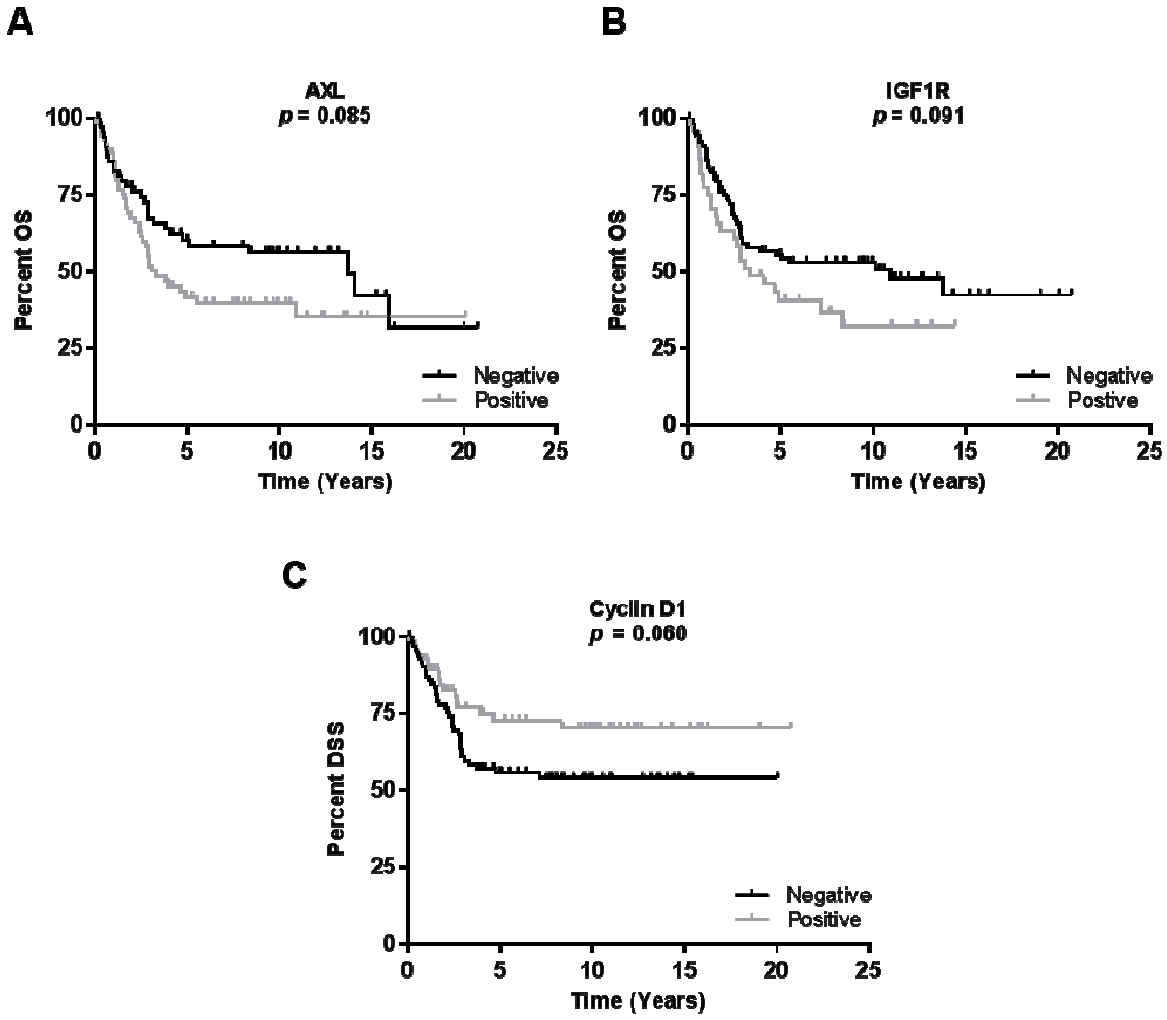

Figure 8. Kaplan-Meier survival curves based on protein marker immunostaining (p < 0.10). Kaplan-Meier OS curves for (A) AXL and (B) IGF1R expression and (C) Kaplan-Meier DSS curve for cyclin D1 immunostaining.

Chapter 4

Dual PI3K/mTOR inhibition has strong antitumorigenic effects in UPS cell lines and results in IGF1R activation.

As UPS is an uncommon malignancy, cell strains/lines are rare and, therefore, it is difficult to conduct preclinical investigations of novel therapies. Our laboratory has established several UPS cell strains and cell lines from patient tumor samples whose histologies have been verified by pathologists who are experts in the STS Field (Table 1). These bioresources are karyotypically complex and can grow in adherent cultures over several passages; furthermore, the migration and invasion abilities of these cells can be assessed *in vitro* (Figure 9). In addition, some of these cell strains/lines are tumorigenic in mice and can be utilized to model UPS tumorigenesis and evaluate therapeutic efficacy *in vivo* (Figures 9 and 12).

The PI3K/mTOR signaling pathway is active in UPS cell lines and cell strains

After determining that PI3K/mTOR signaling is active in UPS patient tumor samples, we wished to assess the status of this pathway in UPS cell strains/lines. Currently, there is no known originating cell or tissue type for UPS; therefore, human mesenchymal stem cells (hMSCs) were used as a normal control as previous studies have found molecular similarities between hMSC and UPS cells (33-35). Western blot analysis determined that PI3K/mTOR signaling is active in a panel of RA-UPS and sporadic UPS cells as evidenced by high levels of pAKT, pS6K, and p4EBP1 compared to the hMSC control (Figure 10).

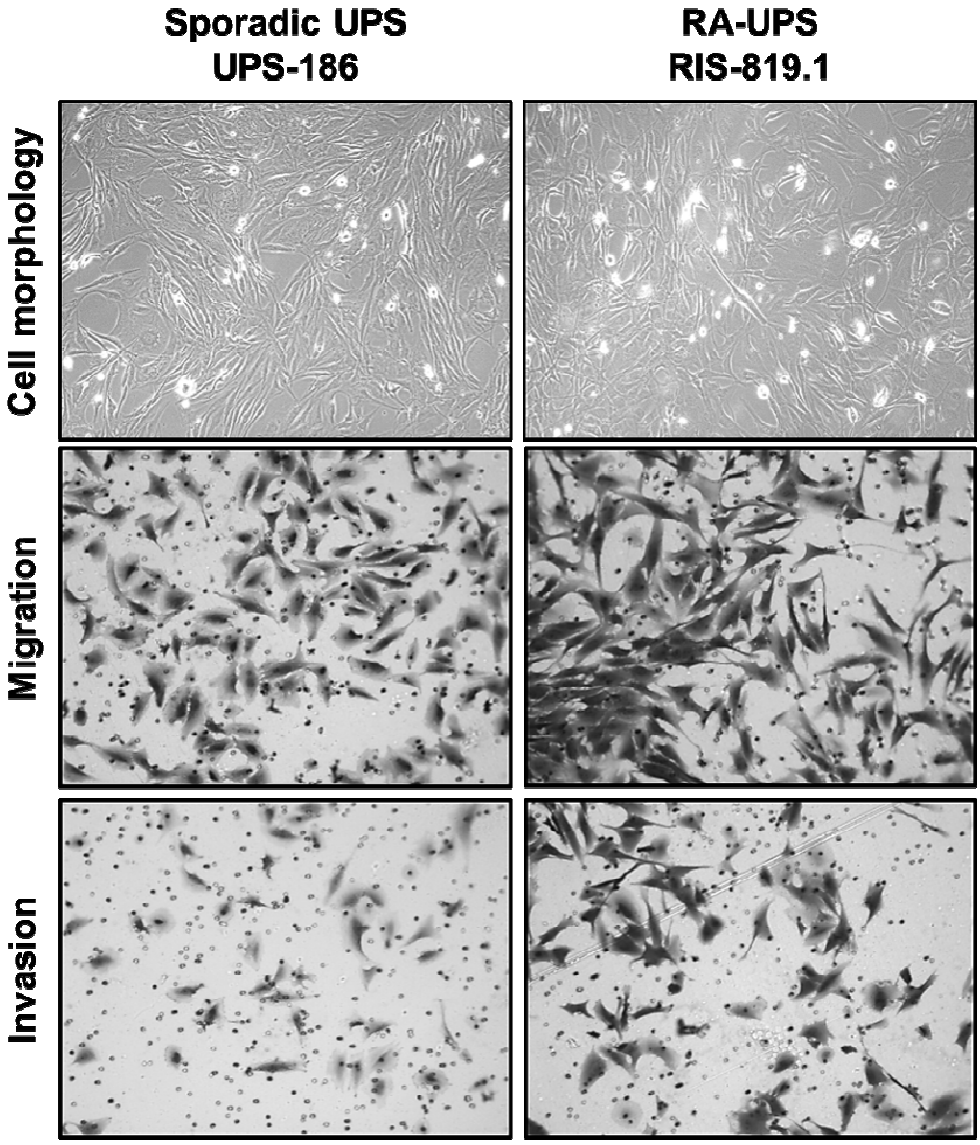

Figure 9. UPS cell lines can be used for preclinical investigations. Representative images of UPS-186 and RIS-819.1 in adherent culture (magnification: 100x) and after assessment for migration and invasion in modified Boyden chamber assays (magnification: 200x).

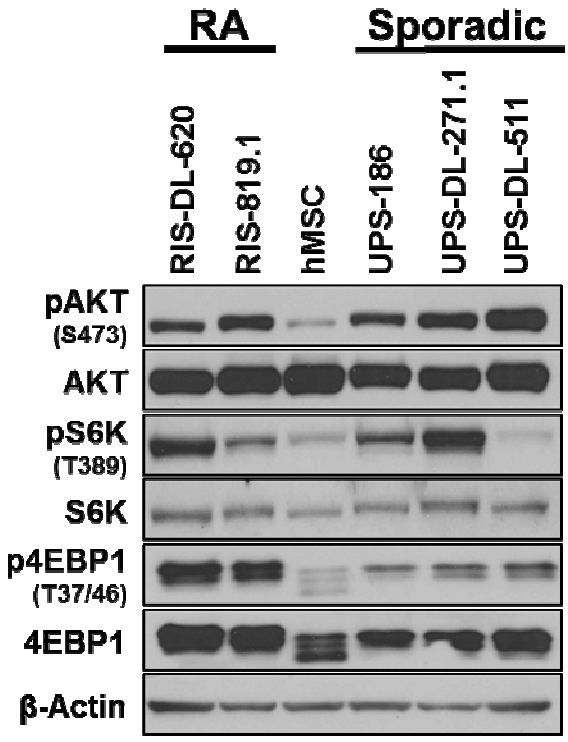

Figure 10. PI3K/mTOR signaling is active in UPS cell lines and cell strains. Whole cell lysates obtained from a panel of RA-UPS and sporadic UPS cell strains and cell lines were subjected to western blot analysis for total and activated (phosphorylated) AKT, S6K, and 4EPB1. hMSC served as the normal control.

A dual PI3K/mTOR inhibitor, PI-103, can block cell proliferation, migration, and invasion in the RA-UPS cell line RIS-819.1

In order to determine the extent to which PI3K/mTOR signaling supports UPS tumorigenesis, we elected to pharmacologically inhibit pathway activity using several dual PI3K/mTOR inhibitors. We first treated the RA-UPS cell line RIS-819.1 with increasing micromolar doses of PI-103, a dual PI3K/mTOR inhibitor which inhibits PI3K and mTOR at varying IC50 values (PI3K p110α IC50: 2 nM, mTOR IC50: 30 nM) (232). We observed a decrease in PI3K/mTOR signaling in RIS-819.1 cells treated with PI-103 (range: 0 – 5 μM) over 4 hours (Figure 11A). A reduction in signaling, as measured by a decrease in pAKT and pS6K, was not achieved until 0.5 μM PI-103 and p4EBP1 attenuation was not noted until 5 μM PI-103. A decrease in cell proliferation with PI-103 treatment was recorded and an EC50 of 0.68 μM was calculated (Figure 11B). Signaling through the PI3K/mTOR pathway can facilitate cell motility; when inappropriately activated, these cellular processes can support tumor growth, invasion, and metastasis (69, 92, 121). Therefore, we assessed the effect of PI-103 on RIS-819.1 migration and invasion. Overnight (16 hour) incubation with 0.5 μM of PI-103 resulted in a ~20% decrease in migration and 60% decrease in invasion (Figure 11C).

We assessed the *in vivo* antitumor efficacy of PI-103 using the RIS-819.1 implant model (Figure 12). Animals that were treated with 50 mg/kg PI-103 daily had significantly smaller tumor volumes when compared to the control group ($p = 0.045$) (Figure 13A). In addition, a significant reduction in *ex vivo* tumor weight was observed in treated animals versus the control ($p = 0.031$) (Figure 13B).

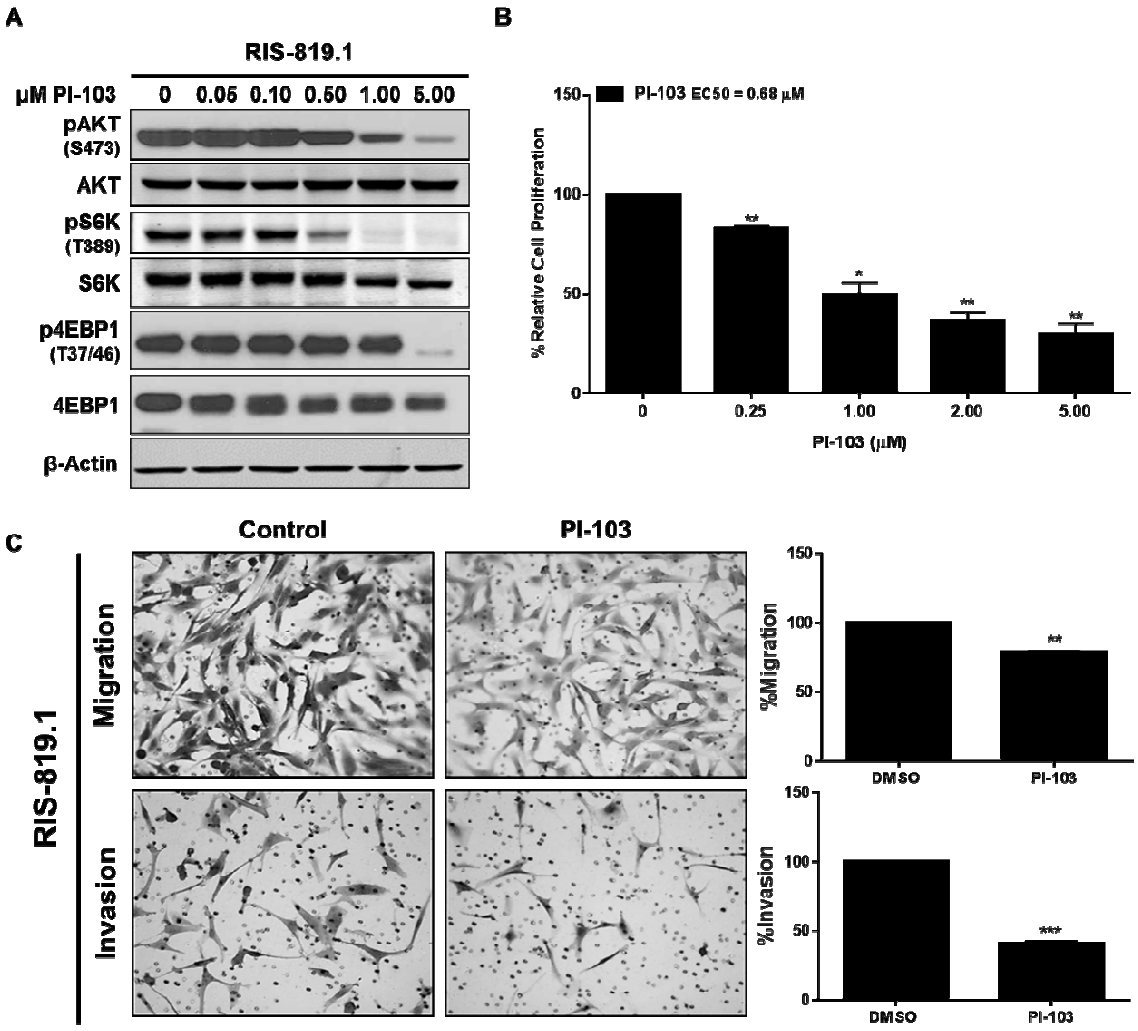

Figure 11. PI-103 treatment attenuates PI3K/mTOR signaling, proliferation, and migration and invasion *in vitro*. (A) Immunoblotting of RIS-819.1 whole cell lysates after PI-103 treatment for 4 hours. (B) RIS-819.1 cells were treated with increasing concentrations of PI-103 for 96 hours and cell viability was assessed by MTS assay and an EC50 value of 0.68 μM was calculated. Data obtained from duplicate experiments (C) RIS-819.1 cell migration and invasion abilities were evaluated after a 16 hour incubation with 0.5 μM PI-103 in modified Boyden chambers. Data obtained from duplicate experiments. Representative images of the lower surface of the Boyden chamber is shown at 200x magnification. The graphs depict the mean of duplicate experiments; error bars are the SEM. (* = $p < 0.05$; ** = $p < 0.01$; *** = $p < 0.001$)

.

Figure 12. Flow chart describing the general design of *in vivo* experiments using the RIS-819.1 implant mouse model.

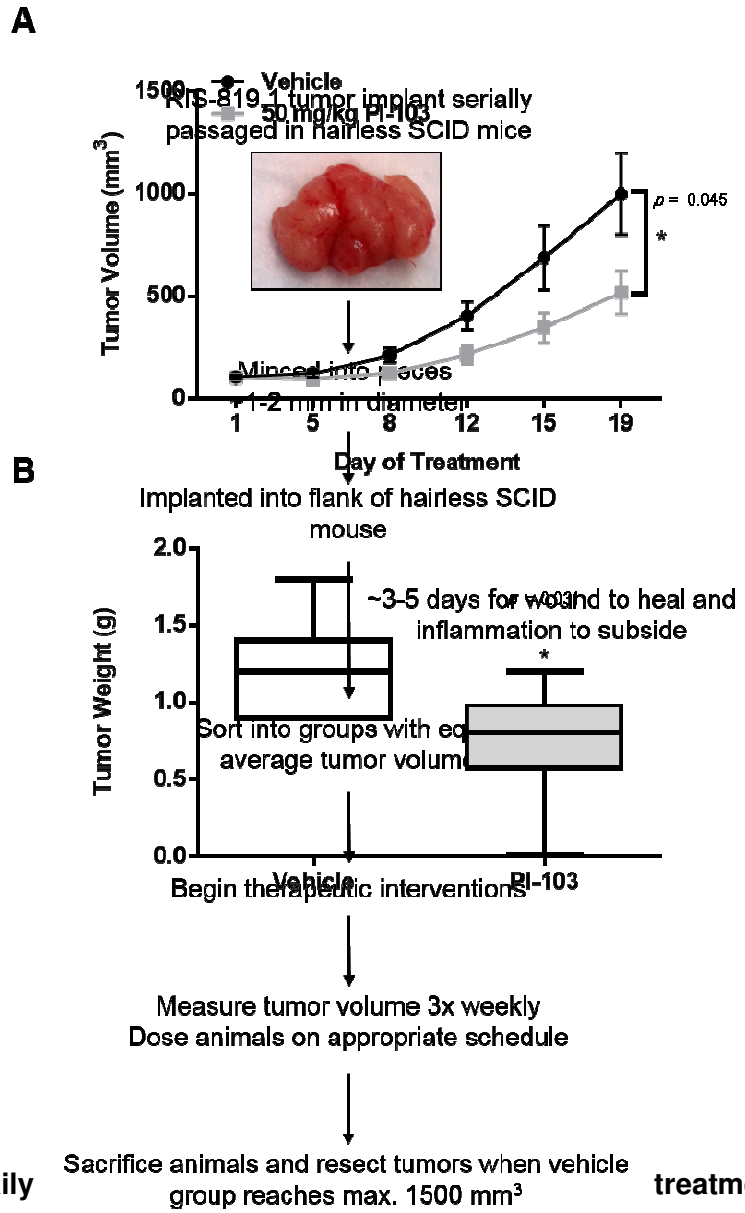

Figure 13. Daily treatment with PI-103 reduces tumor volume and weight *in vivo*. (A) Tumor volume throughout the dosing period and (B) end-point tumor volume for mice harboring RIS-819.1 implants and treated with either vehicle or 50 mg/kg PI-103. Vehicle control: n =7; PI-103: n = 8. (* = $p < 0.05$; ** = $p < 0.01$; *** = $p < 0.001$)

XL765, a clinically viable PI3K/mTOR inhibitor, reduces RIS-819.1 tumorigenicity

PI-103 is capable of blocking PI3K/mTOR signaling both *in vitro* and *in vivo*; however, this compound has not moved into clinical trials as it is rapidly metabolized by mouse models (151). Through a collaborative effort with Sanofi-Aventis, we were provided with the dual PI3K/mTOR inhibitor XL765 (PI3K p110α IC50: 39 nM, mTOR IC50: 157 nM) (233). Furthermore, this targeted agent has been evaluated in clinical trials, both as a single agent and with chemotherapy or targeted therapy, in patients with with glioma, breast cancer, or other advanced solid tumors (Table 7) (174, 178-180, 234). In order to assess the efficacy of XL765 to block PI3K/mTOR signaling and, thus, PI3K/mTOR-dependent tumorigenesis, we evaluated XL765 treatment in RIS-819.1 and an additional cell line, UPS-186, which was generated from a sporadic UPS (Figure 9). Similar to PI-103, XL765 treatment attenuated signaling through the PI3K/mTOR pathway in both cell lines after 48 hours of treatment; this signaling inhibition persisted through 96 hours of treatment (Figure 14A). Both cell lines were responsive to XL765 treatment, with calculated EC50 values of 1.44 μM (UPS-186) and 1.06 μM (RIS-819.1) (Figure 14B). Furthermore, XL765 diminished migratory and invasive capacities of both cell lines after incubation with drug in modified Boyden chambers (Figure 14C).

Table 7. Clinical trial information* associated with the small molecule inhibitors used in this study.

Name	Target	Company	Clinical Trial Phase	Tumor type	Combination
PI-103	PI3K and mTOR	Astellas Pharmaceuticals	N/A	N/A	N/A
XL765	PI3K and mTOR	Exelixis/Sanofi-Aventis	Phase I	Glioma	Temozolomide, radiation
			Phase I	Advanced solid tumors	N/A
			Phase I	Solid tumors	Erlotinib
			Phase I/II	Hormone receptor positive/ HER2 negative breast cancer	Letrozole
			Phase I	Recurrent glioma	N/A
BGT226	PI3K and mTOR	Novartis	Phase I	Solid tumors	N/A
			Phase I/II	Advanced solid tumors	N/A
AEW541	IGF1R	Novartis	N/A	N/A	N/A

*Information obtained from searches of clinicaltrials.gov for the indicated drug

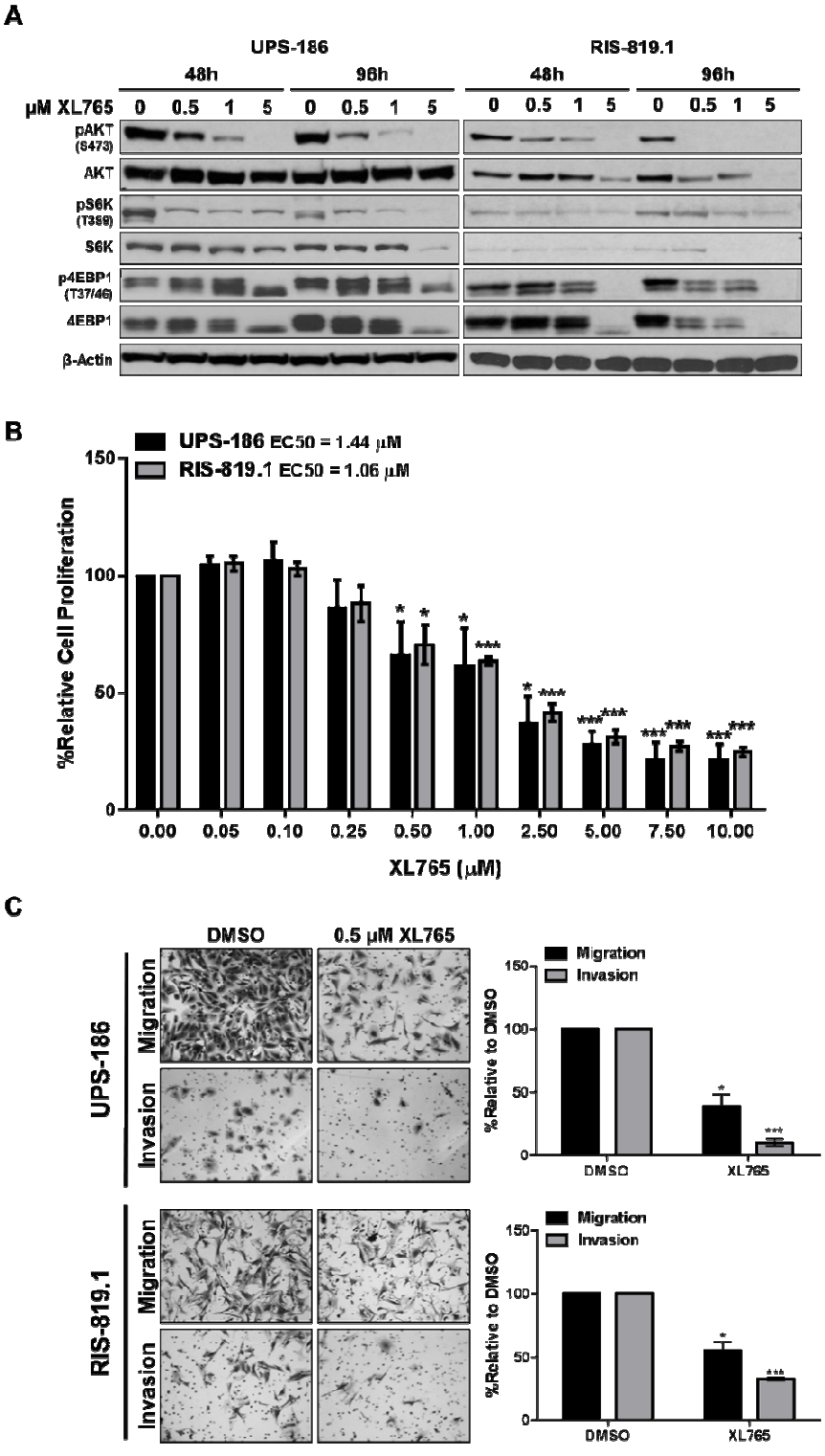
A
UPS-186
RIS-819.1
48h
96h
48h
96h
μM XL765 0 0.5 1 5 0 0.5 1 5 0 0.5 1 5 0 0.5 1 5
pAKT (S473)
AKT
pS6K (T389)
S6K
p4EBP1 (T37/46)
4EBP1
β-Actin
B
UPS-186 EC50 = 1.44 μM
RIS-819.1 EC50 = 1.06 μM
%Relative Cell Proliferation
150
100
50
0
0.00 0.05 0.10 0.25 0.50 1.00 2.50 5.00 7.50 10.00
XL765 (μM)
C
DMSO
0.5 μM XL765
UPS-186
Migration
Invasion
RIS-819.1
Migration
Invasion
Migration
Invasion
%Relative to DMSO
150
100
50
0
DMSO
XL765

Figure 14. XL765 inhibits signaling through the PI3K/mTOR pathway and reduces cell proliferation *in vitro*. (A) Levels of activated and total AKT, S6K, and 4EBP1 were detected via immunoblotting after treatment with micromolar doses of XL765. (B) Cell lines were treated with escalating doses of XL765. Proliferation was assessed using an MTS assay. (C) UPS-186 and RIS-819.1 cells were incubated in modified Boyden chambers with DMSO or 0.5 µM XL765 in low-serum (1%FBS in 1x DMEM/F12) conditions for 16 hours. FBS (5%) was used as a chemoattractant. Representative images of the lower surface of the Boyden chamber is shown at 20x magnification. The graphs depict the mean of triplicate experiments; error bars are the SEM. (* = $p < 0.05$; ** = $p < 0.01$; *** = $p < 0.001$)

We then evaluated XL765 in the RIS-819.1 mouse model of UPS. Animals were treated twice daily with 30 mg/kg XL765. A 75% reduction in tumor volume was noted in the XL765-treated arm when compared to the control vehicle group ($p < 0.001$) (Figure 15A). Furthermore, average XL765-treated tumor weight was significantly less than the control ($p = 0.025$) (Figure 15B).

Treatment with XL765 results in increased IGF1R activation in vitro

Although the PI3K/mTOR pathway was inhibited via XL765, tumor growth was not abolished *in vivo*. Therefore, we turned our attention to potential mechanisms of resistance to PI3K/mTOR blockade. RPPA analysis of a sporadic UPS cell line and RIS-819.1 revealed that total IGF1R protein levels were elevated following XL765 treatment (Figure 16A), suggesting that upregulation of this receptor could override the inhibitory effects of a PI3K/mTOR blockade.

Previous studies have indicated that activation of IGF1R and/or the MAPK pathway could provide a means to evade targeted PI3K/mTOR inhibition (141, 142, 145, 182). We observed an increase in IGF1R activity, as measured by phosphorylation of the receptor at Y1135/1136 after 48 and 96 hours of XL765 treatment (Figure 16B). In addition, we observed an increase in pMEK1/2 with XL765 treatment in UPS-186 at both 48 and 96 hours; however, we did not observe a similar increase in RIS-819.1 at 96 hours, indicating the potential for cell-line dependent modes of resistance.

Furthermore, the increase in MEK1/2 phosphorylation did not necessarily correlate with downstream ERK activation.

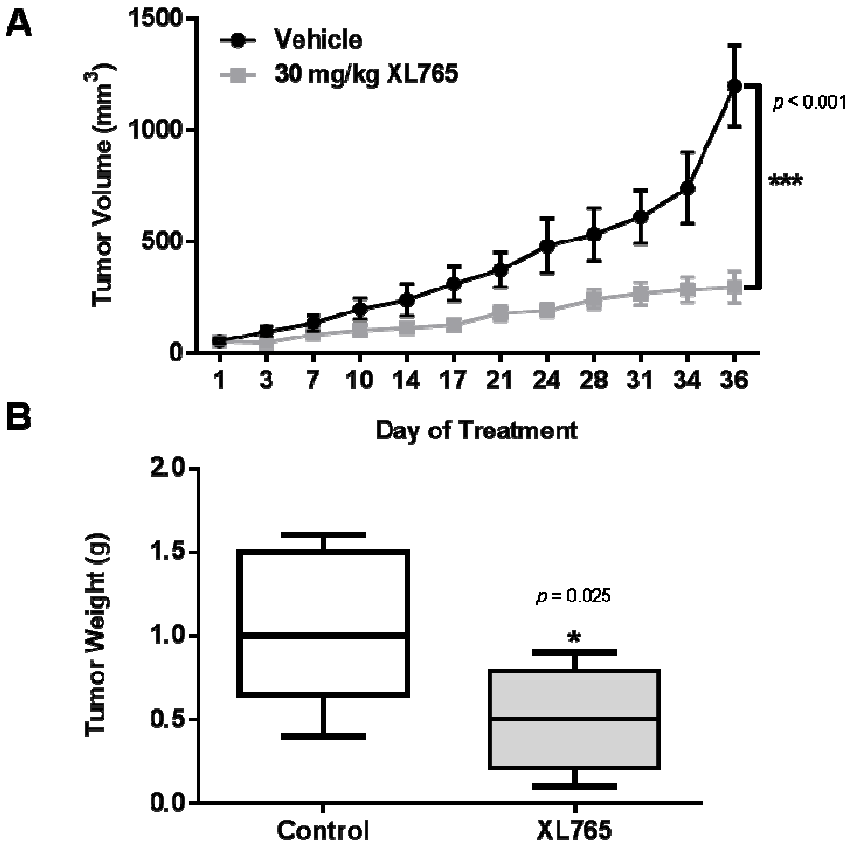

Figure 15. Reduction of tumor volume and weight in XL765-treated animals. Twice daily administration of 30 mg/kg XL765 resulted in significantly decreased (A) *in vivo* tumor volume and (B) *ex vivo* tumor weight when compared to the the control group. Vehicle control arm: n = 6 and XL765-treated arm: n = 6. (* = $p < 0.05$; ** = $p < 0.01$; *** = $p < 0.001$)

A

Linear Ratio (XL765-treated/Untreated)	Sporadic	RA	Average	Protein
	0.948	1.067	1.007	AXL pT702
	1.019	0.881	0.950	c-KIT
	0.956	0.935	0.946	c-MET pY1235
	1.278	0.983	1.130	EGFR
	0.537	0.978	0.758	EGFR pY1173
	0.975	1.011	0.993	EGFR pY992
	1.111	0.967	1.039	EGFR Y1068
	1.051	1.004	1.028	HER2 pY1248
	0.809	1.049	0.929	HER3
	1.128	1.062	1.095	HER3 pY1298
	1.633	1.665	1.649	IGF1Rβ

B

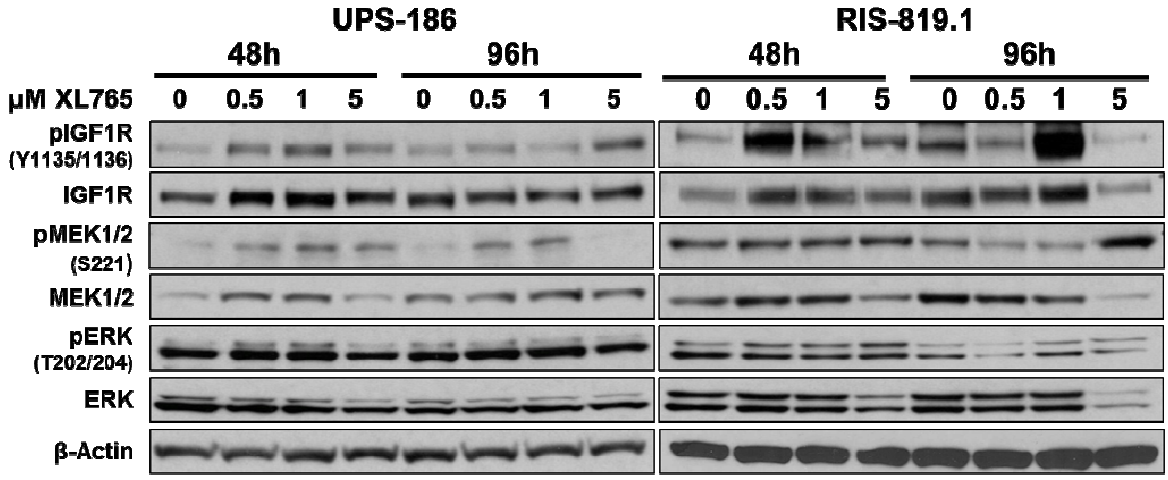

Figure 16. Upregulation of IGF1R in response to XL765 treatment. (A) Heat map generated from RPPA analysis of upstream receptor tyrosine kinases from sporadic UPS cells or RIS-819.1 cells treated with XL765 for 48 hours. Displayed values are the linear ratios comparing protein expression of XL765-treated cells to that of untreated cells. (B) Validation of RPPA data was performed by western blot analysis for UPS-186 and RIS-819.1 following treated with

increasing doses of XL765 over 48 or 96 hours. Expression of the indicated proteins was assessed by immunoblotting.

BGT226 inhibits PI3K/mTOR activity and UPS cell proliferation, migration, and invasion

BGT226 is a commercially available dual PI3K/mTOR inhibitor, which inhibits PI3K and mTOR activity at a low nanomolar range (175).This drug has been demonstrated to potently inhibit tumor cell proliferation in multiple cancer models both *in vitro* and *in vivo*, primarily through a G_0/G_1 arrest (152, 157, 158, 166, 172). In addition, this compound recently completed a phase I clinical trial in patients with advanced solid tumors (175); according to clinicaltrials.gov, a phase I/II trial in patients with advanced solid malignancies, including breast cancer, has also concluded although the results have yet to be released (Table 7).

BGT226-mediated inhibition of PI3K and mTOR in UPS-186 and RIS-819.1 suppressed phosphorylation of AKT and downstream kinases S6K and 4EBP1 after 2 hours; dephosphorylation was maintained after 96 hours of treatment (Figure 17A). Substantial antiproliferative effects were detected after 96 hour treatment with low nanomolar concentrations of BGT226, with calculated EC50 values of 6.81 nM and 4.17 nM for UPS-186 and RIS-819.1, respectively (Figure 17B). Diminished cell proliferation was linked to both a G_1 cell cycle arrest and the induction of apoptosis (Figure 17C). Interestingly, a greater proportion of apoptotic cells were detected with increasing concentrations of BGT226 in the RA-UPS cell line RIS-819.1 than in the sporadic cell line UPS-186.

To examine the effects of BGT226 on UPS cell migration and invasion, UPS-186 and RIS-819.1 were cultured in low-serum (1% FBS in DMEM/F12) to suppress proliferation and to promote migration towards the chemoattractant (5% FBS in

DMEM/F12). Cell migration and invasion were reduced in a dose-dependent manner in both cell lines; however, these processes were not fully inhibited even at the highest dose of BGT226 evaluated (100 nM) (Figure 17D). Furthermore, although the concentrations of BGT226 used exceeded EC50 values, an increase in cell death was not observed during the 16 hour time point (data not shown).

BGT226 reduces in vivo *tumorigenecity and results in increased IGF1R activation*

Based on the substantial effects of BGT226 treatment seen *in vitro*, we then assessed the efficacy of BGT226 treatment in the RIS-819.1 tumor implant mouse model. After initially treating all arms daily (7 days/week) for 1 week, treatment was reduced to 5 days/week in the 15 mg/kg BGT226 arm to remedy the observed weight loss in those animals; treatment continued for an additional 17 days. Oral administration of BGT226 once daily was sufficient to reduce RIS-819.1 xenograft volume by 47.4% and 63.6% in the 10 mg/kg and 15 mg/kg arm, respectively, when compared to the vehicle; in addition, the difference in tumor volumes between the vehicle and the 15 mg/kg BGT226 group achieved statistical significance ($p = 0.05$) (Figure 18A). A trend of decreased tumor weight in the BGT226-treated arms compared to the control was noted (Figure 18B). Immunohistochemical (IHC) analysis of downstream effectors of PI3K/mTOR signaling revealed that pAKT, pS6K, and p4EBP1 were downregulated in the treatment xenografts compared to the vehicle control, indicating that target inhibition was achieved; however, no differences in Ki67 or CC3 immunostaining was noted (Figure 18C). Interestingly, we detected increased levels of pIGF1R in BGT226-treated xenografts via both IHC analysis and immunoblotting (Figure 18D). Similar to the observations made following XL765 treatment, the same phenomenon was seen *in vitro* via western blot analysis of whole

A

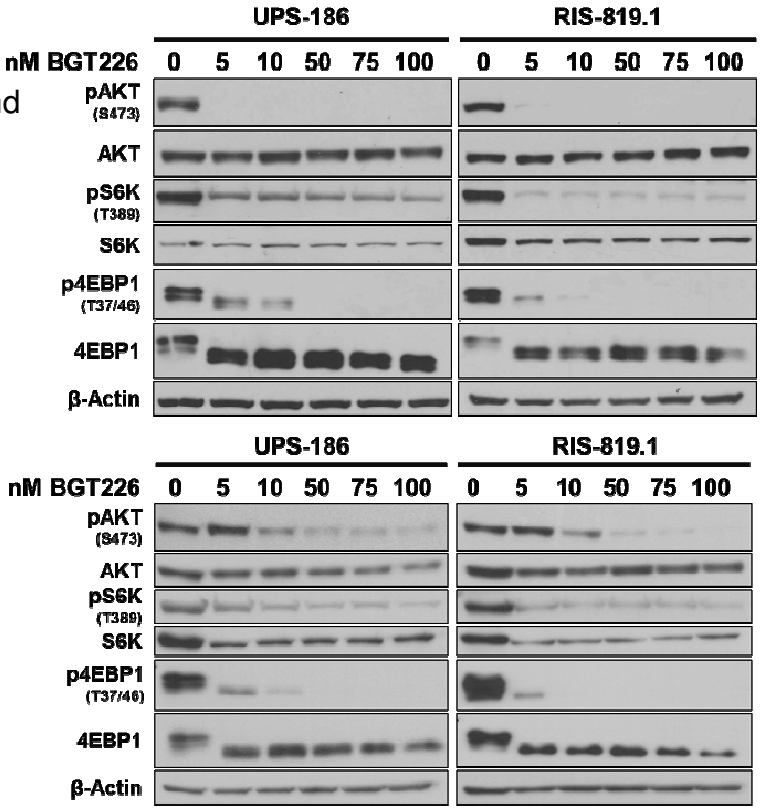

cell lysates harvested from UPS-186 and RIS-819.1 treated with BGT226 for 2 and 96 hours (Figure 19A).

B

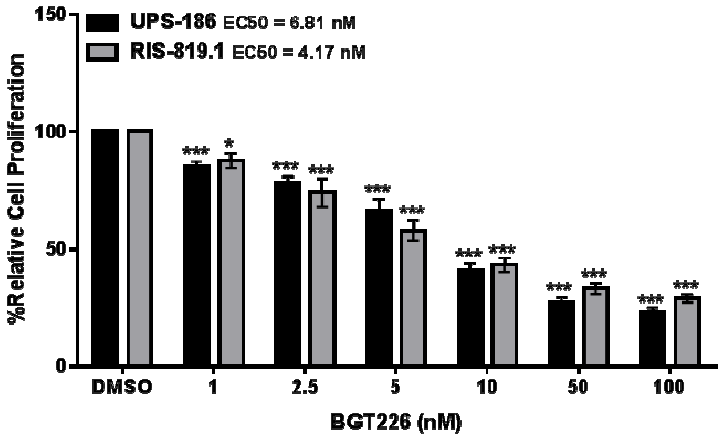

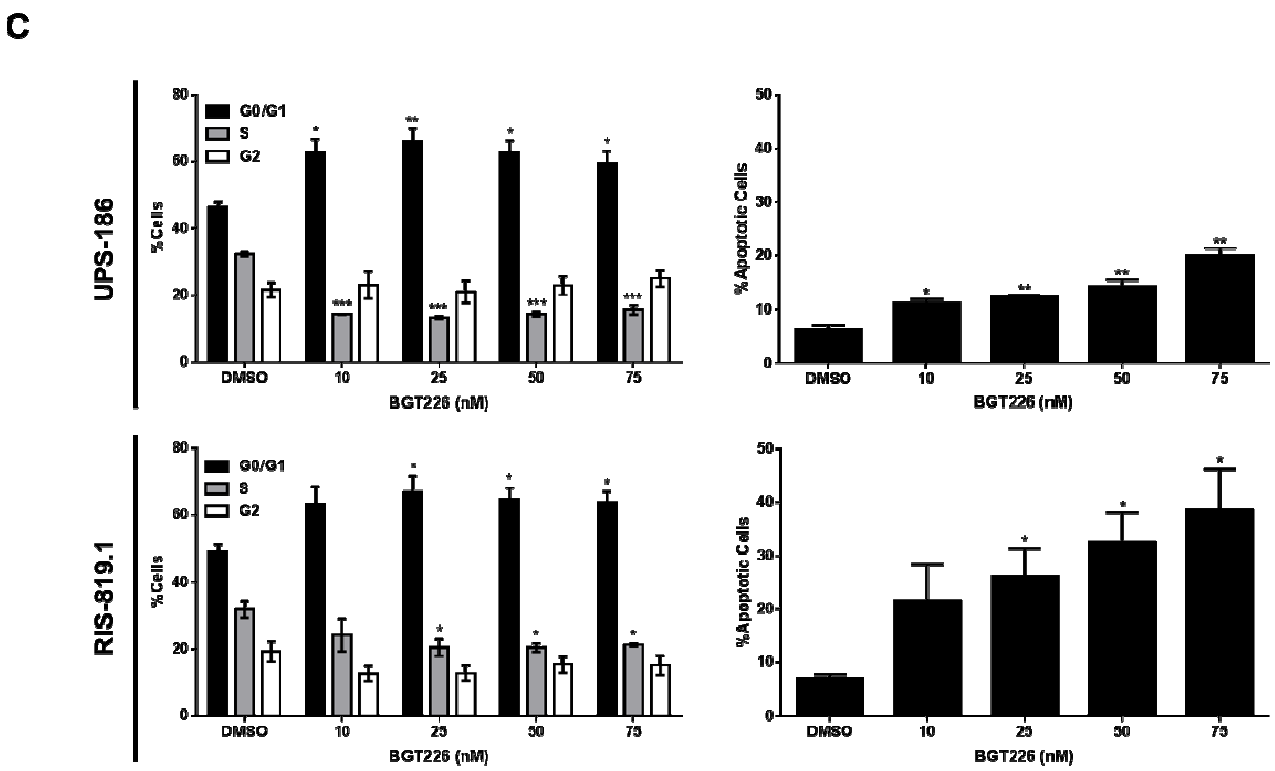
C
UPS-186
RIS-819.1
G0/G1
S
G2
% Cells
% Apoptotic Cells
DMSO
10
25
50
75
BGT226 (nM)

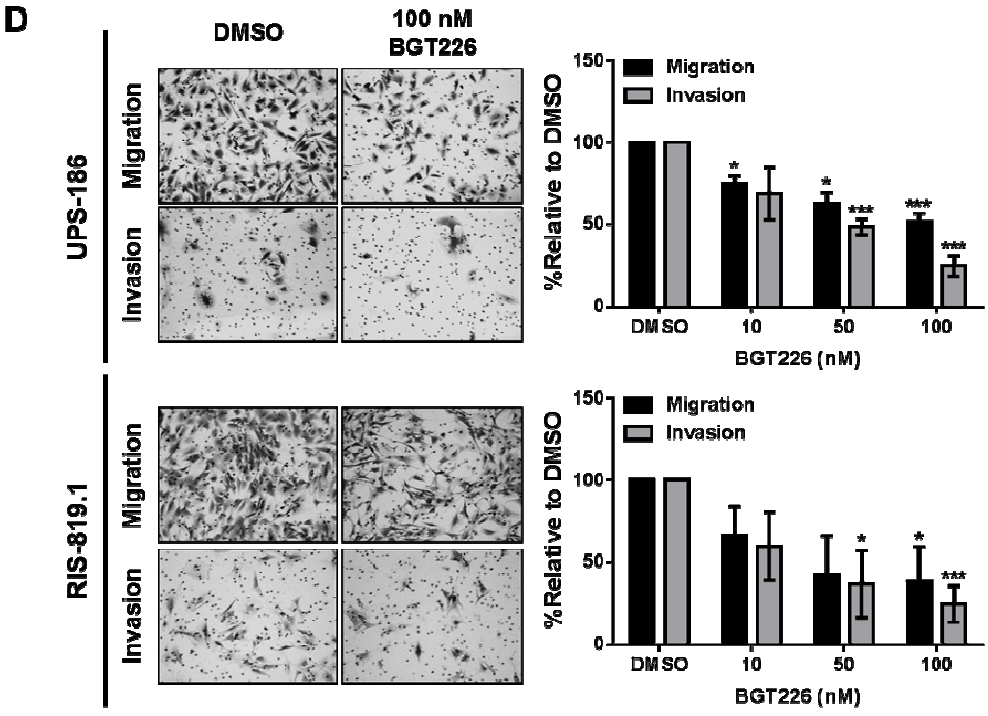
D
DMSO
100 nM BGT226
UPS-186
RIS-819.1
Migration
Invasion
%Relative to DMSO
DMSO
10
50
100
BGT226 (nM)

Figure 17. Blockade of the PI3K/mTOR pathway by BGT226 inhibits protumorigenic processes *in vitro*. (A) Representative western blots of whole cell lysates from a sporadic UPS cell line (UPS-186) and a RA-UPS cell line (RIS-819.1) after incubation with increasing doses of BGT226 for 2 (top) and 96 (bottom) hours. (B) Diminished UPS cell proliferation in response to 96 hours of BGT226 treatment was measured by MTS assay in UPS-186 and RIS-819.1 and the individual EC50s were determined. (C) Cell cycle distribution (left) and apoptosis levels (right) were evaluated in two UPS cell lines by FACS analysis after 48 and 96 hours of BGT226 treatment, respectively. (D) The effects of BGT226 on UPS-186 and RIS-819.1 cell migration and invasion were assessed by modified Boyden chamber assays. Representative images of cells treated with DMSO or 100 nM BGT226 are displayed (total magnification: 200x). The graphs depict the mean of triplicate experiments; error bars are the SEM. (* = $p < 0.05$; ** = $p < 0.01$; *** = $p < 0.001$)

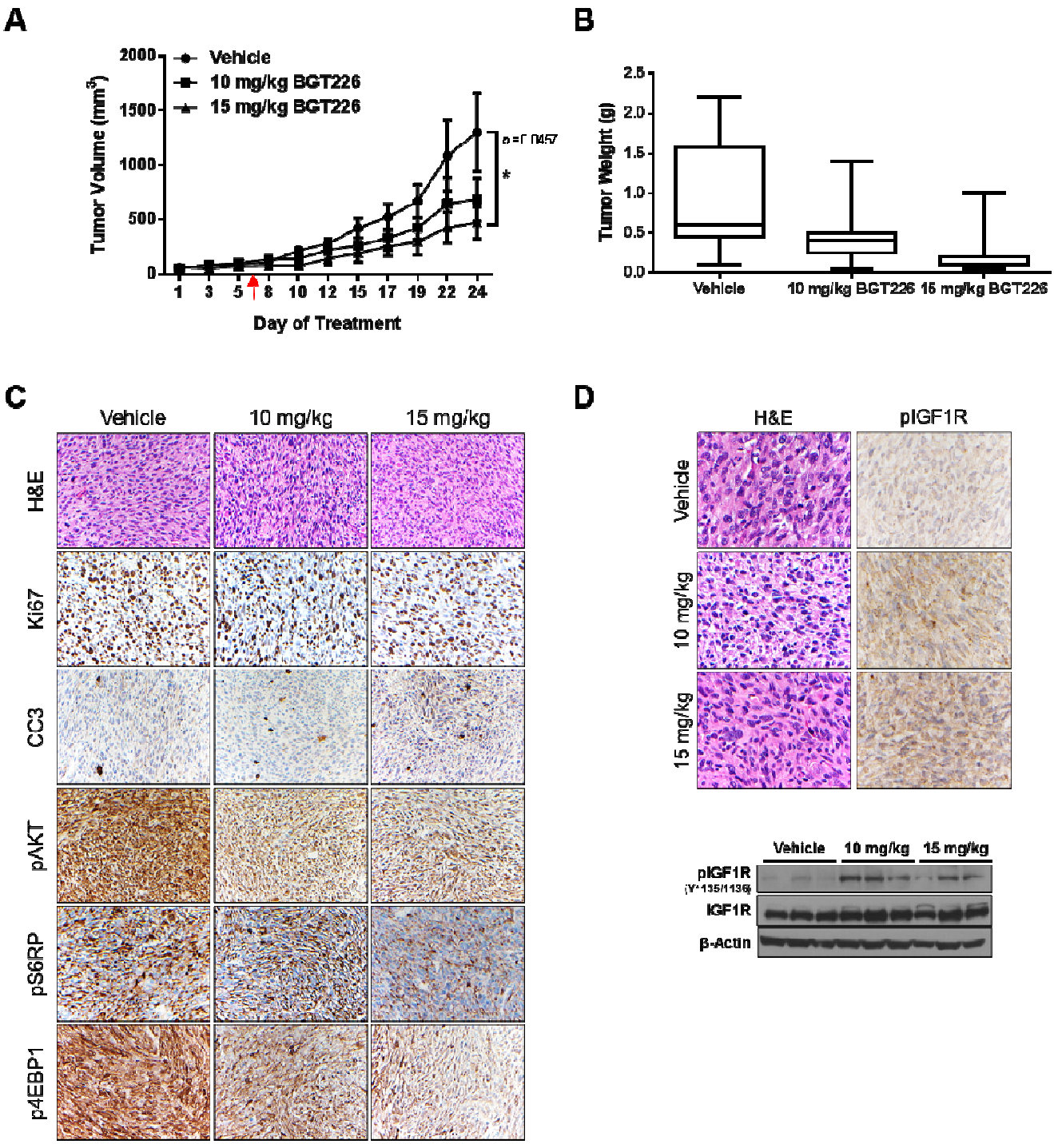

Figure 18. Daily administration of BGT226 reduces tumor volume and blocks PI3K/mTOR signaling, while activating IGF1R *in vivo*. (A) Hairless SCID mice harboring RIS-819.1

implants were treated with either vehicle (n=6) or BGT226 (10 mg/kg or 15 mg/kg, n=7 for both groups) via daily oral gavage; tumor volumes were measured three times per week. The arrow indicates the change in the treatment schedule for 15 mg/kg BGT226 group (from 7d/wk to 5d/wk). Values displayed are the mean volumes ± SEM. (* = $p < 0.05$) (B) Tumor weight was measured *ex vivo.* (C) Representative photographs (magnification: 200x) of IHC performed on RIS-819.1 xenografts from vehicle and BGT226-treated animals for markers of proliferation (Ki67), apoptosis (CC3), and markers of PI3K/mTOR activity (pAKT, pS6RP, and p4EBP1). (D) Detection of IGF1R activation (pIGF1R) in vehicle and BGT226-treated xenografts via IHC (top, magnification: 200x) and western blot (bottom).

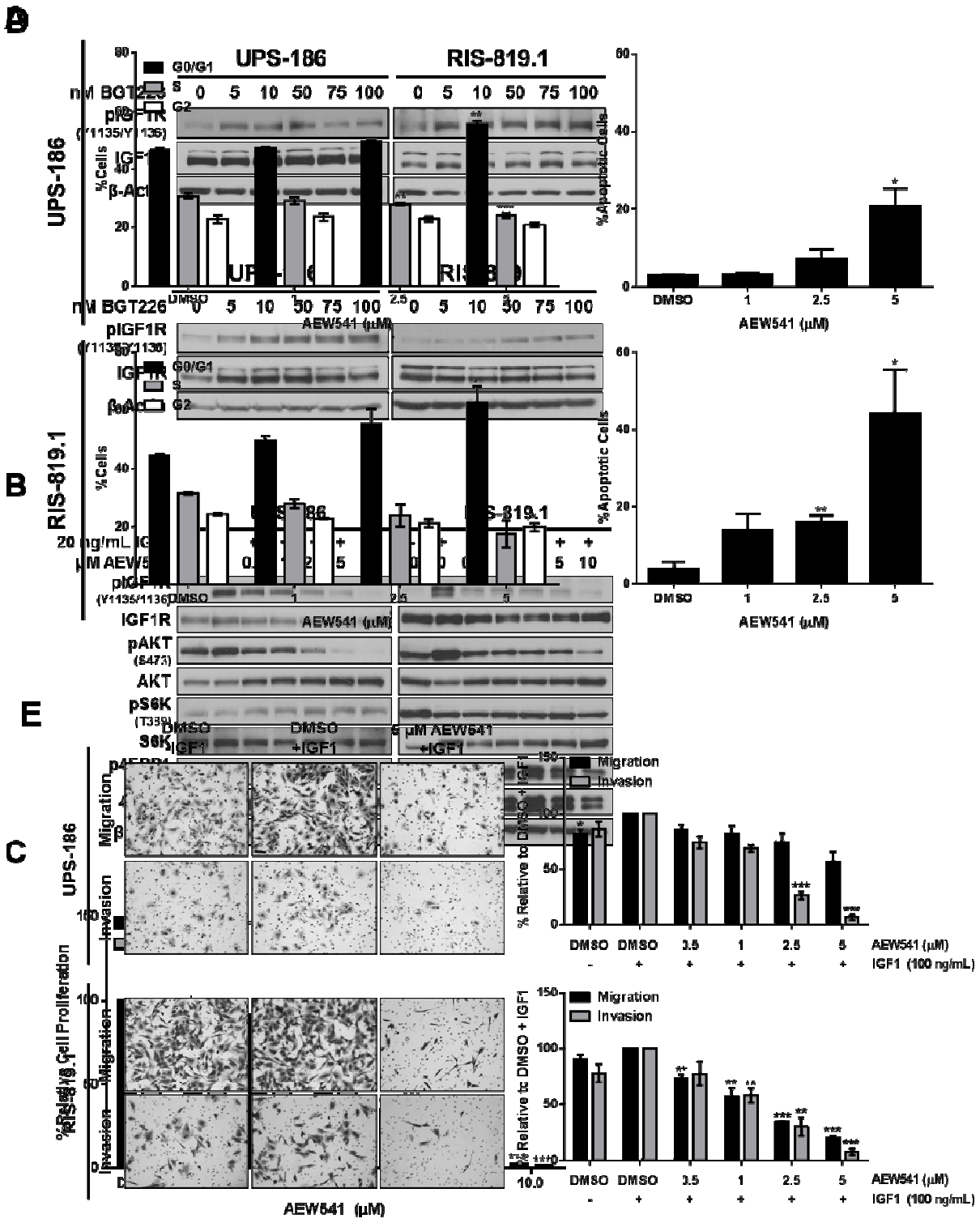
A
UPS-186
RIS-819.1
G0/G1
S
G2
nM BGT226
0 5 10 50 75 100
pIGF1R
(Y1135/Y1136)
IGF1R
β-Actin
%Cells
%Apoptotic Cells
DMSO
1
2.5
5
AEW541 (μM)
B
20 ng/mL IGF1
μM AEW541
pAKT
(S473)
AKT
pS6K
(T389)
S6K
E
DMSO
DMSO +IGF1
5 μM AEW541 +IGF1
C
Migration
Invasion
% Relative to DMSO + IGF1
3.5
IGF1 (100 ng/mL)
% Relative Cell Proliferation

Figure 19. IGF1R is activated in response to BGT226-mediated PI3K/mTOR blockade and is attenuated by AEW541. (A) Detection of phospho- and total IGF1R in UPS cell lines incubated with BGT226 for 2 and 96 hours. (B) Western blot analysis of UPS-186 and RIS-819.1 cells pre-treated with increasing concentrations of AEW541, then stimulated with 20

ng/mL IGF1. (C) UPS cell proliferation decreased in the presence of AEW541 ± 20 ng/mL IGF1. (D) Cell cycle analysis and detection of apoptosis indicated an accumulation of cells in the G_1 phase of the cell cycle and an induction of apoptosis after AEW541 treatment. (E) Incubation with AEW541 for 16 hours reduced UPS cell migration and invasion. Representative images of cells treated with DMSO, DMSO + 100 ng/mL IGF1, or 5 μM AEW541 + 100 ng/mL IGF1 are displayed (magnification: 200x). The graphical representations of the data are the mean of triplicate experiments; error bars are the SEM. (* = $p < 0.05$; ** = $p < 0.01$; *** = $p < 0.001$)

Chapter 5

Co-targeting PI3K, mTOR, and IGF1R drastically reduces tumorigenicity.

The IGF1R inhibitor AEW541 hinders UPS cell viability, migration, and invasion

Small molecule inhibitors against IGF1R may also target the highly homologous insulin receptor (IR). Therefore, we selected the small molecule inhibitor AEW541 to block IGF1R activation following BGT226 treatment as it displays a higher affinity for IGF1R over IR. (210). We evaluated the ability of AEW541 to block IGF1R activation by incubating UPS-186 and RIS-819.1 cell lines with increasing micromolar concentrations of drug, followed by acute exposure to recombinant IGF1. Western blot analysis demonstrated that AEW541 reduced IGF1R activation at all concentrations tested, with the highest level of inhibition achieved at concentrations greater than 1 µM (Figure 19B). While AEW541 downregulated pAKT in both cell lines, it did not strongly effect the activation status of S6K or 4EBP1, suggesting that IGF1R is not solely responsible for PI3K/mTOR pathway activation in UPS.

IGF1R can regulate cell growth and proliferation through PI3K/mTOR and/or MAPK pathway activation (191); accordingly, inhibition of the receptor via AEW541 elicited strong antiproliferative effects in UPS cell lines (EC50 values: UPS-186 = 4.39 µM and RIS-819.1 = 4.96 µM) resulting from a significant increase in G_1 phase and concomitant decrease in S phase of the cell cycle and the induction of apoptosis in both cell lines (Figure 19C and D). Similar to BGT226 treatment, more apoptotic cells were detected in RIS-819.1 when compared to UPS-186.

Activation of IGF1R has been linked to tumor invasion and metastasis; therefore, we investigated the effect of IGF1R inhibition via AEW541 on cell migration and invasion (195). UPS-186 and RIS-819.1 cells were seeded in low-serum conditions in modified Boyden chambers; recombinant IGF1 was used as an additional chemoattractant in order to evaluate the efficacy of AEW541 to block both IGF1R activation and subsequent promotion of cell migration and invasion. The sensitivity of RIS-819.1 to AEW541 is further reflected by the significant dose-dependent decline in both migration and invasion with treatment (Figure 19E). In contrast, the only significant effects observed in UPS-186 were decreases in invasion with AEW541 concentrations greater than 2.5 μM. Taken together, these results demonstrate that AEW541 successfully attenuates IGF1R activation, even after stimulation with exogenous ligand, and exerts anti-tumor effects *in vitro* in both cell lines tested. While RIS-819.1 and UPS-186 exhibit varying sensitivities to AEW541, our data suggest that AEW541 could be used to prevent IGF1R activation resulting from treatment with BGT226.

BGT226 and AEW541 co-treatment does not significantly enhance in vitro *antitumor effects*

To investigate potential synergistic drug interactions, UPS-186 and RIS-819.1 cells were treated with fixed concentrations of BGT226 (range: 0-10 nM) and/or AEW541 (range: 0-2.5 μM) for 96 hours and combination index (CI) values were calculated (Figure 20A). According to the CI values, synergistic interactions occurred in 80% of drug combinations tested in UPS-186 and 60% of those in RIS-819.1; however, the corresponding drug effects for the majority of synergistic drug combinations were not substantial, with less than 50% cell death after treatment with AEW541 and BGT226 concentrations below their EC50 values. In addition, minimal effects on cell cycle

distribution and apoptosis levels in UPS-186 and RIS-819.1 were observed after treatment with synergistic concentrations of AEW541 and BGT226, further confirming the lack of antiproliferative effects (Figure 20B).

Despite the lack of antiproliferative effects seen *in vitro*, synergistic drug combinations were capable of preventing activation the PI3K/mTOR signaling cascade and IGF1R after IGF1 stimulation more effectively than either drug alone (Figure 20C). Furthermore, combination treatment did not alter the phosphorylation status of MAPK pathway components MEK1/2 and ERK, suggesting that this signaling cascade is not activated as a compensatory response to PI3K/mTOR and IGF1R blockade (Figure 20D).

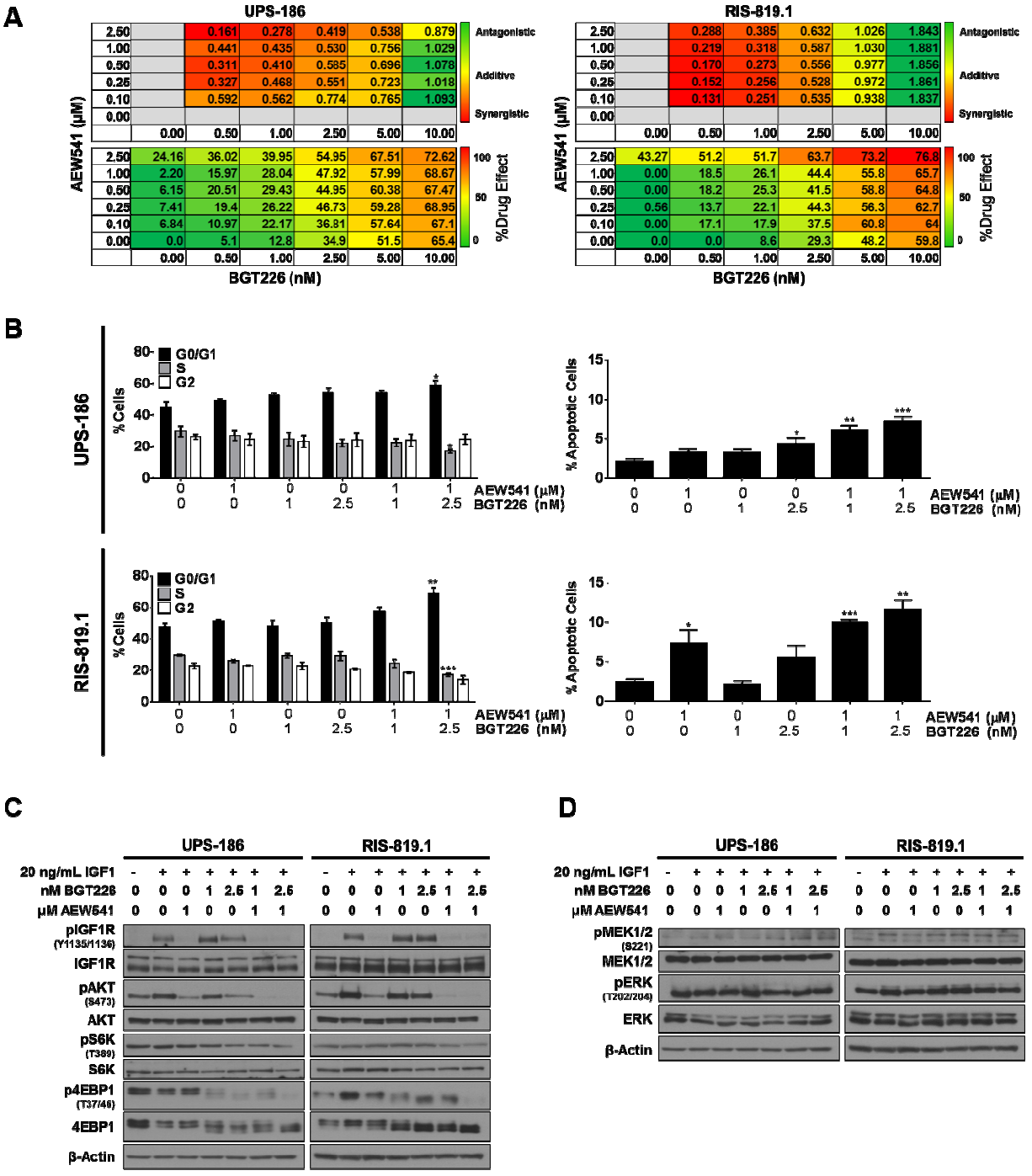

Figure 20. BGT226 and AEW541 act synergistically to block PI3K/mTOR signaling and IGF1R activation *in vitro*. (A) Combination index (CI) values (top), calculated using the CompuSyn software, and drug effect percentages ([1 – relative cell proliferation] x 100%; bottom) were obtained by triplicate MTS experiments using UPS-186 or RIS-819.1. (B) Cell

cycle distribution (left) and percentage of apoptotic cells (right) were measured in UPS-186 and RIS-819.1 cells after 48 and 96 hours of treatment, respectively. (C) Effects on IGF1R and effector molecules of PI3K/mTOR signaling were assayed by western blot following co-treatment with AEW541 and BGT226 and subsequent stimulation with recombinant IGF1. (D) Expression of activated and total MAPK pathway components MEK1/2 and ERK was evaluated by western blot analysis after incubation with AEW541 and/or BGT226 and subsequent acute exposure to IGF1. The graphical representations of the data are the mean of triplicate experiments; error bars are the SEM. (* = $p < 0.05$; ** = $p < 0.01$; *** = $p < 0.001$)

In vivo *tumor growth is strongly inhibited by combination therapy*

Given the negative effect on PI3K/mTOR signal transduction from combination treatment *in vitro*, we evaluated combined inhibition of PI3K/mTOR and IGF1R in RIS-819.1 xenografts. Mice treated daily with single agent BGT226 or AEW541 had comparable tumor volumes to the vehicle group (Figure 21A). Strikingly, combination treatment significantly reduced xenograft volumes by nearly 85% compared to tumors in the vehicle group ($p = 0.020$) and by 80% compared to either single agent (AEW541: $p = 0.007$; BGT226 $p = 0.005$); a significant decrease in tumor weight between the combination and either the control or single agent arms was also noted ($p = 0.026$, <0.001, and 0.002; combination versus control, BGT226, and AEW541, respectively) (Figure 21B). Excitingly, one animal in the combination arm had complete regression of its tumor within the first 2 weeks of treatment. IHC analysis revealed that AEW541 and BGT226 co-treatment reduced cell proliferation via decreased Ki67 staining when compared to vehicle or single agent therapy, but had little effect on apoptosis as determined by CC3 staining (Figure 21C). PI3K/mTOR signaling was more strongly inhibited by the combination treatment, as evidenced by downregulation of pAKT, pS6RP, and p4EBP1; furthermore, AEW541 prevented BGT226-associated IGF1R activation in the combination arm.

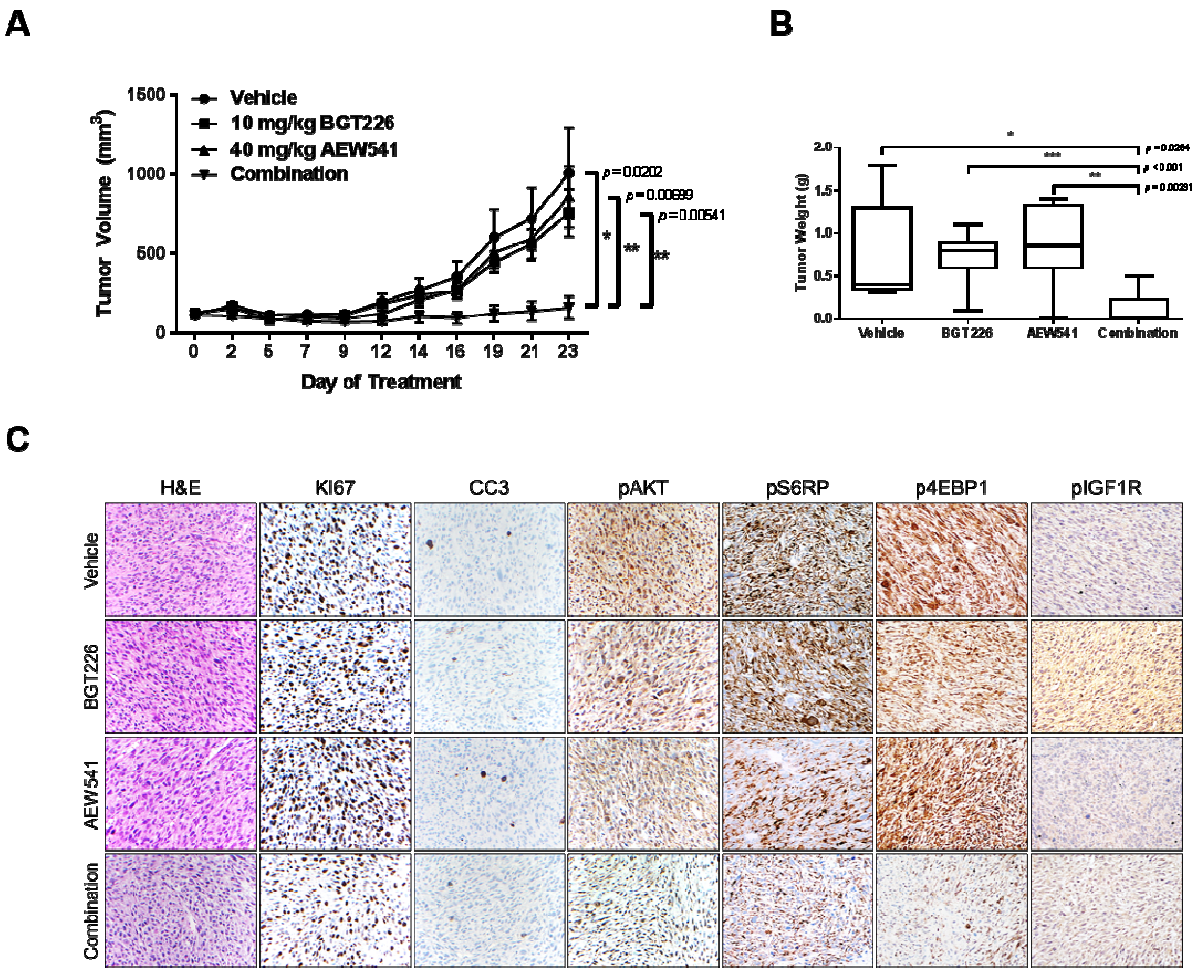

Figure 21. Combination therapy drastically reduces tumor volume *in vivo*. (A) Tumor volumes of RIS-819.1 xenografts treated with vehicle (*n*=7), BGT226 (10 mg/kg, *n*=7), AEW541 (40 mg/kg, *n*=6), and combination (*n*=6) are presented as mean volumes ± SEMs. (B) *Ex vivo* tumor weight was recorded upon termination of the experiment. (C) Control and inhibitor-treated xenografts were subjected to IHC analysis for protein markers of cell proliferation (Ki67), apoptotic cell death (CC3), and indicators of target inhibition (pAKT, pS6RP, p4EBP1, and pIGF1R). Representative images are shown (magnification: 200x).

Chapter 6

Diminished UPS cell migration and invasion after combination therapy is linked to p27 localization.

Combination of BGT226 and AEW541 has synergistic effects on in vitro *cell migration and invasion*

Combination treatment did not significantly alter cell proliferation; however, the substantial antitumor effects of co-targeting PI3K, mTOR, and IGF1R *in vivo* suggested that combination treatment may affect other protumorigenic processes such as cell migration and invasion. The addition of IGF1 as a chemoattractant enhanced the migratory and invasive capacities of both UPS-186 and RIS-819.1 in modified Boyden chambers (Figure 22A). AEW541 treatment alone decreased migration and invasion by nearly 20% in both cell lines tested. Surprisingly, BGT226-treated cells were able to migrate and invade at levels similar to or exceeding the control, suggesting that IGF1R activation may override the inhibitory effects of BGT226. In UPS-186, co-treatment with AEW541 and BGT226 reduced cell migration and invasion by approximately 50% and 75%, respectively, compared to the DMSO + IGF1 controls. Similarly, we observed a significant decrease in both migration and invasion (approximately 60% and 80%, compared to the respective controls) in combination-treated RIS-819.1. Trypan blue exclusion determined that the concentrations of AEW541 and BGT226 used in combination did not induce cell death (data not shown).

Negative effects on migration and invasion by combination treatment are linked to p27 nuclear localization and increased RhoA activity

Nuclear $p27^{Kip1}$ (p27) is a key regulator of the G_1/S transition in the cell cycle; however, p27 can also localize to the cytoplasm, where it can promote cell motility through its interaction with and inhibition of the small GTPase RhoA (124). Aberrant PI3K/mTOR signaling can facilitate the cytoplasmic sequestration of p27 through AKT-mediated phosphorylation at T157 and T198, which blocks p27 nuclear import (116-118). We performed a nuclear and cytoplasmic fractionation after single agent and combination treatment in RIS-819.1 cells, followed by western blot analysis to determine the effects of combination treatment on the subcellular localization of p27. We observed equal distribution of p27 in the cytoplasm and the nucleus in DMSO-treated cells (Figure 22B). BGT226 decreased cytoplasmic p27, while nuclear levels were not altered; AEW541 did not significantly affect cytoplasmic or nuclear p27 when compared to the control cells. Interestingly, combination of AEW541 and BGT226 effectively reduced cytoplasmic p27 levels, while simultaneously increasing nuclear levels. To determine the potential downstream effect on RhoA, we employed a colorimetric assay to evaluate RhoA activity in RIS-819.1 cells treated with BGT226 and AEW541 alone and in combination. Cells cultured in low-serum conditions exhibited low endogenous RhoA activity, which increased after stimulation with FBS with or without IGF1 (Figure 22C). Combination treatment resulted in a significant 1.5 fold increase in RhoA activity, while either single agent had no significant effect. These data suggest that PI3K/mTOR signaling contributes to UPS cell migration and invasion through the promotion of p27 cytoplasmic localization; co-targeting of PI3K, mTOR, and IGF1R can reduce cytoplasmic p27 while simultaneously increasing nuclear levels.

A
UPS-186
RIS-819.1
Invasion
Migration
AEW541 (1 μM)
BGT226 (25 nM)
IGF1 (100 ng/mL)
Migration
Invasion
% Relative to DMSO + IGF1

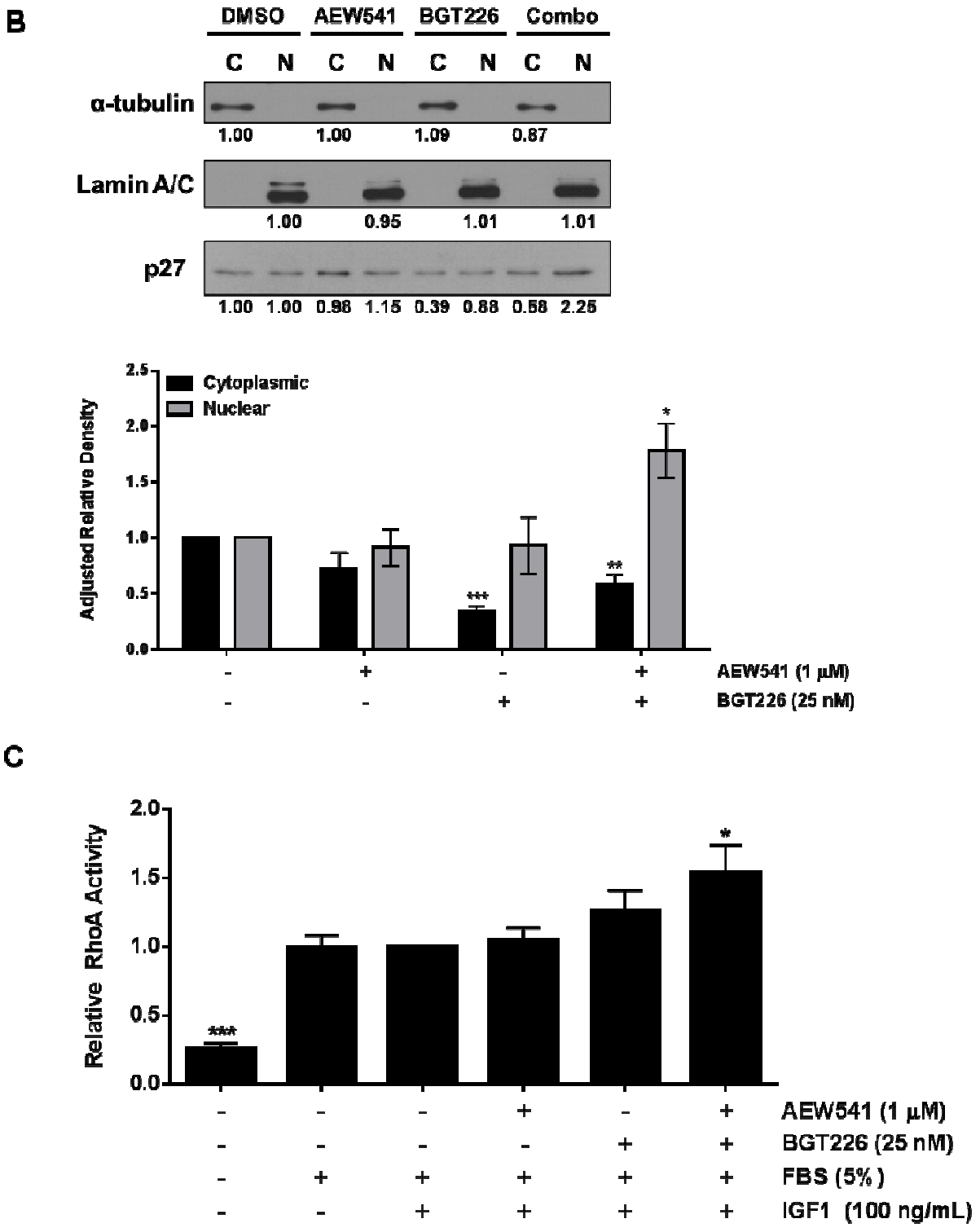
B
DMSO
AEW541
BGT226
Combo
C N C N C N C N
α-tubulin
1.00 1.00 1.09 0.87
Lamin A/C
1.00 0.95 1.01 1.01
p27
1.00 1.00 0.98 1.15 0.39 0.88 0.58 2.25
Cytoplasmic
Nuclear
Adjusted Relative Density
2.5
2.0
1.5
1.0
0.5
0.0
***
**
*
- + - + AEW541 (1 μM)
- - + + BGT226 (25 nM)
C
Relative RhoA Activity
2.0
1.5
1.0
0.5
0.0
***
*
- - - + - + AEW541 (1 μM)
- - - - + + BGT226 (25 nM)
- + + + + + FBS (5%)
- - + + + + IGF1 (100 ng/mL)

Figure 22. Reduction of migration and invasion after co-treatment is associated with localization of p27 to the nucleus and increased RhoA activity. (A) Combination of AEW541 and BGT226 reduced UPS cell migration and invasion as evaluated by modified Boyden chamber assays. (B) p27 localization was determined by nuclear and cytoplasmic fractionation of cell lysates, followed by immunoblot analysis and calculation of relative protein levels by densitometry. Fraction purity was assessed by α-tubulin (cytoplasmic) and lamin A/C (nuclear). (C) The effect of combination treatment on RhoA activity was assayed. Relative RhoA activity is displayed. ($* = p < 0.05$; $** = p < 0.01$; $*** = p < 0.001$)

Chapter 7

Discussion, Conclusions, and Future Directions

UPS is an aggressive subtype of STS devoid of any specificcharacteristics indicative of the tissue of origin nor any known specific recurring genetic aberrations. The standard of care is surgical excision with negative margins; for unresectable or metastatic disease, neoadjuvant systemic chemotherapy or radiation therapy may be considered. However, UPSs are generally chemoresistant; furthermore, clinical trials evaluating kinase-targeted therapies which are sometimes moderately effective in other STS subtypes have reported minimal responses in UPS patients. The aggressiveness of the disease and the poor response to available therapies is reflected in the five-year survival rate of only 65-70%. Therefore, novel molecular targets must be identified and evaluated in order to offer more effacacious therapies and improve UPS patient outcome.

Previous studies have revealed that active PI3K/mTOR signaling molecules are negative molecular prognosticators of STS patient OS and DSS (130-132). Moreover, our laboratory demonstrated that specifically 20% of UPS patients evaluated in a TMA-based study had high levels of pAKT immunostaining, which was indicative of poor DSS (135). These data indicate that active PI3K/mTOR signaling may contribute to UPS tumorigenesis and disease progression in a subset of patients and that this cohort may benefit from targeted therapy against this pathway. Here, we expand upon these

findings and show that the PI3K/mTOR pathway is indeed active in UPS patient samples derived from both sporadic and RA tumors by correlating the expression of several proteins downstream of PI3K and mTOR along with upstream activating RTKs. Furthermore, we demonstrate that UPS cell strains and cell lines developed in our laboratory harbor active PI3K/mTOR signaling, allowing us to more fully interrogate this pathway in preclinical models *in vitro* and *in vivo*.

Dysregulation of the PI3K/mTOR pathway has been reported as a driver of tumorigenesis in several tumor types, including subtypes of STS. Aberrant activation of the pathway can occur through multiple mechanisms: (1) mutations within the PI3K isoforms, (2) loss of the tumor suppressor *PTEN*, and/or (3) the upregulation and/or abnormal activation of upstream RTKs (61). We are currently sequencing *PIK3CA*, the gene encoding catalytic PI3K subunit p110α, to discern whether any activating mutations are present in UPS tumor samples and cell strains/cell lines; however, previous studies indicate that *PIK3CA* mutations are rare in UPS and are most likely not at the root of pathway activation (235).

PTEN loss may be responsible for unchecked PI3K/mTOR activity, as chromosome 10q is frequently lost in pleomorphic sarcomas (namely, UPS and LMS) and corresponds to decreased *PTEN* expression levels (37, 38); in contrast, our data suggests that *PTEN* loss is an unlikely driver of UPS sarcomagenesis, as the majority of patient tumor samples (96%) exhibited PTEN immunostaining. However, a previous study identified several discrepancies between PTEN IHC and array comparative genomic hybridization results, suggesting a potential bias in IHC (236). Interrogation of an expanded cohort of UPS patient tumor samples at the genomic and transcriptomic

levels could provide a clearer assessment of the *PTEN* status in these tumors and better articulate the role of PTEN in UPS tumorigenesis.

The upregulation and/or constitutive activation of RTKs are known drivers of oncogenesis in multiple subtypes of STS (235, 237-239). To date, no mutations in candidate RTKs have been detected in UPS patient samples or cell strains/cell lines (240). Data from Specific Aim 1 demonstrates that there is differential expression of several RTKs: AXL, EGFR, MET, and IGF1R in tumors from our UPS patient cohort. Not only do these receptors represent potential activators of PI3K/mTOR signaling and other protumorigenic pathways (i.e. MAPK), but they could be exploited as molecular prognosticators of patient survival, predictive biomarkers for therapy response, and targets for antitumor therapy. However, the contributions of these RTKs in UPS tumorigenesis are not yet fully understood and should be the topic of future investigations.

While defining the specific mechanism of PI3K/mTOR activation was out of the scope of this dissertation, we identified that this pathway is indeed upregulated in UPS patient-derived tumor samples, cell strains, and cell lines and therefore is an attractive candidate for anti-UPS targeted therapy. In order to assess the contributions of this pathway to UPS tumorigenesis, we used three different small molecule inhibitors against PI3K and mTOR signaling both *in vitro* and *in vivo*.

PI-103 and XL765 attenuated PI3K/mTOR signaling and reduced *in vitro* cell proliferation, migration, and invasion at micromolar concentrations within the range of EC50s calculated for other human tumor cell lines (151, 159, 170, 232, 241). In contrast, low nanomolar concentrations of BGT226 were sufficient to completely abrogate pathway activation, cause potent antiproliferative effects, and effectively block

cell migration and invasion, similar to the results obtained in other tumor types (152, 157, 158, 166, 172, 242). Administration of these dual PI3K/mTOR inhibitors as single agents in a UPS mouse model was sufficient to reduce, but not eliminate, *in vivo* tumorigenicity as well as block the activation of PI3K and mTOR effectors. In addition, cell proliferation and death (as measured by Ki67 and CC3 immunostaining, respectively) were virtually unaltered in xenografts following BGT226 treatment. The continued growth, albeit delayed, of UPS xenografts treated with any of these PI3K/mTOR inhibitors combined with the lack of antiproliferative effects following BGT226 treatment suggested that compensatory signaling pathways were activated in response to treatment and were able to promote tumor progression.

Similar to previous studies, we found that dual PI3K/mTOR inhibitors prevented the compensatory activation of AKT following treatment with rapalogues or other mTOR kinase inhibitors observed in previous studies (140, 143, 148, 149). However, other mechanisms of resistance have been reported. The PI3K/mTOR pathway and the MAPK pathway negatively regulate one another; the blockade of one pathway releases the inhibitory hold on the other and, in essence, promotes the activation of that pathway. Several studies have demonstrated increased MAPK activity in tumor cells treated with anti-PI3K/mTOR therapy; co-inhibition of these pathways is currently being evaluated in preclinical studies and clinical trials (141, 169, 182, 231, 243, 244). In our study, we noted an increase in MEK1/2 phosphorylation in UPS cells treated with increasing concentrations of XL765 without any effect on the activation of the downstream effector kinase ERK; in addition, no such compensation was detected in UPS cells after incubation with BGT226. These data indicate that the MAPK pathway is most likely not involved in acquired resistance to BGT226 treatment and therefore co-

targeting this pathway would have minimal effects on tumorigenesis. Immunoblot analysis revealed that IGF1R is activated in response to PI3K/mTOR inhibition following XL765 or BGT226 treatment; furthermore, immunostaining for pIGF1R in BGT226-treated xenografts detected increased activation of the receptor when compared to the control.

Previous studies have reported that IGF1R expression and activation increases in response to targeted inhibition of PI3K/mTOR signaling components. AKT negatively regulates the FOXO family of transcription factors through phosphorylation-mediated nuclear import prevention. Anti-AKT therapy in a panel of human cancer cell lines representing multiple tumor types increased the expression of several RTKs, including IGF1R, which was dependent on FOXO transcriptional activity; furthermore, the activation status of these RTKs was elevated relative to the untreated control (142). We did not assess the status of FOXO-dependent *IGF1R* transcription in this study; however, we did note a slight increase in the protein levels of total IGF1R after long-term (96 hour) BGT226 treatment. As increased pIGF1R was detected after 2 hours of BGT226 treatment, it is likely that activation in response to PI3K/mTOR inhibition occurs independently of IGF1R protein expression, although increased protein levels may enhance activation status. Additional studies into the mechanism of IGF1R upregulation following PI3K/mTOR inhibition are warranted.

Our data, along with other preclinical and clinical studies, support the co-targeting of PI3K/mTOR pathway components along with IGF1R to enhance the antitumorigenic effects of either single agent. Treatment of acute myeloid leukemia cells with the rapalogue RAD001 resulted in compensatory activation of AKT; co-treatment of these cells with RA001 and an anti-IGF1R mAb prevented the increase in pAKT expression

(148). Inhibition of PI3K/mTOR catalytic activity in matrix-attached ovarian cancer cell lines using the small molecule inhibitor BEZ235 resulted in increased IGF1R expression and activation; subsequent knockdown of IGF1R restored sensitivity to the drug (145). Similarly, synergistic interactions between a small molecule inhibitor against PI3K and an anti-IGF1R mAb attenuating IGF1-stimulated growth in a hematopoietic cell line model (217). In addition, several clinical trials have evaluated the combination of IGF1R inhibition with targeted therapy against mTOR in patients with advanced solid tumors to varying degrees of anticancer efficacy (223, 225).

Calculated CI values denoted strong synergistic drug interactions between BGT226 and AEW541. Incubation with these synergistic concentrations did not substantially improve the overall drug efficacy despite the strong suppression of PI3K/mTOR pathway activation. This is consistent with other studies demonstrating that PI3K/mTOR inhibitors generally result in a G_0/G_1 arrest, as this pathway regulates cell proliferation by the regulation of G_1 cyclins and CDKis at the transcript and protein levels (245, 246); however, cytotoxic effects have been reported and are usually dependent on drug concentration (152, 157, 158, 166, 168, 170, 247). Similarly, the effects of targeted inhibition of IGF1R using AEW541 are generally cytostatic and results in a G_1 cell cycle arrest; apoptosis following AEW541 treatment has been reported, but is highly dependent on cell sensitivity, drug concentration, and incubation time (212, 248-251). Likewise, in our study, the reduction in cell viability observed with single agent BGT226 or AEW541 is largely attributed to a G_1 cell cycle arrest and to a lesser extent an induction of apoptosis, albeit with higher doses of drug. While anti-IGF1R therapy can potentiate the cytotoxic effects of systemic chemotherapy (219, 252), combination treatment using small molecule inhibitors against IGF1R and

PI3K/mTOR did not substantially increase the induction of apoptosis; rather, it merely enhanced the G_1 cell cycle arrest in both cell lines evaluated.

A previous study showed that pharmacologic blockade of PI3K and mTOR catalytic activity did not strongly affect metastatic breast cancer cell proliferation; however, the migratory and invasive capacities of these cells were significantly impaired as a result of decreased levels of cytoplasmic p27 (121). Similarly, UPS cell migration and invasion was strongly downregulated by targeted inhibition of PI3K, mTOR, and IGF1R, despite minimal effects on cell proliferation, cell cycle progression, and apoptosis. Furthermore, co-treatment resulted in a significant decrease of cytoplasmic p27 while concomitantly increasing nuclear levels of the protein; these alterations in p27 localization corresponded to an increase of RhoA activity. In addition, the increased levels of nuclear p27 could result in a G_1 cell cycle arrest and thus reduce UPS cell proliferation. Interestingly, the levels of cytoplasmic p27 decreased dramatically with single agent BGT226 treatment without affecting cell motility, though this could be attributed to the lack of IGF1 stimulation prior to fractionation. Our data shows that IGF1 stimulation renders UPS cells insensitive to the negative effects of BGT226 on migration and invasion. It is possible that IGF1-mediated IGF1R stimulation increases cytoplasmic p27 to a level that cannot be affected by BGT226 treatment.

While the cytoplasmic localization of p27 and corresponding inhibition of RhoA activity surely contribute to UPS cell motility, it is evident that additional mechanisms of cell migration and invasion are involved. Both mTORC1 and mTORC2 have been shown to facilitate IGF1-stimulated cell migration (253). Furthermore, mTORC2 has been demonstrated to regulate actin cytoskeleton reorganization and cell migration through Rho family GTPase activity (254, 255). Activation of Rac1 in response to PI3K

activity requires the Rac GEF PIP_3-dependent Rac exchanger 1 (P-REX1) and is essential for lamellopodia formation in response to growth factor stimulation (256). A previous study reported that P-REX1 can be activated by IGF1 and enhances the IGF1-mediated phosphorylation of AKT through direct interaction; furthermore, P-REX1 can also interact with mTORC2 to promote Rac1 activation (92, 257). In addition, constitutively active AKT can enhance Rac1 activation and vice versa, indicating the potential for a positive feedback loop during PI3K-mediated cell migration (258). Our data demonstrate that phosphorylation of AKT at S473 is abrogated by co-treatment, indicating that mTORC2 function is compromised. Co-treatment with AEW541 and BGT226 inhibit IGF1R and mTORC2, which could suppress Rac1 activity through the elimination of the P-REX1/mTORC2 interaction and thus reduce cell migration. Investigations regarding the pro-migratory activity of mTORC2 and its effect on Rac1 activation following co-treatment with BGT226 and AEW541 should be conducted to better articulate its role in UPS cell migration and invasion.

In addition, IGF1R activation and resulting downstream PI3K/mTOR signaling regulates several matrix metalloproteinases (MMPs) which degrade both extracellular matrix and non-matrix substrates in order to facilitate cell migration and invasion (259-263). In addition, MMPs can increase IGF1 bioavailability through the degradation of insulin-like growth factor binding proteins and thus enhance IGF1R activation and promote cell survival and growth during the invasion process (264-266). The co-inhibition of IGF1R and PI3K/mTOR could substantially reduce MMP production and explain the profound decrease in UPS cell invasion observed *in vitro*. Future studies should evaluate the levels of MMP production and secretion following combined inhibition of IGF1R, PI3K, and mTOR.

Although *in vitro* cell viability was not greatly affected by BGT226 and AEW541 at synergistic concentrations, the "vertical blockade" – that is, targeting multiple components within the same pathway – has proven effective in mouse models of other cancers targeting PI3K/mTOR signaling (167, 267-269). Indeed, we found that combination therapy administered to a mouse model of UPS resulted in drastically decreased tumor volume and weight when compared to the control which could attributed in part to a reduction in cell proliferation as well as improved target inhibition. However, we did not observe complete reduction in tumor cell proliferation, nor any difference in apoptotic cell death that could account for the significant difference in tumor volume and weight between the combination-treated and the control arms. Given the importance of PI3K/mTOR signaling and IGF1R activity for invasive tumor growth and angiogenesis (62, 160, 212, 270-275), co-targeting of PI3K, mTOR, and IGF1R would have a substantial negative effect on these tumorigenic processes, thus limiting the supply of nutrients and oxygen to tumor cells and preventing primary tumor expansion and metastatic spread, while possibly promoting cell death in an apoptosis-independent manner.

Excitingly, one tumor completely regressed within two weeks of treatment onset, suggesting that combination therapy may be highly effective in UPS, resulting in disease-stabilization or instances of tumor regression. However, an increase in tumor growth, though slight, was noted in the remaining animals receiving combination treatment, suggesting that long term treatment may reveal other potential mechanisms of adaptive resistance (i.e. activation of the MAPK pathway or an oncogenic RTK) which could be incorporated into combination therapy. Future studies should focus on

the effect of *in vivo* combination therapy on long-term survival while exploring the possibility for compensatory activation of other protumorigenic molecules or pathways.

Numerous preclinical studies have supported developing anti-IGF1R targeted therapies for the treatment of different human malignancies (193-195, 202, 205, 208, 212). Phase I and II clinical trials evaluating mAbs against IGF1R for the treatment of advanced solid tumors of various histologies demonstrated anticancer activity in some patients (209, 224, 276-280); however, the majority of advanced phase clinical trials evaluating IGF1R as a therapeutic target have been discontinued due to a lack of efficacy in the majority of patients (213-216). Targeting IGF1R with mAbs increases receptor internalization, while IR expression increases in response to anti-IGF1R therapy (213). In addition, targeted inhibition of IGF1R has been linked to dysregulated endocrine signaling, which promotes growth hormone production and the subsequent increase in IGF1 and insulin production (213). The resulting increase in IR activation could attenuate the antitumor response to IGF1R inhibition or even promote disease progression in the presence of treatment (191, 208).

Despite the disappointing reports from Phase II and III clinical trials, evidence demonstrating anti-IGF1R efficacy in some patients raises the possibility that a subset of patients could benefit from this type of therapy and highlights the need for predictive biomarkers to identify these populations. We found that pIGF1R expression correlated to poorer OS and DSS in our cohort of sporadic and RA-UPS patients. In addition, total and activated IGF1R were more highly expressed in RA-UPS patient tumors samples compared to the majority of sporadic UPS samples. However, a small subset (25-30%) of sporadic UPS tumor samples expressed high levels of IGF1R and pIGF1R. RA-UPS are generally more aggressive than sporadic UPS, as illustrated by the dramatically

shortened DSS times and higher propensity for recurrent disease in RA-UPS patients (60); however, no known molecular alterations have yet been identified as unique markers of disease setting. While no protein markers in our panel could differentiate between disease settings with complete specificity, pIGF1R may indicate overall disease aggressiveness, as it was expressed predominantly in RA-UPS and in a subset of sporadic UPS. Further studies should include samples representative of recurrent and metastatic disease when examining the utility of pIGF1R as a biomarker for disease stage, patient response to therapy, and DSS times.

These data are further supported by our *in vitro* results. pIGF1R expression is elevated in response to PI3K/mTOR inhibition both *in vitro* and *in vivo* and combined inhibition of all three molecules using BGT226 and AEW541 is synergistic. Interestingly, the RA-UPS-derived cell line RIS-819.1 was more sensitive to targeted inhibition of PI3K, mTOR, and IGF1R than the sporadic UPS cell line UPS-186 as evidenced by increased apoptosis with single agent or combination treatment and an enhanced G_1 cell cycle arrest following co-treatment. However, UPS-186 still exhibited compensatory IGF1R activation in response to PI3K/mTOR signaling blockade and was sensitive to combined inhibition with BGT226 and AEW541. Together, these observations and data indicate that activated IGF1R may not necessarily differentiate between disease settings, but rather could be utilized as a marker of tumor aggression, a predictor of patient response to therapy, and/or a molecular prognosticator of survival.

Conclusions and future directions

UPS is a devastating malignancy for which there are limited therapeutic options for patients and no known biomarkers to predict patient response to therapy. In this study, we demonstrate that targeted PI3K, mTOR, and IGF1R in tandem exerts strong synergistic antitumor effects *in vivo* and downregulates UPS cell migration and invasion in part through the cytoplasmic sequestration of p27. Our data support co-targeting this pathway in a vertical blockade as a novel therapeutic avenue for these patients. In addition, we propose that IGF1R is a molecular prognosticator for patient outcome and may be useful in the identification of extremely aggressive subtypes of RA and sporadic UPS. Future investigations are necessary to understand the complete mechanism by which IGF1R and PI3K/mTOR signaling regulate UPS cell migration and invasion in addition to modulation of p27 subcellular localization. Additionally, the interrogation of IGF1R and components of the PI3K/mTOR pathway could further validate the utility of these molecules as predictive biomarkers for UPS patient response to therapy; in addition, studies examining the effects of combined inhibition of PI3K, mTOR, and IGF1R on long-term survival could provide additional support the evaluation of this combination cohorts of UPS patients.

Chapter 8

Appendices

Appendix 1

The manuscript described below has been submitted for publication and involves the data discussed in Specific Aim 2 and Specific Aim 3 from this dissertation.

May CD, Bolshakov S, Landers SM, Ingram DR, Ma XY, Kivlin CM, Kalam AA, Lazar AJ, and Torres KE. *Co-targeting PI3K, mTOR, and IGF1R with small molecule inhibitors for the treatment of undifferentiated pleomorphic sarcoma.* Submitted for publication.

Appendix 2

The manuscript described below has been submitted for publication and involves the data discussed in Specific Aim 1 from this dissertation. Data from this Aim were previously presented at the 68th Society for Surgical Oncology Annual Cancer Symposium, March 2015, Houston, Texas.

Roland CL, Dineen SP, Watson KL, Al Sannaa GA, Feig R, **May CD**, Ingram DR, Wang WL, Lazar AJ, Ravi V, Hunt KK, Cormier JN, Feig BW, and Torres KE. *Variations in Protein Expression are Associated with Survival Outcomes in Patients with Undifferentiated Pleomorphic Sarcomas.* Submitted for the 68th Society of Surgical Oncology Annual Cancer Symposium, March 25-28, 2015, Houston, Texas.

Appendix 3

The manuscript described below has been submitted for publication and contains data from a side project investigating the receptor tyrosine kinase AXL for its role in liposarcomagenesis.

May CD, Garnett J, Ma XY, Ingram DR, Al-Sannaa GA, Demicco EG, Han L, Zhang Y, Kivlin CM, Bolshakov S, Landers SM, Kalam AA, Wang WL, Lazar AJ, Pollock RE, Lev D, and Torres KE. *Role of AXL as a potential therapeutic target for pleomorphic and dedifferentiated liposarcomas.* Submitted for publication.

Chapter 9

References

1. Siegel RL, Miller KD, Jemal A. Cancer statistics, 2015. CA Cancer J Clin. 2015;65:5-29.

2. Koscielniak E, Morgan M, Treuner J. Soft tissue sarcoma in children: prognosis and management. Paediatr Drugs. 2002;4:21-8.

3. Singer S, Demetri GD, Baldini EH, Fletcher CD. Management of soft-tissue sarcomas: an overview and update. Lancet Oncol. 2000;1:75-85.

4. Brennan MF, Antonescu CR, Maki RG. Management of soft tissue sarcoma. New York: Springer; 2013.

5. Goldblum JR, Folpe AL, Weiss SW, Enzinger FM, Weiss SW. Enzinger and Weiss's soft tissue tumors. 6th ed. Philadelphia, PA: Saunders/Elsevier; 2014.

6. Gustafson P. Soft tissue sarcoma. Epidemiology and prognosis in 508 patients. Acta Orthop Scand Suppl. 1994;259:1-31.

7. American Cancer Society. Cancer Facts & Figures 2015. Atlanta: American Cancer Society; 2015.

8. Howlader N, Noone A, Krapcho M. SEER Cancer Statistics Review, 1975-2011, based on November 2013 SEER data submission, posted to the SEER web site, April 2014. Bethesda, MD: National Cancer Institute. 2014.

9. Riggi N, Cironi L, Suva ML, Stamenkovic I. Sarcomas: genetics, signalling, and cellular origins. Part 1: The fellowship of TET. J Pathol. 2007;213:4-20.

10. Wardelmann E, Schildhaus HU, Merkelbach-Bruse S, Hartmann W, Reichardt P, Hohenberger P, Buttner R. Soft tissue sarcoma: from molecular diagnosis to selection of treatment. Pathological diagnosis of soft tissue sarcoma amid molecular biology and targeted therapies. Ann Oncol. 2010;21 Suppl 7:vii265-9.

11. Helman LJ, Meltzer P. Mechanisms of sarcoma development. Nat Rev Cancer. 2003;3:685-94.

12. van de Rijn M, Fletcher JA. Genetics of soft tissue tumors. Annu Rev Pathol. 2006;1:435-66.

13. Guillou L, Aurias A. Soft tissue sarcomas with complex genomic profiles. Virchows Arch. 2010;456:201-17.

14. Goldblum JR. An approach to pleomorphic sarcomas: can we subclassify, and does it matter? Mod Pathol. 2014;27 Suppl 1:S39-46.

15. Kelleher FC, Viterbo A. Histologic and genetic advances in refining the diagnosis of "undifferentiated pleomorphic sarcoma". Cancers (Basel). 2013;5:218-33.

16. Dei Tos AP. Classification of pleomorphic sarcomas: where are we now? Histopathology. 2006;48:51-62.

17. Ozzello L, Stout AP, Murray MR. Cultural characteristics of malignant histiocytomas and fibrous xanthomas. Cancer. 1963;16:331-44.

18. O'Brien JE, Stout AP. Malignant Fibrous Xanthomas. Cancer. 1964;17:1445-55.

19. Enzinger FM, Weiss SW. Soft tissue tumors. St. Louis: Mosby; 1983.

20. Enzinger FM. Malignant fibrous histiocytoma 20 years after Stout. Am J Surg Pathol. 1986;10 Suppl 1:43-53.

21. Matushansky I, Charytonowicz E, Mills J, Siddiqi S, Hricik T, Cordon-Cardo C. MFH classification: differentiating undifferentiated pleomorphic sarcoma in the 21st Century. Expert Rev Anticancer Ther. 2009;9:1135-44.

22. Fletcher CD. The evolving classification of soft tissue tumours: an update based on the new WHO classification. Histopathology. 2006;48:3-12.

23. Hollowood K, Fletcher CD. Malignant fibrous histiocytoma: morphologic pattern or pathologic entity? Semin Diagn Pathol. 1995;12:210-20.

24. Meister P. Malignant fibrous histiocytoma: histomorphological pattern or tumor type. Pathol Res Pract. 1996;192:877-81.

25. Fletcher CD. Pleomorphic malignant fibrous histiocytoma: fact or fiction? A critical reappraisal based on 159 tumors diagnosed as pleomorphic sarcoma. Am J Surg Pathol. 1992;16:213-28.

26. Fletcher CD, Gustafson P, Rydholm A, Willen H, Akerman M. Clinicopathologic re-evaluation of 100 malignant fibrous histiocytomas: prognostic relevance of subclassification. J Clin Oncol. 2001;19:3045-50.

27. Montgomery E, Fisher C. Myofibroblastic differentiation in malignant fibrous histiocytoma (pleomorphic myofibrosarcoma): a clinicopathological study. Histopathology. 2001;38:499-509.

28. Nakayama R, Nemoto T, Takahashi H, Ohta T, Kawai A, Seki K, Yoshida T, Toyama Y, Ichikawa H, Hasegawa T. Gene expression analysis of soft tissue sarcomas: characterization and reclassification of malignant fibrous histiocytoma. Mod Pathol. 2007;20:749-59.

29. Wood GS, Beckstead JH, Turner RR, Hendrickson MR, Kempson RL, Warnke RA. Malignant fibrous histiocytoma tumor cells resemble fibroblasts. Am J Surg Pathol. 1986;10:323-35.

30. Fletcher CDM, Unni KK, Mertens F. Pathology and Genetics of Soft Tissue and Bone: World Health Organization Classification of Tumors. Lyon, France: IARC Press; 2002.

31. Fletcher CDM, Bridge JA, Hogendoom PCW, Mertens F. World health organization classification of tumours of soft tissue and bone. 4th ed: Lyon: IARC press; 2013.

32. Siegel R, Naishadham D, Jemal A. Cancer statistics, 2012. CA Cancer J Clin. 2012;62:10-29.

33. Xiao W, Mohseny AB, Hogendoorn PC, Cleton-Jansen AM. Mesenchymal stem cell transformation and sarcoma genesis. Clin Sarcoma Res. 2013;3:10.

34. Rodriguez R, Rubio R, Menendez P. Modeling sarcomagenesis using multipotent mesenchymal stem cells. Cell Res. 2012;22:62-77.

35. Matushansky I, Hernando E, Socci ND, Mills JE, Matos TA, Edgar MA, Singer S, Maki RG, Cordon-Cardo C. Derivation of sarcomas from mesenchymal stem cells via inactivation of the Wnt pathway. J Clin Invest. 2007;117:3248-57.

36. Li Q, Hisha H, Takaki T, Adachi Y, Li M, Song C, Feng W, Okazaki S, Mizokami T, Kato J, Inaba M, Hosaka N, Maki M, Ikehara S. Transformation potential of bone

marrow stromal cells into undifferentiated high-grade pleomorphic sarcoma. J Cancer Res Clin Oncol. 2010;136:829-38.

37. Silveira SM, Villacis RA, Marchi FA, Barros Filho Mde C, Drigo SA, Neto CS, Lopes A, da Cunha IW, Rogatto SR. Genomic signatures predict poor outcome in undifferentiated pleomorphic sarcomas and leiomyosarcomas. PLoS One. 2013;8:e67643.

38. Gibault L, Perot G, Chibon F, Bonnin S, Lagarde P, Terrier P, Coindre JM, Aurias A. New insights in sarcoma oncogenesis: a comprehensive analysis of a large series of 160 soft tissue sarcomas with complex genomics. J Pathol. 2011;223:64-71.

39. Derre J, Lagace R, Nicolas A, Mairal A, Chibon F, Coindre JM, Terrier P, Sastre X, Aurias A. Leiomyosarcomas and most malignant fibrous histiocytomas share very similar comparative genomic hybridization imbalances: an analysis of a series of 27 leiomyosarcomas. Lab Invest. 2001;81:211-5.

40. Nielsen TO, West RB, Linn SC, Alter O, Knowling MA, O'Connell JX, Zhu S, Fero M, Sherlock G, Pollack JR, Brown PO, Botstein D, van de Rijn M. Molecular characterisation of soft tissue tumours: a gene expression study. Lancet. 2002;359:1301-7.

41. Carneiro A, Francis P, Bendahl PO, Fernebro J, Akerman M, Fletcher C, Rydholm A, Borg A, Nilbert M. Indistinguishable genomic profiles and shared prognostic markers in undifferentiated pleomorphic sarcoma and leiomyosarcoma: different sides of a single coin? Lab Invest. 2009;89:668-75.

42. Lee YF, John M, Edwards S, Clark J, Flohr P, Maillard K, Edema M, Baker L, Mangham DC, Grimer R, Wooster R, Thomas JM, Fisher C, Judson I, Cooper CS.

Molecular classification of synovial sarcomas, leiomyosarcomas and malignant fibrous histiocytomas by gene expression profiling. Br J Cancer. 2003;88:510-5.

43. Francis P, Namlos HM, Muller C, Eden P, Fernebro J, Berner JM, Bjerkehagen B, Akerman M, Bendahl PO, Isinger A, Rydholm A, Myklebost O, Nilbert M. Diagnostic and prognostic gene expression signatures in 177 soft tissue sarcomas: hypoxia-induced transcription profile signifies metastatic potential. BMC Genomics. 2007;8:73.

44. Schmitt T, Kasper B. New medical treatment options and strategies to assess clinical outcome in soft-tissue sarcoma. Expert Rev Anticancer Ther. 2009;9:1159-67.

45. Nascimento AF, Raut CP. Diagnosis and management of pleomorphic sarcomas (so-called "MFH") in adults. J Surg Oncol. 2008;97:330-9.

46. Donato Di Paola E, Nielsen OS, Tissue ES, Bone Sarcoma G. The EORTC soft tissue and bone sarcoma group. European Organisation for Research and Treatment of Cancer. Eur J Cancer. 2002;38 Suppl 4:S138-41.

47. Chugh R, Wathen JK, Maki RG, Benjamin RS, Patel SR, Meyers PA, Priebat DA, Reinke DK, Thomas DG, Keohan ML, Samuels BL, Baker LH. Phase II multicenter trial of imatinib in 10 histologic subtypes of sarcoma using a bayesian hierarchical statistical model. J Clin Oncol. 2009;27:3148-53.

48. Maki RG, D'Adamo DR, Keohan ML, Saulle M, Schuetze SM, Undevia SD, Livingston MB, Cooney MM, Hensley ML, Mita MM, Takimoto CH, Kraft AS, Elias AD, Brockstein B, Blachere NE, Edgar MA, Schwartz LH, Qin LX, Antonescu CR, Schwartz GK. Phase II study of sorafenib in patients with metastatic or recurrent sarcomas. J Clin Oncol. 2009;27:3133-40.

49. George S, Merriam P, Maki RG, Van den Abbeele AD, Yap JT, Akhurst T, Harmon DC, Bhuchar G, O'Mara MM, D'Adamo DR, Morgan J, Schwartz GK, Wagner

AJ, Butrynski JE, Demetri GD, Keohan ML. Multicenter phase II trial of sunitinib in the treatment of nongastrointestinal stromal tumor sarcomas. J Clin Oncol. 2009;27:3154-60.

50. Sleijfer S, Ray-Coquard I, Papai Z, Le Cesne A, Scurr M, Schoffski P, Collin F, Pandite L, Marreaud S, De Brauwer A, van Glabbeke M, Verweij J, Blay JY. Pazopanib, a multikinase angiogenesis inhibitor, in patients with relapsed or refractory advanced soft tissue sarcoma: a phase II study from the European organisation for research and treatment of cancer-soft tissue and bone sarcoma group (EORTC study 62043). J Clin Oncol. 2009;27:3126-32.

51. Salo JC, Lewis JJ, Woodruff JM, Leung DH, Brennan MF. Malignant fibrous histiocytoma of the extremity. Cancer. 1999;85:1765-72.

52. Le Doussal V, Coindre JM, Leroux A, Hacene K, Terrier P, Bui NB, Bonichon F, Collin F, Mandard AM, Contesso G. Prognostic factors for patients with localized primary malignant fibrous histiocytoma: a multicenter study of 216 patients with multivariate analysis. Cancer. 1996;77:1823-30.

53. Zagars GK, Mullen JR, Pollack A. Malignant fibrous histiocytoma: outcome and prognostic factors following conservation surgery and radiotherapy. Int J Radiat Oncol Biol Phys. 1996;34:983-94.

54. Engellau J, Anderson H, Rydholm A, Bauer HC, Hall KS, Gustafson P, Akerman M, Meis-Kindblom J, Alvegard TA, Nilbert M, Scandinavian Sarcoma G. Time dependence of prognostic factors for patients with soft tissue sarcoma: a Scandinavian Sarcoma Group Study of 338 malignant fibrous histiocytomas. Cancer. 2004;100:2233-9.

55. Mark RJ, Poen JC, Tran LM, Fu YS, Juillard GF. Angiosarcoma. A report of 67 patients and a review of the literature. Cancer. 1996;77:2400-6.

56. Gladdy RA, Qin LX, Moraco N, Edgar MA, Antonescu CR, Alektiar KM, Brennan MF, Singer S. Do radiation-associated soft tissue sarcomas have the same prognosis as sporadic soft tissue sarcomas? J Clin Oncol. 2010;28:2064-9.

57. Laskin WB, Silverman TA, Enzinger FM. Postradiation soft tissue sarcomas. An analysis of 53 cases. Cancer. 1988;62:2330-40.

58. Riad S, Biau D, Holt GE, Werier J, Turcotte RE, Ferguson PC, Griffin AM, Dickie CI, Chung PW, Catton CN, O'Sullivan B, Wunder JS. The clinical and functional outcome for patients with radiation-induced soft tissue sarcoma. Cancer. 2012;118:2682-92.

59. Cha C, Antonescu CR, Quan ML, Maru S, Brennan MF. Long-term results with resection of radiation-induced soft tissue sarcomas. Ann Surg. 2004;239:903-9; discussion 9-10.

60. Dineen SP, Roland CL, Feig R, May C, Zhou S, Demicco E, Sannaa GA, Ingram D, Wang WL, Ravi V, Guadagnolo A, Lev D, Pollock RE, Hunt K, Cormier J, Lazar A, Feig B, Torres KE. Radiation-Associated Undifferentiated Pleomorphic Sarcoma is Associated with Worse Clinical Outcomes than Sporadic Lesions. Ann Surg Oncol. 2015.

61. Thorpe LM, Yuzugullu H, Zhao JJ. PI3K in cancer: divergent roles of isoforms, modes of activation and therapeutic targeting. Nat Rev Cancer. 2014;15:7-24.

62. Engelman JA. Targeting PI3K signalling in cancer: opportunities, challenges and limitations. Nat Rev Cancer. 2009;9:550-62.

63. Rameh LE, Chen CS, Cantley LC. Phosphatidylinositol (3,4,5)P3 interacts with SH2 domains and modulates PI 3-kinase association with tyrosine-phosphorylated proteins. Cell. 1995;83:821-30.

64. Yu J, Wjasow C, Backer JM. Regulation of the p85/p110alpha phosphatidylinositol 3'-kinase. Distinct roles for the n-terminal and c-terminal SH2 domains. J Biol Chem. 1998;273:30199-203.

65. Pal I, Mandal M. PI3K and Akt as molecular targets for cancer therapy: current clinical outcomes. Acta Pharmacol Sin. 2012;33:1441-58.

66. Sarbassov DD, Guertin DA, Ali SM, Sabatini DM. Phosphorylation and regulation of Akt/PKB by the rictor-mTOR complex. Science. 2005;307:1098-101.

67. Vanhaesebroeck B, Stephens L, Hawkins P. PI3K signalling: the path to discovery and understanding. Nat Rev Mol Cell Biol. 2012;13:195-203.

68. Stambolic V, Woodgett JR. Functional distinctions of protein kinase B/Akt isoforms defined by their influence on cell migration. Trends Cell Biol. 2006;16:461-6.

69. Ridley AJ, Schwartz MA, Burridge K, Firtel RA, Ginsberg MH, Borisy G, Parsons JT, Horwitz AR. Cell migration: integrating signals from front to back. Science. 2003;302:1704-9.

70. Laplante M, Sabatini DM. mTOR signaling in growth control and disease. Cell. 2012;149:274-93.

71. Chiarini F, Evangelisti C, McCubrey JA, Martelli AM. Current treatment strategies for inhibiting mTOR in cancer. Trends Pharmacol Sci. 2014.

72. Zhou H, Huang S. mTOR signaling in cancer cell motility and tumor metastasis. Crit Rev Eukaryot Gene Expr. 2010;20:1-16.

73. Shimobayashi M, Hall MN. Making new contacts: the mTOR network in metabolism and signalling crosstalk. Nat Rev Mol Cell Biol. 2014;15:155-62.

74. Laplante M, Sabatini DM. mTOR signaling at a glance. J Cell Sci. 2009;122:3589-94.

75. Sabatini DM. mTOR and cancer: insights into a complex relationship. Nat Rev Cancer. 2006;6:729-34.

76. Vezina C, Kudelski A, Sehgal SN. Rapamycin (AY-22,989), a new antifungal antibiotic. I. Taxonomy of the producing streptomycete and isolation of the active principle. J Antibiot (Tokyo). 1975;28:721-6.

77. Sarbassov DD, Ali SM, Sengupta S, Sheen JH, Hsu PP, Bagley AF, Markhard AL, Sabatini DM. Prolonged rapamycin treatment inhibits mTORC2 assembly and Akt/PKB. Mol Cell. 2006;22:159-68.

78. Inoki K, Li Y, Zhu T, Wu J, Guan KL. TSC2 is phosphorylated and inhibited by Akt and suppresses mTOR signalling. Nat Cell Biol. 2002;4:648-57.

79. Manning BD, Tee AR, Logsdon MN, Blenis J, Cantley LC. Identification of the tuberous sclerosis complex-2 tumor suppressor gene product tuberin as a target of the phosphoinositide 3-kinase/akt pathway. Mol Cell. 2002;10:151-62.

80. Potter CJ, Pedraza LG, Xu T. Akt regulates growth by directly phosphorylating Tsc2. Nat Cell Biol. 2002;4:658-65.

81. Inoki K, Li Y, Xu T, Guan KL. Rheb GTPase is a direct target of TSC2 GAP activity and regulates mTOR signaling. Genes Dev. 2003;17:1829-34.

82. Tee AR, Manning BD, Roux PP, Cantley LC, Blenis J. Tuberous sclerosis complex gene products, Tuberin and Hamartin, control mTOR signaling by acting as a GTPase-activating protein complex toward Rheb. Curr Biol. 2003;13:1259-68.

83. Long X, Lin Y, Ortiz-Vega S, Yonezawa K, Avruch J. Rheb binds and regulates the mTOR kinase. Curr Biol. 2005;15:702-13.

84. Song MS, Salmena L, Pandolfi PP. The functions and regulation of the PTEN tumour suppressor. Nat Rev Mol Cell Biol. 2012;13:283-96.

85. Populo H, Lopes JM, Soares P. The mTOR signalling pathway in human cancer. Int J Mol Sci. 2012;13:1886-918.

86. Nojima H, Tokunaga C, Eguchi S, Oshiro N, Hidayat S, Yoshino K, Hara K, Tanaka N, Avruch J, Yonezawa K. The mammalian target of rapamycin (mTOR) partner, raptor, binds the mTOR substrates p70 S6 kinase and 4E-BP1 through their TOR signaling (TOS) motif. J Biol Chem. 2003;278:15461-4.

87. Gingras AC, Gygi SP, Raught B, Polakiewicz RD, Abraham RT, Hoekstra MF, Aebersold R, Sonenberg N. Regulation of 4E-BP1 phosphorylation: a novel two-step mechanism. Genes Dev. 1999;13:1422-37.

88. Sonenberg N, Gingras AC. The mRNA 5' cap-binding protein eIF4E and control of cell growth. Curr Opin Cell Biol. 1998;10:268-75.

89. Jastrzebski K, Hannan KM, Tchoubrieva EB, Hannan RD, Pearson RB. Coordinate regulation of ribosome biogenesis and function by the ribosomal protein S6 kinase, a key mediator of mTOR function. Growth Factors. 2007;25:209-26.

90. Ma XM, Blenis J. Molecular mechanisms of mTOR-mediated translational control. Nat Rev Mol Cell Biol. 2009;10:307-18.

91. Gan X, Wang J, Su B, Wu D. Evidence for direct activation of mTORC2 kinase activity by phosphatidylinositol 3,4,5-trisphosphate. J Biol Chem. 2011;286:10998-1002.

92. Kim EK, Yun SJ, Ha JM, Kim YW, Jin IH, Yun J, Shin HK, Song SH, Kim JH, Lee JS, Kim CD, Bae SS. Selective activation of Akt1 by mammalian target of rapamycin complex 2 regulates cancer cell migration, invasion, and metastasis. Oncogene. 2011;30:2954-63.

93. Garcia-Echeverria C. Allosteric and ATP-competitive kinase inhibitors of mTOR for cancer treatment. Bioorg Med Chem Lett. 2010;20:4308-12.

94. Yuan TL, Cantley LC. PI3K pathway alterations in cancer: variations on a theme. Oncogene. 2008;27:5497-510.

95. Rodon J, Dienstmann R, Serra V, Tabernero J. Development of PI3K inhibitors: lessons learned from early clinical trials. Nat Rev Clin Oncol. 2013;10:143-53.

96. Courtney KD, Corcoran RB, Engelman JA. The PI3K pathway as drug target in human cancer. J Clin Oncol. 2010;28:1075-83.

97. West KA, Castillo SS, Dennis PA. Activation of the PI3K/Akt pathway and chemotherapeutic resistance. Drug Resist Updat. 2002;5:234-48.

98. Larrea MD, Wander SA, Slingerland JM. p27 as Jekyll and Hyde: regulation of cell cycle and cell motility. Cell Cycle. 2009;8:3455-61.

99. Chu IM, Hengst L, Slingerland JM. The Cdk inhibitor p27 in human cancer: prognostic potential and relevance to anticancer therapy. Nat Rev Cancer. 2008;8:253-67.

100. Borriello A, Bencivenga D, Criscuolo M, Caldarelli I, Cucciolla V, Tramontano A, Borgia A, Spina A, Oliva A, Naviglio S, Della Ragione F. Targeting p27Kip1 protein: its relevance in the therapy of human cancer. Expert Opin Ther Targets. 2011;15:677-93.

101. Nakayama KI, Hatakeyama S, Nakayama K. Regulation of the cell cycle at the G1-S transition by proteolysis of cyclin E and p27Kip1. Biochem Biophys Res Commun. 2001;282:853-60.

102. Wander SA, Zhao D, Slingerland JM. p27: a barometer of signaling deregulation and potential predictor of response to targeted therapies. Clin Cancer Res. 2011;17:12-8.

103. Besson A, Dowdy SF, Roberts JM. CDK inhibitors: cell cycle regulators and beyond. Dev Cell. 2008;14:159-69.

104. Koff A, Ohtsuki M, Polyak K, Roberts JM, Massague J. Negative regulation of G1 in mammalian cells: inhibition of cyclin E-dependent kinase by TGF-beta. Science. 1993;260:536-9.

105. Polyak K, Kato JY, Solomon MJ, Sherr CJ, Massague J, Roberts JM, Koff A. p27Kip1, a cyclin-Cdk inhibitor, links transforming growth factor-beta and contact inhibition to cell cycle arrest. Genes Dev. 1994;8:9-22.

106. Slingerland JM, Hengst L, Pan CH, Alexander D, Stampfer MR, Reed SI. A novel inhibitor of cyclin-Cdk activity detected in transforming growth factor beta-arrested epithelial cells. Mol Cell Biol. 1994;14:3683-94.

107. Sherr CJ, Roberts JM. CDK inhibitors: positive and negative regulators of G1-phase progression. Genes Dev. 1999;13:1501-12.

108. Grimmler M, Wang Y, Mund T, Cilensek Z, Keidel EM, Waddell MB, Jakel H, Kullmann M, Kriwacki RW, Hengst L. Cdk-inhibitory activity and stability of p27Kip1 are directly regulated by oncogenic tyrosine kinases. Cell. 2007;128:269-80.

109. Chu I, Sun J, Arnaout A, Kahn H, Hanna W, Narod S, Sun P, Tan CK, Hengst L, Slingerland J. p27 phosphorylation by Src regulates inhibition of cyclin E-Cdk2. Cell. 2007;128:281-94.

110. Shanmugasundaram K, Block K, Nayak BK, Livi CB, Venkatachalam MA, Sudarshan S. PI3K regulation of the SKP-2/p27 axis through mTORC2. Oncogene. 2013;32:2027-36.

111. Boehm M, Yoshimoto T, Crook MF, Nallamshetty S, True A, Nabel GJ, Nabel EG. A growth factor-dependent nuclear kinase phosphorylates p27(Kip1) and regulates cell cycle progression. EMBO J. 2002;21:3390-401.

112. Deng X, Mercer SE, Shah S, Ewton DZ, Friedman E. The cyclin-dependent kinase inhibitor p27Kip1 is stabilized in G(0) by Mirk/dyrk1B kinase. J Biol Chem. 2004;279:22498-504.

113. Rodier G, Montagnoli A, Di Marcotullio L, Coulombe P, Draetta GF, Pagano M, Meloche S. p27 cytoplasmic localization is regulated by phosphorylation on Ser10 and is not a prerequisite for its proteolysis. EMBO J. 2001;20:6672-82.

114. Besson A, Gurian-West M, Chen X, Kelly-Spratt KS, Kemp CJ, Roberts JM. A pathway in quiescent cells that controls p27Kip1 stability, subcellular localization, and tumor suppression. Genes Dev. 2006;20:47-64.

115. Connor MK, Kotchetkov R, Cariou S, Resch A, Lupetti R, Beniston RG, Melchior F, Hengst L, Slingerland JM. CRM1/Ran-mediated nuclear export of p27(Kip1) involves a nuclear export signal and links p27 export and proteolysis. Mol Biol Cell. 2003;14:201-13.

116. Liang J, Zubovitz J, Petrocelli T, Kotchetkov R, Connor MK, Han K, Lee JH, Ciarallo S, Catzavelos C, Beniston R, Franssen E, Slingerland JM. PKB/Akt

phosphorylates p27, impairs nuclear import of p27 and opposes p27-mediated G1 arrest. Nat Med. 2002;8:1153-60.

117. Viglietto G, Motti ML, Bruni P, Melillo RM, D'Alessio A, Califano D, Vinci F, Chiappetta G, Tsichlis P, Bellacosa A, Fusco A, Santoro M. Cytoplasmic relocalization and inhibition of the cyclin-dependent kinase inhibitor p27(Kip1) by PKB/Akt-mediated phosphorylation in breast cancer. Nat Med. 2002;8:1136-44.

118. Shin I, Yakes FM, Rojo F, Shin NY, Bakin AV, Baselga J, Arteaga CL. PKB/Akt mediates cell-cycle progression by phosphorylation of p27(Kip1) at threonine 157 and modulation of its cellular localization. Nat Med. 2002;8:1145-52.

119. Sekimoto T, Fukumoto M, Yoneda Y. 14-3-3 suppresses the nuclear localization of threonine 157-phosphorylated p27(Kip1). EMBO J. 2004;23:1934-42.

120. Fujita N, Sato S, Katayama K, Tsuruo T. Akt-dependent phosphorylation of p27Kip1 promotes binding to 14-3-3 and cytoplasmic localization. J Biol Chem. 2002;277:28706-13.

121. Wander SA, Zhao D, Besser AH, Hong F, Wei J, Ince TA, Milikowski C, Bishopric NH, Minn AJ, Creighton CJ, Slingerland JM. PI3K/mTOR inhibition can impair tumor invasion and metastasis in vivo despite a lack of antiproliferative action in vitro: implications for targeted therapy. Breast Cancer Res Treat. 2013;138:369-81.

122. O'Connor K, Chen M. Dynamic functions of RhoA in tumor cell migration and invasion. Small GTPases. 2013;4:141-7.

123. Denicourt C, Dowdy SF. Cip/Kip proteins: more than just CDKs inhibitors. Genes Dev. 2004;18:851-5.

124. Besson A, Gurian-West M, Schmidt A, Hall A, Roberts JM. p27Kip1 modulates cell migration through the regulation of RhoA activation. Genes Dev. 2004;18:862-76.

125. Hernando E, Charytonowicz E, Dudas ME, Menendez S, Matushansky I, Mills J, Socci ND, Behrendt N, Ma L, Maki RG, Pandolfi PP, Cordon-Cardo C. The AKT-mTOR pathway plays a critical role in the development of leiomyosarcomas. Nat Med. 2007;13:748-53.

126. Gutierrez A, Snyder EL, Marino-Enriquez A, Zhang YX, Sioletic S, Kozakewich E, Grebliunaite R, Ou WB, Sicinska E, Raut CP, Demetri GD, Perez-Atayde AR, Wagner AJ, Fletcher JA, Fletcher CD, Look AT. Aberrant AKT activation drives well-differentiated liposarcoma. Proc Natl Acad Sci U S A. 2011;108:16386-91.

127. Demicco EG, Torres KE, Ghadimi MP, Colombo C, Bolshakov S, Hoffman A, Peng T, Bovee JV, Wang WL, Lev D, Lazar AJ. Involvement of the PI3K/Akt pathway in myxoid/round cell liposarcoma. Mod Pathol. 2012;25:212-21.

128. Friedrichs N, Trautmann M, Endl E, Sievers E, Kindler D, Wurst P, Czerwitzki J, Steiner S, Renner M, Penzel R, Koch A, Larsson O, Tanaka S, Kawai A, Schirmacher P, Mechtersheimer G, Wardelmann E, Buettner R, Hartmann W. Phosphatidylinositol-3'-kinase/AKT signaling is essential in synovial sarcoma. Int J Cancer. 2011;129:1564-75.

129. Keng VW, Rahrmann EP, Watson AL, Tschida BR, Moertel CL, Jessen WJ, Rizvi TA, Collins MH, Ratner N, Largaespada DA. PTEN and NF1 inactivation in Schwann cells produces a severe phenotype in the peripheral nervous system that promotes the development and malignant progression of peripheral nerve sheath tumors. Cancer Res. 2012;72:3405-13.

130. Dobashi Y, Suzuki S, Sato E, Hamada Y, Yanagawa T, Ooi A. EGFR-dependent and independent activation of Akt/mTOR cascade in bone and soft tissue tumors. Mod Pathol. 2009;22:1328-40.

131. Tomita Y, Morooka T, Hoshida Y, Zhang B, Qiu Y, Nakamichi I, Hamada K, Ueda T, Naka N, Kudawara I, Aozasa K. Prognostic significance of activated AKT expression in soft-tissue sarcoma. Clin Cancer Res. 2006;12:3070-7.

132. Valkov A, Kilvaer TK, Sorbye SW, Donnem T, Smeland E, Bremnes RM, Busund LT. The prognostic impact of Akt isoforms, PI3K and PTEN related to female steroid hormone receptors in soft tissue sarcomas. J Transl Med. 2011;9:200.

133. Petricoin EF, 3rd, Espina V, Araujo RP, Midura B, Yeung C, Wan X, Eichler GS, Johann DJ, Jr., Qualman S, Tsokos M, Krishnan K, Helman LJ, Liotta LA. Phosphoprotein pathway mapping: Akt/mammalian target of rapamycin activation is negatively associated with childhood rhabdomyosarcoma survival. Cancer Res. 2007;67:3431-40.

134. Saito T, Oda Y, Kawaguchi K, Takahira T, Yamamoto H, Tamiya S, Tanaka K, Matsuda S, Sakamoto A, Iwamoto Y, Tsuneyoshi M. PTEN/MMAC1 gene mutation is a rare event in soft tissue sarcomas without specific balanced translocations. Int J Cancer. 2003;104:175-8.

135. Lahat G, Zhang P, Zhu QS, Torres K, Ghadimi M, Smith KD, Wang WL, Lazar AJ, Lev D. The expression of c-Met pathway components in unclassified pleomorphic sarcoma/malignant fibrous histiocytoma (UPS/MFH): a tissue microarray study. Histopathology. 2011;59:556-61.

136. Hennessy BT, Smith DL, Ram PT, Lu Y, Mills GB. Exploiting the PI3K/AKT pathway for cancer drug discovery. Nat Rev Drug Discov. 2005;4:988-1004.

137. Wander SA, Hennessy BT, Slingerland JM. Next-generation mTOR inhibitors in clinical oncology: how pathway complexity informs therapeutic strategy. J Clin Invest. 2011;121:1231-41.

138. Liu P, Cheng H, Roberts TM, Zhao JJ. Targeting the phosphoinositide 3-kinase pathway in cancer. Nat Rev Drug Discov. 2009;8:627-44.

139. Burris HA, 3rd. Overcoming acquired resistance to anticancer therapy: focus on the PI3K/AKT/mTOR pathway. Cancer Chemother Pharmacol. 2013;71:829-42.

140. O'Reilly KE, Rojo F, She QB, Solit D, Mills GB, Smith D, Lane H, Hofmann F, Hicklin DJ, Ludwig DL, Baselga J, Rosen N. mTOR inhibition induces upstream receptor tyrosine kinase signaling and activates Akt. Cancer Res. 2006;66:1500-8.

141. Carracedo A, Ma L, Teruya-Feldstein J, Rojo F, Salmena L, Alimonti A, Egia A, Sasaki AT, Thomas G, Kozma SC, Papa A, Nardella C, Cantley LC, Baselga J, Pandolfi PP. Inhibition of mTORC1 leads to MAPK pathway activation through a PI3K-dependent feedback loop in human cancer. J Clin Invest. 2008;118:3065-74.

142. Chandarlapaty S, Sawai A, Scaltriti M, Rodrik-Outmezguine V, Grbovic-Huezo O, Serra V, Majumder PK, Baselga J, Rosen N. AKT inhibition relieves feedback suppression of receptor tyrosine kinase expression and activity. Cancer Cell. 2011;19:58-71.

143. Rodrik-Outmezguine VS, Chandarlapaty S, Pagano NC, Poulikakos PI, Scaltriti M, Moskatel E, Baselga J, Guichard S, Rosen N. mTOR kinase inhibition causes feedback-dependent biphasic regulation of AKT signaling. Cancer Discov. 2011;1:248-59.

144. Muellner MK, Uras IZ, Gapp BV, Kerzendorfer C, Smida M, Lechtermann H, Craig-Mueller N, Colinge J, Duernberger G, Nijman SM. A chemical-genetic screen reveals a mechanism of resistance to PI3K inhibitors in cancer. Nat Chem Biol. 2011;7:787-93.

145. Muranen T, Selfors LM, Worster DT, Iwanicki MP, Song L, Morales FC, Gao S, Mills GB, Brugge JS. Inhibition of PI3K/mTOR leads to adaptive resistance in matrix-attached cancer cells. Cancer Cell. 2012;21:227-39.

146. Tzatsos A, Kandror KV. Nutrients suppress phosphatidylinositol 3-kinase/Akt signaling via raptor-dependent mTOR-mediated insulin receptor substrate 1 phosphorylation. Mol Cell Biol. 2006;26:63-76.

147. Harrington LS, Findlay GM, Gray A, Tolkacheva T, Wigfield S, Rebholz H, Barnett J, Leslie NR, Cheng S, Shepherd PR, Gout I, Downes CP, Lamb RF. The TSC1-2 tumor suppressor controls insulin-PI3K signaling via regulation of IRS proteins. J Cell Biol. 2004;166:213-23.

148. Tamburini J, Chapuis N, Bardet V, Park S, Sujobert P, Willems L, Ifrah N, Dreyfus F, Mayeux P, Lacombe C, Bouscary D. Mammalian target of rapamycin (mTOR) inhibition activates phosphatidylinositol 3-kinase/Akt by up-regulating insulin-like growth factor-1 receptor signaling in acute myeloid leukemia: rationale for therapeutic inhibition of both pathways. Blood. 2008;111:379-82.

149. Wan X, Harkavy B, Shen N, Grohar P, Helman LJ. Rapamycin induces feedback activation of Akt signaling through an IGF-1R-dependent mechanism. Oncogene. 2007;26:1932-40.

150. Willems L, Tamburini J, Chapuis N, Lacombe C, Mayeux P, Bouscary D. PI3K and mTOR signaling pathways in cancer: new data on targeted therapies. Curr Oncol Rep. 2012;14:129-38.

151. Raynaud FI, Eccles S, Clarke PA, Hayes A, Nutley B, Alix S, Henley A, Di-Stefano F, Ahmad Z, Guillard S, Bjerke LM, Kelland L, Valenti M, Patterson L, Gowan S, de Haven Brandon A, Hayakawa M, Kaizawa H, Koizumi T, Ohishi T, Patel S, Saghir

N, Parker P, Waterfield M, Workman P. Pharmacologic characterization of a potent inhibitor of class I phosphatidylinositide 3-kinases. Cancer Res. 2007;67:5840-50.

152. Glienke W, Maute L, Wicht J, Bergmann L. The dual PI3K/mTOR inhibitor NVP-BGT226 induces cell cycle arrest and regulates Survivin gene expression in human pancreatic cancer cell lines. Tumour Biol. 2012;33:757-65.

153. Zou CY, Smith KD, Zhu QS, Liu J, McCutcheon IE, Slopis JM, Meric-Bernstam F, Peng Z, Bornmann WG, Mills GB, Lazar AJ, Pollock RE, Lev D. Dual targeting of AKT and mammalian target of rapamycin: a potential therapeutic approach for malignant peripheral nerve sheath tumor. Mol Cancer Ther. 2009;8:1157-68.

154. Gobin B, Battaglia S, Lanel R, Chesneau J, Amiaud J, Redini F, Ory B, Heymann D. NVP-BEZ235, a dual PI3K/mTOR inhibitor, inhibits osteosarcoma cell proliferation and tumor development in vivo with an improved survival rate. Cancer Lett. 2014;344:291-8.

155. Cho DC, Cohen MB, Panka DJ, Collins M, Ghebremichael M, Atkins MB, Signoretti S, Mier JW. The efficacy of the novel dual PI3-kinase/mTOR inhibitor NVP-BEZ235 compared with rapamycin in renal cell carcinoma. Clin Cancer Res. 2010;16:3628-38.

156. Serra V, Markman B, Scaltriti M, Eichhorn PJ, Valero V, Guzman M, Botero ML, Llonch E, Atzori F, Di Cosimo S, Maira M, Garcia-Echeverria C, Parra JL, Arribas J, Baselga J. NVP-BEZ235, a dual PI3K/mTOR inhibitor, prevents PI3K signaling and inhibits the growth of cancer cells with activating PI3K mutations. Cancer Res. 2008;68:8022-30.

157. Chang KY, Tsai SY, Wu CM, Yen CJ, Chuang BF, Chang JY. Novel phosphoinositide 3-kinase/mTOR dual inhibitor, NVP-BGT226, displays potent growth-

inhibitory activity against human head and neck cancer cells in vitro and in vivo. Clin Cancer Res. 2011;17:7116-26.

158. Baumann P, Schneider L, Mandl-Weber S, Oduncu F, Schmidmaier R. Simultaneous targeting of PI3K and mTOR with NVP-BGT226 is highly effective in multiple myeloma. Anticancer Drugs. 2012;23:131-8.

159. Yu P, Laird AD, Du X, Wu J, Won KA, Yamaguchi K, Hsu PP, Qian F, Jaeger CT, Zhang W, Buhr CA, Shen P, Abulafia W, Chen J, Young J, Plonowski A, Yakes FM, Chu F, Lee M, Bentzien F, Lam ST, Dale S, Matthews DJ, Lamb P, Foster P. Characterization of the activity of the PI3K/mTOR inhibitor XL765 (SAR245409) in tumor models with diverse genetic alterations affecting the PI3K pathway. Mol Cancer Ther. 2014;13:1078-91.

160. Laird AD. XL765 targets tumor growth, survival, and angiogenesis in preclinical models by dual inhibition of PI3K and mTOR. Molecular Cancer Therapeutics. 2007;6:B250-B.

161. Kim S, Dodd RD, Mito JK, Ma Y, Kim Y, Riedel RF, Kirsch DG. Efficacy of phosphatidylinositol-3 kinase inhibitors in a primary mouse model of undifferentiated pleomorphic sarcoma. Sarcoma. 2012;2012:680708.

162. Guo S, Lopez-Marquez H, Fan KC, Choy E, Cote G, Harmon D, Nielsen GP, Yang C, Zhang C, Mankin H, Hornicek FJ, Borger DR, Duan Z. Synergistic effects of targeted PI3K signaling inhibition and chemotherapy in liposarcoma. PLoS One. 2014;9:e93996.

163. Manara MC, Nicoletti G, Zambelli D, Ventura S, Guerzoni C, Landuzzi L, Lollini PL, Maira SM, Garcia-Echeverria C, Mercuri M, Picci P, Scotlandi K. NVP-BEZ235 as a new therapeutic option for sarcomas. Clin Cancer Res. 2010;16:530-40.

164. Katanasaka Y, Kodera Y, Yunokawa M, Kitamura Y, Tamura T, Koizumi F. Synergistic anti-tumor effects of a novel phosphatidyl inositol-3 kinase/mammalian target of rapamycin dual inhibitor BGT226 and gefitinib in non-small cell lung cancer cell lines. Cancer Lett. 2014;347:196-203.

165. Erlich RB, Kherrouche Z, Rickwood D, Endo-Munoz L, Cameron S, Dahler A, Hazar-Rethinam M, de Long LM, Wooley K, Guminski A, Saunders NA. Preclinical evaluation of dual PI3K-mTOR inhibitors and histone deacetylase inhibitors in head and neck squamous cell carcinoma. Br J Cancer. 2012;106:107-15.

166. Kampa-Schittenhelm KM, Heinrich MC, Akmut F, Rasp KH, Illing B, Dohner H, Dohner K, Schittenhelm MM. Cell cycle-dependent activity of the novel dual PI3K-MTORC1/2 inhibitor NVP-BGT226 in acute leukemia. Mol Cancer. 2013;12:46.

167. Ou DL, Lee BS, Lin LI, Liou JY, Liao SC, Hsu C, Cheng AL. Vertical blockade of the IGFR- PI3K/Akt/mTOR pathway for the treatment of hepatocellular carcinoma: the role of survivin. Mol Cancer. 2014;13:2.

168. Fan QW, Cheng CK, Nicolaides TP, Hackett CS, Knight ZA, Shokat KM, Weiss WA. A dual phosphoinositide-3-kinase alpha/mTOR inhibitor cooperates with blockade of epidermal growth factor receptor in PTEN-mutant glioma. Cancer Res. 2007;67:7960-5.

169. Gedaly R, Angulo P, Hundley J, Daily MF, Chen C, Koch A, Evers BM. PI-103 and sorafenib inhibit hepatocellular carcinoma cell proliferation by blocking Ras/Raf/MAPK and PI3K/AKT/mTOR pathways. Anticancer Res. 2010;30:4951-8.

170. Ghadimi MP, Lopez G, Torres KE, Belousov R, Young ED, Liu J, Brewer KJ, Hoffman A, Lusby K, Lazar AJ, Pollock RE, Lev D. Targeting the PI3K/mTOR axis,

alone and in combination with autophagy blockade, for the treatment of malignant peripheral nerve sheath tumors. Mol Cancer Ther. 2012;11:1758-69.

171. Prasad G, Sottero T, Yang X, Mueller S, James CD, Weiss WA, Polley MY, Ozawa T, Berger MS, Aftab DT, Prados MD, Haas-Kogan DA. Inhibition of PI3K/mTOR pathways in glioblastoma and implications for combination therapy with temozolomide. Neuro Oncol. 2011;13:384-92.

172. Fokas E, Yoshimura M, Prevo R, Higgins G, Hackl W, Maira SM, Bernhard EJ, McKenna WG, Muschel RJ. NVP-BEZ235 and NVP-BGT226, dual phosphatidylinositol 3-kinase/mammalian target of rapamycin inhibitors, enhance tumor and endothelial cell radiosensitivity. Radiat Oncol. 2012;7:48.

173. Prevo R, Deutsch E, Sampson O, Diplexcito J, Cengel K, Harper J, O'Neill P, McKenna WG, Patel S, Bernhard EJ. Class I PI3 kinase inhibition by the pyridinylfuranopyrimidine inhibitor PI-103 enhances tumor radiosensitivity. Cancer Res. 2008;68:5915-23.

174. Papadopoulos KP, Tabernero J, Markman B, Patnaik A, Tolcher AW, Baselga J, Shi W, Egile C, Ruiz-Soto R, Laird AD, Miles D, Lorusso PM. Phase I safety, pharmacokinetic, and pharmacodynamic study of SAR245409 (XL765), a novel, orally administered PI3K/mTOR inhibitor in patients with advanced solid tumors. Clin Cancer Res. 2014;20:2445-56.

175. Markman B, Tabernero J, Krop I, Shapiro GI, Siu L, Chen LC, Mita M, Melendez Cuero M, Stutvoet S, Birle D, Anak O, Hackl W, Baselga J. Phase I safety, pharmacokinetic, and pharmacodynamic study of the oral phosphatidylinositol-3-kinase and mTOR inhibitor BGT226 in patients with advanced solid tumors. Ann Oncol. 2012;23:2399-408.

176. Cohen RB, Jänne PA, Engelman JA, Martínez P, Nishida Y, Gendreau S, Wu B, Felip E. A Phase 1 safety and pharmacokinetic (PK) study of PI3K/TORC1/TORC2 inhibitor XL765 (SAR245409) in combination with erlotinib in patients with advanced solid tumors. Screening. 2010;22:D85.

177. Janne PA, Cohen RB, Laird AD, Mace S, Engelman JA, Ruiz-Soto R, Rockich K, Xu J, Shapiro GI, Martinez P, Felip E. Phase I safety and pharmacokinetic study of the PI3K/mTOR inhibitor SAR245409 (XL765) in combination with erlotinib in patients with advanced solid tumors. J Thorac Oncol. 2014;9:316-23.

178. Molckovsky A, Siu LL. First-in-class, first-in-human phase I results of targeted agents: highlights of the 2008 American society of clinical oncology meeting. J Hematol Oncol. 2008;1:20.

179. Nghiemphu P, Omuro AM, Cloughesy T, Mellinghoff IK, Norden AD, Nguyen L, Rajangam K, Wen PY. A phase I safety and pharmacokinetic study of XL765 (SAR245409), a novel PI3K/TORC1/TORC2 inhibitor, in combination with temozolomide (TMZ) in patients (pts) with newly diagnosed malignant glioma. J Clin Oncol. 2010;28:3085.

180. Patnaik A, LoRusso P, Tabernero J, Laird AD, Aggarwal S, Papadopoulos K. Biomarker development for XL765, a potent and selective oral dual inhibitor of PI3K and mTOR currently being administered to patients in a Phase I clinical trial. Molecular Cancer Therapeutics. 2007;6:B265-B.

181. Britschgi A, Andraos R, Brinkhaus H, Klebba I, Romanet V, Muller U, Murakami M, Radimerski T, Bentires-Alj M. JAK2/STAT5 inhibition circumvents resistance to PI3K/mTOR blockade: a rationale for cotargeting these pathways in metastatic breast cancer. Cancer Cell. 2012;22:796-811.

182. Serra V, Scaltriti M, Prudkin L, Eichhorn PJ, Ibrahim YH, Chandarlapaty S, Markman B, Rodriguez O, Guzman M, Rodriguez S, Gili M, Russillo M, Parra JL, Singh S, Arribas J, Rosen N, Baselga J. PI3K inhibition results in enhanced HER signaling and acquired ERK dependency in HER2-overexpressing breast cancer. Oncogene. 2011;30:2547-57.

183. Fujita-Yamaguchi Y, LeBon TR, Tsubokawa M, Henzel W, Kathuria S, Koyal D, Ramachandran J. Comparison of insulin-like growth factor I receptor and insulin receptor purified from human placental membranes. J Biol Chem. 1986;261:16727-31.

184. Ullrich A, Gray A, Tam AW, Yang-Feng T, Tsubokawa M, Collins C, Henzel W, Le Bon T, Kathuria S, Chen E, et al. Insulin-like growth factor I receptor primary structure: comparison with insulin receptor suggests structural determinants that define functional specificity. EMBO J. 1986;5:2503-12.

185. Entingh-Pearsall A, Kahn CR. Differential roles of the insulin and insulin-like growth factor-I (IGF-I) receptors in response to insulin and IGF-I. J Biol Chem. 2004;279:38016-24.

186. Moxham CP, Duronio V, Jacobs S. Insulin-like growth factor I receptor beta-subunit heterogeneity. Evidence for hybrid tetramers composed of insulin-like growth factor I and insulin receptor heterodimers. J Biol Chem. 1989;264:13238-44.

187. Furstenberger G, Senn HJ. Insulin-like growth factors and cancer. Lancet Oncol. 2002;3:298-302.

188. Seccareccia E, Brodt P. The role of the insulin-like growth factor-I receptor in malignancy: an update. Growth Horm IGF Res. 2012;22:193-9.

189. Chitnis MM, Yuen JS, Protheroe AS, Pollak M, Macaulay VM. The type 1 insulin-like growth factor receptor pathway. Clin Cancer Res. 2008;14:6364-70.

190. Rikhof B, de Jong S, Suurmeijer AJ, Meijer C, van der Graaf WT. The insulin-like growth factor system and sarcomas. J Pathol. 2009;217:469-82.

191. Pollak M. The insulin and insulin-like growth factor receptor family in neoplasia: an update. Nat Rev Cancer. 2012;12:159-69.

192. Heidegger I, Pircher A, Klocker H, Massoner P. Targeting the insulin-like growth factor network in cancer therapy. Cancer Biol Ther. 2011;11:701-7.

193. Sell C, Dumenil G, Deveaud C, Miura M, Coppola D, DeAngelis T, Rubin R, Efstratiadis A, Baserga R. Effect of a null mutation of the insulin-like growth factor I receptor gene on growth and transformation of mouse embryo fibroblasts. Mol Cell Biol. 1994;14:3604-12.

194. Sell C, Rubini M, Rubin R, Liu JP, Efstratiadis A, Baserga R. Simian virus 40 large tumor antigen is unable to transform mouse embryonic fibroblasts lacking type 1 insulin-like growth factor receptor. Proc Natl Acad Sci U S A. 1993;90:11217-21.

195. Sachdev D, Zhang X, Matise I, Gaillard-Kelly M, Yee D. The type I insulin-like growth factor receptor regulates cancer metastasis independently of primary tumor growth by promoting invasion and survival. Oncogene. 2010;29:251-62.

196. Arcaro A. Targeting the insulin-like growth factor-1 receptor in human cancer. Front Pharmacol. 2013;4:30.

197. Tognon CE, Sorensen PH. Targeting the insulin-like growth factor 1 receptor (IGF1R) signaling pathway for cancer therapy. Expert Opin Ther Targets. 2012;16:33-48.

198. Cheng H, Dodge J, Mehl E, Liu S, Poulin N, van de Rijn M, Nielsen TO. Validation of immature adipogenic status and identification of prognostic biomarkers in myxoid liposarcoma using tissue microarrays. Hum Pathol. 2009;40:1244-51.

199. Xie Y, Skytting B, Nilsson G, Brodin B, Larsson O. Expression of insulin-like growth factor-1 receptor in synovial sarcoma: association with an aggressive phenotype. Cancer Res. 1999;59:3588-91.

200. Cao L, Yu Y, Darko I, Currier D, Mayeenuddin LH, Wan X, Khanna C, Helman LJ. Addiction to elevated insulin-like growth factor I receptor and initial modulation of the AKT pathway define the responsiveness of rhabdomyosarcoma to the targeting antibody. Cancer Res. 2008;68:8039-48.

201. Yang J, Ylipaa A, Sun Y, Zheng H, Chen K, Nykter M, Trent J, Ratner N, Lev DC, Zhang W. Genomic and molecular characterization of malignant peripheral nerve sheath tumor identifies the IGF1R pathway as a primary target for treatment. Clin Cancer Res. 2011;17:7563-73.

202. Busund LT, Ow KT, Russell P, Crowe PJ, Yang JL. Expression of insulin-like growth factor mitogenic signals in adult soft-tissue sarcomas: significant correlation with malignant potential. Virchows Arch. 2004;444:142-8.

203. Jones HE, Goddard L, Gee JM, Hiscox S, Rubini M, Barrow D, Knowlden JM, Williams S, Wakeling AE, Nicholson RI. Insulin-like growth factor-I receptor signalling and acquired resistance to gefitinib (ZD1839; Iressa) in human breast and prostate cancer cells. Endocr Relat Cancer. 2004;11:793-814.

204. Lu Y, Zi X, Zhao Y, Mascarenhas D, Pollak M. Insulin-like growth factor-I receptor signaling and resistance to trastuzumab (Herceptin). J Natl Cancer Inst. 2001;93:1852-7.

205. Liu YC, Leu CM, Wong FH, Fong WS, Chen SC, Chang C, Hu CP. Autocrine stimulation by insulin-like growth factor I is involved in the growth, tumorigenicity and chemoresistance of human esophageal carcinoma cells. J Biomed Sci. 2002;9:665-74.

206. Kurmasheva RT, Houghton PJ. IGF-I mediated survival pathways in normal and malignant cells. Biochim Biophys Acta. 2006;1766:1-22.

207. Kim TR, Cho EW, Paik SG, Kim IG. Hypoxia-induced SM22alpha in A549 cells activates the IGF1R/PI3K/Akt pathway, conferring cellular resistance against chemo- and radiation therapy. FEBS Lett. 2012;586:303-9.

208. Gualberto A, Pollak M. Emerging role of insulin-like growth factor receptor inhibitors in oncology: early clinical trial results and future directions. Oncogene. 2009;28:3009-21.

209. Rodon J, DeSantos V, Ferry RJ, Jr., Kurzrock R. Early drug development of inhibitors of the insulin-like growth factor-I receptor pathway: lessons from the first clinical trials. Mol Cancer Ther. 2008;7:2575-88.

210. Garcia-Echeverria C, Pearson MA, Marti A, Meyer T, Mestan J, Zimmermann J, Gao J, Brueggen J, Capraro HG, Cozens R, Evans DB, Fabbro D, Furet P, Porta DG, Liebetanz J, Martiny-Baron G, Ruetz S, Hofmann F. In vivo antitumor activity of NVP-AEW541-A novel, potent, and selective inhibitor of the IGF-IR kinase. Cancer Cell. 2004;5:231-9.

211. Girnita A, Girnita L, del Prete F, Bartolazzi A, Larsson O, Axelson M. Cyclolignans as inhibitors of the insulin-like growth factor-1 receptor and malignant cell growth. Cancer Res. 2004;64:236-42.

212. Scotlandi K, Manara MC, Nicoletti G, Lollini PL, Lukas S, Benini S, Croci S, Perdichizzi S, Zambelli D, Serra M, Garcia-Echeverria C, Hofmann F, Picci P. Antitumor activity of the insulin-like growth factor-I receptor kinase inhibitor NVP-AEW541 in musculoskeletal tumors. Cancer Res. 2005;65:3868-76.

213. Yee D. Insulin-like growth factor receptor inhibitors: baby or the bathwater? J Natl Cancer Inst. 2012;104:975-81.

214. Guha M. Anticancer IGF1R classes take more knocks. Nat Rev Drug Discov. 2013;12:250.

215. Robertson JF, Ferrero JM, Bourgeois H, Kennecke H, de Boer RH, Jacot W, McGreivy J, Suzuki S, Zhu M, McCaffery I, Loh E, Gansert JL, Kaufman PA. Ganitumab with either exemestane or fulvestrant for postmenopausal women with advanced, hormone-receptor-positive breast cancer: a randomised, controlled, double-blind, phase 2 trial. Lancet Oncol. 2013;14:228-35.

216. King H, Aleksic T, Haluska P, Macaulay VM. Can we unlock the potential of IGF-1R inhibition in cancer therapy? Cancer Treat Rev. 2014;40:1096-105.

217. Bertrand FE, Steelman LS, Chappell WH, Abrams SL, Shelton JG, White ER, Ludwig DL, McCubrey JA. Synergy between an IGF-1R antibody and Raf/MEK/ERK and PI3K/Akt/mTOR pathway inhibitors in suppressing IGF-1R-mediated growth in hematopoietic cells. Leukemia. 2006;20:1254-60.

218. Singh RK, Gaikwad SM, Jinager A, Chaudhury S, Maheshwari A, Ray P. IGF-1R inhibition potentiates cytotoxic effects of chemotherapeutic agents in early stages of chemoresistant ovarian cancer cells. Cancer Lett. 2014;354:254-62.

219. Bitelman C, Sarfstein R, Sarig M, Attias-Geva Z, Fishman A, Werner H, Bruchim I. IGF1R-directed targeted therapy enhances the cytotoxic effect of chemotherapy in endometrial cancer. Cancer Lett. 2013;335:153-9.

220. Reidy DL, Vakiani E, Fakih MG, Saif MW, Hecht JR, Goodman-Davis N, Hollywood E, Shia J, Schwartz J, Chandrawansa K, Dontabhaktuni A, Youssoufian H, Solit DB, Saltz LB. Randomized, phase II study of the insulin-like growth factor-1

receptor inhibitor IMC-A12, with or without cetuximab, in patients with cetuximab- or panitumumab-refractory metastatic colorectal cancer. J Clin Oncol. 2010;28:4240-6.

221. Molife LR, Fong PC, Paccagnella L, Reid AH, Shaw HM, Vidal L, Arkenau HT, Karavasilis V, Yap TA, Olmos D, Spicer J, Postel-Vinay S, Yin D, Lipton A, Demers L, Leitzel K, Gualberto A, de Bono JS. The insulin-like growth factor-I receptor inhibitor figitumumab (CP-751,871) in combination with docetaxel in patients with advanced solid tumours: results of a phase Ib dose-escalation, open-label study. Br J Cancer. 2010;103:332-9.

222. Langer CJ, Novello S, Park K, Krzakowski M, Karp DD, Mok T, Benner RJ, Scranton JR, Olszanski AJ, Jassem J. Randomized, phase III trial of first-line figitumumab in combination with paclitaxel and carboplatin versus paclitaxel and carboplatin alone in patients with advanced non-small-cell lung cancer. J Clin Oncol. 2014;32:2059-66.

223. Quek R, Wang Q, Morgan JA, Shapiro GI, Butrynski JE, Ramaiya N, Huftalen T, Jederlinic N, Manola J, Wagner AJ, Demetri GD, George S. Combination mTOR and IGF-1R inhibition: phase I trial of everolimus and figitumumab in patients with advanced sarcomas and other solid tumors. Clin Cancer Res. 2011;17:871-9.

224. Olmos D, Postel-Vinay S, Molife LR, Okuno SH, Schuetze SM, Paccagnella ML, Batzel GN, Yin D, Pritchard-Jones K, Judson I, Worden FP, Gualberto A, Scurr M, de Bono JS, Haluska P. Safety, pharmacokinetics, and preliminary activity of the anti-IGF-1R antibody figitumumab (CP-751,871) in patients with sarcoma and Ewing's sarcoma: a phase 1 expansion cohort study. Lancet Oncol. 2010;11:129-35.

225. Naing A, Kurzrock R, Burger A, Gupta S, Lei X, Busaidy N, Hong D, Chen HX, Doyle LA, Heilbrun LK, Rohren E, Ng C, Chandhasin C, LoRusso P. Phase I trial of

cixutumumab combined with temsirolimus in patients with advanced cancer. Clin Cancer Res. 2011;17:6052-60.

226. Lahat G, Zhu QS, Huang KL, Wang S, Bolshakov S, Liu J, Torres K, Langley RR, Lazar AJ, Hung MC, Lev D. Vimentin is a novel anti-cancer therapeutic target; insights from in vitro and in vivo mice xenograft studies. PLoS One. 2010;5:e10105.

227. Keniry M, Parsons R. The role of PTEN signaling perturbations in cancer and in targeted therapy. Oncogene. 2008;27:5477-85.

228. Tibes R, Qiu Y, Lu Y, Hennessy B, Andreeff M, Mills GB, Kornblau SM. Reverse phase protein array: validation of a novel proteomic technology and utility for analysis of primary leukemia specimens and hematopoietic stem cells. Mol Cancer Ther. 2006;5:2512-21.

229. Stambolic V, Suzuki A, de la Pompa JL, Brothers GM, Mirtsos C, Sasaki T, Ruland J, Penninger JM, Siderovski DP, Mak TW. Negative regulation of PKB/Akt-dependent cell survival by the tumor suppressor PTEN. Cell. 1998;95:29-39.

230. Hollander MC, Blumenthal GM, Dennis PA. PTEN loss in the continuum of common cancers, rare syndromes and mouse models. Nat Rev Cancer. 2011;11:289-301.

231. Mendoza MC, Er EE, Blenis J. The Ras-ERK and PI3K-mTOR pathways: cross-talk and compensation. Trends Biochem Sci. 2011;36:320-8.

232. Raynaud FI, Eccles SA, Patel S, Alix S, Box G, Chuckowree I, Folkes A, Gowan S, De Haven Brandon A, Di Stefano F, Hayes A, Henley AT, Lensun L, Pergl-Wilson G, Robson A, Saghir N, Zhyvoloup A, McDonald E, Sheldrake P, Shuttleworth S, Valenti M, Wan NC, Clarke PA, Workman P. Biological properties of potent inhibitors of class I

phosphatidylinositide 3-kinases: from PI-103 through PI-540, PI-620 to the oral agent GDC-0941. Mol Cancer Ther. 2009;8:1725-38.

233. Garcia-Echeverria C, Sellers WR. Drug discovery approaches targeting the PI3K/Akt pathway in cancer. Oncogene. 2008;27:5511-26.

234. Braña I, LoRusso P, Baselga J, Heath E, Patnaik A, Gendreau S, Laird AD, Papadopoulos K. A Phase 1 dose-escalation study of the safety, pharmacokinetics and pharmacodynamics of XL765 (SAR245409), a PI3K/TORC1/TORC2 inhibitor administered orally to patients with advanced malignancies. bid. 2010;16:5.

235. Barretina J, Taylor BS, Banerji S, Ramos AH, Lagos-Quintana M, Decarolis PL, Shah K, Socci ND, Weir BA, Ho A, Chiang DY, Reva B, Mermel CH, Getz G, Antipin Y, Beroukhim R, Major JE, Hatton C, Nicoletti R, Hanna M, Sharpe T, Fennell TJ, Cibulskis K, Onofrio RC, Saito T, Shukla N, Lau C, Nelander S, Silver SJ, Sougnez C, Viale A, Winckler W, Maki RG, Garraway LA, Lash A, Greulich H, Root DE, Sellers WR, Schwartz GK, Antonescu CR, Lander ES, Varmus HE, Ladanyi M, Sander C, Meyerson M, Singer S. Subtype-specific genomic alterations define new targets for soft-tissue sarcoma therapy. Nat Genet. 2010;42:715-21.

236. Gibault L, Ferreira C, Perot G, Audebourg A, Chibon F, Bonnin S, Lagarde P, Vacher-Lavenu MC, Terrier P, Coindre JM, Aurias A. From PTEN loss of expression to RICTOR role in smooth muscle differentiation: complex involvement of the mTOR pathway in leiomyosarcomas and pleomorphic sarcomas. Mod Pathol. 2012;25:197-211.

237. Bai Y, Li J, Fang B, Edwards A, Zhang G, Bui M, Eschrich S, Altiok S, Koomen J, Haura EB. Phosphoproteomics identifies driver tyrosine kinases in sarcoma cell lines and tumors. Cancer Res. 2012;72:2501-11.

238. Heinrich MC, Corless CL, Duensing A, McGreevey L, Chen CJ, Joseph N, Singer S, Griffith DJ, Haley A, Town A, Demetri GD, Fletcher CD, Fletcher JA. PDGFRA activating mutations in gastrointestinal stromal tumors. Science. 2003;299:708-10.

239. Wunder JS, Nielsen TO, Maki RG, O'Sullivan B, Alman BA. Opportunities for improving the therapeutic ratio for patients with sarcoma. Lancet Oncol. 2007;8:513-24.

240. Becerikli M, Wieczorek S, Stricker I, Nambiar S, Rittig A, Epplen JT, Tannapfel A, Lehnhardt M, Steinstraesser L, Jacobsen F. Numerical and structural chromosomal anomalies in undifferentiated pleomorphic sarcoma. Anticancer Res. 2014;34:7119-27.

241. El Haibi CP, Sharma PK, Singh R, Johnson PR, Suttles J, Singh S, Lillard JW, Jr. PI3Kp110-, Src-, FAK-dependent and DOCK2-independent migration and invasion of CXCL13-stimulated prostate cancer cells. Mol Cancer. 2010;9:85.

242. Sanchez CG, Ma CX, Crowder RJ, Guintoli T, Phommaly C, Gao F, Lin L, Ellis MJ. Preclinical modeling of combined phosphatidylinositol-3-kinase inhibition with endocrine therapy for estrogen receptor-positive breast cancer. Breast Cancer Res. 2011;13:R21.

243. Will M, Qin AC, Toy W, Yao Z, Rodrik-Outmezguine V, Schneider C, Huang X, Monian P, Jiang X, de Stanchina E, Baselga J, Liu N, Chandarlapaty S, Rosen N. Rapid induction of apoptosis by PI3K inhibitors is dependent upon their transient inhibition of RAS-ERK signaling. Cancer Discov. 2014;4:334-47.

244. Shimizu T, Tolcher AW, Papadopoulos KP, Beeram M, Rasco DW, Smith LS, Gunn S, Smetzer L, Mays TA, Kaiser B, Wick MJ, Alvarez C, Cavazos A, Mangold GL, Patnaik A. The clinical effect of the dual-targeting strategy involving PI3K/AKT/mTOR

and RAS/MEK/ERK pathways in patients with advanced cancer. Clin Cancer Res. 2012;18:2316-25.

245. Gao N, Flynn DC, Zhang Z, Zhong XS, Walker V, Liu KJ, Shi X, Jiang BH. G1 cell cycle progression and the expression of G1 cyclins are regulated by PI3K/AKT/mTOR/p70S6K1 signaling in human ovarian cancer cells. Am J Physiol Cell Physiol. 2004;287:C281-91.

246. Manning BD, Cantley LC. AKT/PKB signaling: navigating downstream. Cell. 2007;129:1261-74.

247. Park S, Chapuis N, Bardet V, Tamburini J, Gallay N, Willems L, Knight ZA, Shokat KM, Azar N, Viguie F, Ifrah N, Dreyfus F, Mayeux P, Lacombe C, Bouscary D. PI-103, a dual inhibitor of Class IA phosphatidylinositide 3-kinase and mTOR, has antileukemic activity in AML. Leukemia. 2008;22:1698-706.

248. Hopfner M, Huether A, Sutter AP, Baradari V, Schuppan D, Scherubl H. Blockade of IGF-1 receptor tyrosine kinase has antineoplastic effects in hepatocellular carcinoma cells. Biochem Pharmacol. 2006;71:1435-48.

249. Tanno B, Mancini C, Vitali R, Mancuso M, McDowell HP, Dominici C, Raschella G. Down-regulation of insulin-like growth factor I receptor activity by NVP-AEW541 has an antitumor effect on neuroblastoma cells in vitro and in vivo. Clin Cancer Res. 2006;12:6772-80.

250. Moser C, Schachtschneider P, Lang SA, Gaumann A, Mori A, Zimmermann J, Schlitt HJ, Geissler EK, Stoeltzing O. Inhibition of insulin-like growth factor-I receptor (IGF-IR) using NVP-AEW541, a small molecule kinase inhibitor, reduces orthotopic pancreatic cancer growth and angiogenesis. Eur J Cancer. 2008;44:1577-86.

251. Tazzari PL, Tabellini G, Bortul R, Papa V, Evangelisti C, Grafone T, Martinelli G, McCubrey JA, Martelli AM. The insulin-like growth factor-I receptor kinase inhibitor NVP-AEW541 induces apoptosis in acute myeloid leukemia cells exhibiting autocrine insulin-like growth factor-I secretion. Leukemia. 2007;21:886-96.

252. Juan HC, Tsai HT, Chang PH, Huang CY, Hu CP, Wong FH. Insulin-like growth factor 1 mediates 5-fluorouracil chemoresistance in esophageal carcinoma cells through increasing survivin stability. Apoptosis. 2011;16:174-83.

253. Liu L, Li F, Cardelli JA, Martin KA, Blenis J, Huang S. Rapamycin inhibits cell motility by suppression of mTOR-mediated S6K1 and 4E-BP1 pathways. Oncogene. 2006;25:7029-40.

254. Sarbassov DD, Ali SM, Kim DH, Guertin DA, Latek RR, Erdjument-Bromage H, Tempst P, Sabatini DM. Rictor, a novel binding partner of mTOR, defines a rapamycin-insensitive and raptor-independent pathway that regulates the cytoskeleton. Curr Biol. 2004;14:1296-302.

255. Jacinto E, Loewith R, Schmidt A, Lin S, Ruegg MA, Hall A, Hall MN. Mammalian TOR complex 2 controls the actin cytoskeleton and is rapamycin insensitive. Nat Cell Biol. 2004;6:1122-8.

256. Parri M, Chiarugi P. Rac and Rho GTPases in cancer cell motility control. Cell Commun Signal. 2010;8:23.

257. Hernandez-Negrete I, Carretero-Ortega J, Rosenfeldt H, Hernandez-Garcia R, Calderon-Salinas JV, Reyes-Cruz G, Gutkind JS, Vazquez-Prado J. P-Rex1 links mammalian target of rapamycin signaling to Rac activation and cell migration. J Biol Chem. 2007;282:23708-15.

258. Higuchi M, Masuyama N, Fukui Y, Suzuki A, Gotoh Y. Akt mediates Rac/Cdc42-regulated cell motility in growth factor-stimulated cells and in invasive PTEN knockout cells. Curr Biol. 2001;11:1958-62.

259. McCawley LJ, Matrisian LM. Matrix metalloproteinases: they're not just for matrix anymore! Curr Opin Cell Biol. 2001;13:534-40.

260. Zhang D, Bar-Eli M, Meloche S, Brodt P. Dual regulation of MMP-2 expression by the type 1 insulin-like growth factor receptor: the phosphatidylinositol 3-kinase/Akt and Raf/ERK pathways transmit opposing signals. J Biol Chem. 2004;279:19683-90.

261. Long L, Navab R, Brodt P. Regulation of the Mr 72,000 type IV collagenase by the type I insulin-like growth factor receptor. Cancer Res. 1998;58:3243-7.

262. Li S, Zhang D, Yang L, Burnier JV, Wang N, Lin R, Lee ER, Glazer RI, Brodt P. The IGF-I receptor can alter the matrix metalloproteinase repertoire of tumor cells through transcriptional regulation of PKC-{alpha}. Mol Endocrinol. 2009;23:2013-25.

263. Zhang D, Samani AA, Brodt P. The role of the IGF-I receptor in the regulation of matrix metalloproteinases, tumor invasion and metastasis. Horm Metab Res. 2003;35:802-8.

264. Nakamura M, Miyamoto S, Maeda H, Ishii G, Hasebe T, Chiba T, Asaka M, Ochiai A. Matrix metalloproteinase-7 degrades all insulin-like growth factor binding proteins and facilitates insulin-like growth factor bioavailability. Biochem Biophys Res Commun. 2005;333:1011-6.

265. Miyamoto S, Yano K, Sugimoto S, Ishii G, Hasebe T, Endoh Y, Kodama K, Goya M, Chiba T, Ochiai A. Matrix metalloproteinase-7 facilitates insulin-like growth factor bioavailability through its proteinase activity on insulin-like growth factor binding protein 3. Cancer Res. 2004;64:665-71.

266. Sadowski T, Dietrich S, Koschinsky F, Sedlacek R. Matrix metalloproteinase 19 regulates insulin-like growth factor-mediated proliferation, migration, and adhesion in human keratinocytes through proteolysis of insulin-like growth factor binding protein-3. Mol Biol Cell. 2003;14:4569-80.

267. D'Amato V, Rosa R, D'Amato C, Formisano L, Marciano R, Nappi L, Raimondo L, Di Mauro C, Servetto A, Fusciello C, Veneziani BM, De Placido S, Bianco R. The dual PI3K/mTOR inhibitor PKI-587 enhances sensitivity to cetuximab in EGFR-resistant human head and neck cancer models. Br J Cancer. 2014;110:2887-95.

268. O'Brien NA, McDonald K, Tong L, von Euw E, Kalous O, Conklin D, Hurvitz SA, di Tomaso E, Schnell C, Linnartz R, Finn RS, Hirawat S, Slamon DJ. Targeting PI3K/mTOR overcomes resistance to HER2-targeted therapy independent of feedback activation of AKT. Clin Cancer Res. 2014;20:3507-20.

269. Belmont PJ, Jiang P, McKee TD, Xie T, Isaacson J, Baryla NE, Roper J, Sinnamon MJ, Lee NV, Kan JL, Guicherit O, Wouters BG, O'Brien CA, Shields D, Olson P, VanArsdale T, Weinrich SL, Rejto P, Christensen JG, Fantin VR, Hung KE, Martin ES. Resistance to dual blockade of the kinases PI3K and mTOR in KRAS-mutant colorectal cancer models results in combined sensitivity to inhibition of the receptor tyrosine kinase EGFR. Sci Signal. 2014;7:ra107.

270. Brader S, Eccles SA. Phosphoinositide 3-kinase signalling pathways in tumor progression, invasion and angiogenesis. Tumori. 2004;90:2-8.

271. Reinmuth N, Fan F, Liu W, Parikh AA, Stoeltzing O, Jung YD, Bucana CD, Radinsky R, Gallick GE, Ellis LM. Impact of insulin-like growth factor receptor-I function on angiogenesis, growth, and metastasis of colon cancer. Lab Invest. 2002;82:1377-89.

272. Woo JK, Choi Y, Oh SH, Jeong JH, Choi DH, Seo HS, Kim CW. Mucin 1 enhances the tumor angiogenic response by activation of the AKT signaling pathway. Oncogene. 2012;31:2187-98.

273. Gariboldi MB, Ravizza R, Monti E. The IGFR1 inhibitor NVP-AEW541 disrupts a pro-survival and pro-angiogenic IGF-STAT3-HIF1 pathway in human glioblastoma cells. Biochem Pharmacol. 2010;80:455-62.

274. Heidegger I, Kern J, Ofer P, Klocker H, Massoner P. Oncogenic functions of IGF1R and INSR in prostate cancer include enhanced tumor growth, cell migration and angiogenesis. Oncotarget. 2014;5:2723-35.

275. Karar J, Maity A. PI3K/AKT/mTOR Pathway in Angiogenesis. Front Mol Neurosci. 2011;4:51.

276. Kurzrock R, Patnaik A, Aisner J, Warren T, Leong S, Benjamin R, Eckhardt SG, Eid JE, Greig G, Habben K, McCarthy CD, Gore L. A phase I study of weekly R1507, a human monoclonal antibody insulin-like growth factor-I receptor antagonist, in patients with advanced solid tumors. Clin Cancer Res. 2010;16:2458-65.

277. Tolcher AW, Sarantopoulos J, Patnaik A, Papadopoulos K, Lin CC, Rodon J, Murphy B, Roth B, McCaffery I, Gorski KS, Kaiser B, Zhu M, Deng H, Friberg G, Puzanov I. Phase I, pharmacokinetic, and pharmacodynamic study of AMG 479, a fully human monoclonal antibody to insulin-like growth factor receptor 1. J Clin Oncol. 2009;27:5800-7.

278. Haluska P, Shaw HM, Batzel GN, Yin D, Molina JR, Molife LR, Yap TA, Roberts ML, Sharma A, Gualberto A, Adjei AA, de Bono JS. Phase I dose escalation study of the anti insulin-like growth factor-I receptor monoclonal antibody CP-751,871 in patients with refractory solid tumors. Clin Cancer Res. 2007;13:5834-40.

279. Ramalingam SS, Spigel DR, Chen D, Steins MB, Engelman JA, Schneider C-P, Novello S, Eberhardt WEE, Crino L, Habben K, Liu L, Jänne PA, Brownstein CM, Reck M. Randomized Phase II Study of Erlotinib in Combination With Placebo or R1507, a Monoclonal Antibody to Insulin-Like Growth Factor-1 Receptor, for Advanced-Stage Non–Small-Cell Lung Cancer. Journal of Clinical Oncology. 2011;29:4574-80.

280. Pappo AS, Patel SR, Crowley J, Reinke DK, Kuenkele K-P, Chawla SP, Toner GC, Maki RG, Meyers PA, Chugh R, Ganjoo KN, Schuetze SM, Juergens H, Leahy MG, Geoerger B, Benjamin RS, Helman LJ, Baker LH. R1507, a Monoclonal Antibody to the Insulin-Like Growth Factor 1 Receptor, in Patients With Recurrent or Refractory Ewing Sarcoma Family of Tumors: Results of a Phase II Sarcoma Alliance for Research Through Collaboration Study. Journal of Clinical Oncology. 2011;29:4541-7.

Vitae

Caitlin Denise May was born in Lake Forest, Illinois, on October 26, 1987, the daughter of Catherine Sue May and Paul Dennis May. After graduating from Monsignor John R. Hackett Catholic Central High School, Kalamazoo, Michigan in 2005, she enrolled at Grand Valley State University, Allendale, Michigan. She received the degree of Bachelor of Science with a major in Cell and Molecular Biology, with an Emphasis in Chemistry and Genetics, from GVSU in April, 2009. During her last year at GVSU, she was an undergraduate intern at the Van Andel Research Institute in Grand Rapids, Michigan, where she worked in the Laboratory of Genome Integrity and Tumorigenesis under the direction of Dr. Michael Weinreich. In August of 2009, she entered The University of Texas Graduate School of Biomedical Sciences at Houston/MD Anderson Cancer Center, where she investigated novel combination therapies for the treatment of undifferentiated pleomorphic sarcoma.